NTNU – Trondheim
Norwegian University of
Science and Technology

Micro-Nano enhanced surfaces for investigation of oil-water separation

Åsmund Bryne Retterstøl

Master of Energy and Environmental Engineering
Submission date: Januar 2015
Supervisor: Carlos Alberto Dorao, EPT

Norwegian University of Science and Technology
Department of Energy and Process Engineering

Acknowledgments

I would like to express my great appreciation and gratitude to my supervisor during the work related to this Masters' Thesis, Carlos A. Dorao, for all the support and guidance throughout the semester.

Preface

This master thesis is the result of the work I preformed at the Department of Energy and Process Engineering during the fall of 2014 and conclude my Master of Science degree in Energy and Environmental Engineering at the Norwegian University of Science and Technology (NTNU). The topic of this thesis is an experimental study of droplet dynamic related to oil-water gravity separators, with focus on the droplet interaction with the liquid-liquid interface. This is a critical parameter for the sizing of the separators. Furthermore, alternatives for improving the visualization of the test cell will be evaluated. This thesis consist of a literature study and the extensive experimental work performed during the duration of the semester. The supervisor of this Master's Thesis has been Carlos A. Dorao.

Abstract

Separator are an important part of the oil processing. The fluid mixture extracted from an oil well contains large amount of water, and is separated by using large separators. A gravitational separator relies on the difference in density to separate the phases. To increase the efficiency of these separators it is important to understand the underlying physics of the of the separation process. This requires experimental work. However, the oil interaction with the with the test cell reduce the visibility of the process.

There were two main objectives in this thesis. One was to investigate the separation of oil – water, and the other was to investigate the possibility to control the wettability of the glass surface of the test cell.

The separation time for a mixture of oil and water, depend on both the settling velocity of the droplets and the coalescence time. These depend both, on the properties of the oil and the droplet size. In this thesis focus on the separation time, and the velocity of the droplet – interface coalescence. The experiment was conducted by using a small glass vessel, filled with the same amount of oil and water. The liquids were mixed for different amount of time, and the separation was visualized by using a near infrared high-speed camera. Both crude oil-water, and Exxol D80 – water mixtures was investigated. The separation velocity of the mixtures was measured by tracking the movement of the interface over time.

The separation velocity of the mixtures did decrease with mixing time. Both for Exxol – water and crude oil – water. These results were compared with the terminal velocity of a single droplet. The result indicates that the hindering effect of neighboring droplets significantly affect the dynamic of the separation process. Further work is needed to quantify this effect.

The other main objective was to investigate the possibility to control the wettability of the glass surface of the test cell. The wettability of a surface depended on the shape, roughness and energy of the surface. The nano-micro enhanced surfaces were fabricated at the NTNU NanoLab. A thin layer of aluminum and Indium Tin Oxide (ITO) was deposit on different glass samples using a sputtering technic. Different surfaces were created by changing the duration of the sputtering. The roughness of these samples was measured using an Atomic Force Microscope. The surface wettability was then investigated by measuring the contact angle with both oil and water.

The enhanced surfaces did improve the hydrophobic properties, however there was no change in the oleophobic properties. Only one surface in this thesis was hydrophobic, that was an ITO surface that was sputtered for 30 minutes. The hydrophobic properties of the samples, was not just related to the roughness of the surface. This shows that there are other properties that are equally important, such as surface energy and the possibility for air pockets between the surface and liquid. Further work is needed to create a surface for the test cell. The surface energy of the samples should be low to create an oleophobic surface.

Sammendrag

Separatorer er en viktig del av olje prosessering. Det er store mengder vann i væsken som pumpes opp av olje brønner, som separeres av store separatorer. Gravitasjons separatorer bruker foskjellen i tetthet til å separere de forskjellige fasene. For å øke effektiviteten til disse separatorene er det viktig å forstå den underliggende fysikken i en separasjons prosess. Dette krever eksperimentelt arbeid. Likevel er det utfordrende at interaksjonen mellom oljen og test cellen minker synligheten av denne prosessen.

I denne avhandlingen er det to hoved oppgaver. Den ene er å undersøke separasjonen av en blanding av olje og vann. Den andre er å undersøke muligheten til å kontrollere fuktingen a glass overflaten som blir brukt i test cellen.

Separasjons tiden for blandingen av olje og vann, avhenger både av den synkehastigheten til dråpene og koalesens tiden. Disse avhenger både av egenskapene til oljen og størrelsen til dråpen. I denne oppgaven er det fokusert på separasjonstiden, og hastigheten av dråpe - grensesnitt koalesens. Eksperimentene ble utført ved at en lite glass beholder ble fylt med lik mengde olje og vann. Væskene ble blandet i forskjellige tidslengder, og separasjonen ble visualisert med et nær infrarødt høyhastighet kamera. Både råolje – vann og Exxol D80 – vann blandinger ble undersøkt. Hastigheten til separasjonen ble målt ved å følge bevegelsen til grensesnittet over tid.

Separasjons hastigheten til blandingen sank med blandetid. Både for Exxol – vann og råolje – vann. Disse resultatene ble sammenlignet med terminal hastigheten til en enslig dråpe. Resultatet tyder på at hindrings effekten av nærliggende dråper tydelig påvirker dynamikken av separasjons prosessen. Det trengs mer arbeid for å angi størrelsen av denne effekten.

Den andre hovedoppgaven oppgaven var å undersøke muligheten til å kontrollere fuktingen av glass overflaten som blir brukt i test cellen. Fuktingen av en overflate avhenger av form, ruhet og energien til overflaten. De nano-micro forbedrede overflatene ble laget på NTNU NanoLab. Et tynt lag av aluminium og Indium Tinn Oksid (ITO) ble lagt på en forskjellige glass eksemplarer ved hjelp av en «sputter» teknikk. Forskjellige overflater ble laget ved å forandre «sputter» tiden. Ruheten ble målt ved å bruke en atomkraftmikroskop. Fuktheten til overflatene ble så undersøkt ved å måle kontakt graden med både vann og olje.

De forbedrede overflatene forbedret de hydrofobe egenskapene, men det var ingen forskjell i de olje frastøtende egenskapene. Bare en overflate i denne oppgaven var hydrofob. Det var en ITO overflate som hadde blitt «sputtered» i 30 minutter. De hydrofobe egenskapene til overflaten til prøvene, var ikke bare relatert til ruheten av overflatene. Hvilket viser at det er andre egenskaper som er viktige, slik som overflate energi og muligheten for luftlommer mellom overflaten og væsken. Mer arbeid trengs for å skape en overflate for test cellen. Overflate energi av prøven bør være lav for å kunne lage en overflate som frastøter olje.

Contents

Acknowledgments i
Preface ii
Abstract iii
Sammendrag iv
List of Figures vii
List of Tables ix
List of Symbols x
1. Introduction 1
1.1. Background 1
1.2. Objective 2
1.3. Scope of Work 2
1.4. Thesis Structure 2
2. Theory 3
2.1. Coalescence 3
2.1.1. Modeling 4
2.2. Terminal Velocity 7
2.3. Wetting 8
2.3.1. Surface Energy 8
2.3.2. Contact Angle 9
2.4. Hydrophobic and Oleophobic surface 11
2.4.1. Sputtering 11
2.4.2. Atomic Force Microscope 12
3. Experimental Work 13
3.1. Experimental Setup for Oil – Water Separation 14
3.1.1. Procedure 16
3.1.2. Light 16
3.1.3. Vessel 17
3.1.4. Mixer 18
3.1.5. Camera 19
3.1.6. Droplet size measuring 20
3.2. Enhanced Surface 21
3.2.1. Procedure 22
3.2.2. Sputter 22
3.2.3. Atomic Force Microscope 23
3.3. Experimental Setup for Measuring Contact Angle 25

3.3.1. Procedure 26
3.3.2. Camera 26
3.3.3. Syringe Controller 27
3.3.4. Computer tool for measurement 27
3.4. Error Analyses 28
3.4.1. Oil and Water Separation 28
3.4.2. Enhanced Surface 28
3.4.3. Contact Angle 28
4. Oil – Water separation 29
4.1. Crude Oil and Water 29
4.1.1. Results 29
4.1.2. Discussion 36
4.2. Exxol D80 and Water 39
4.2.1. Result 39
4.2.2. Discussion 44
5. Nano Enhanced surface 45
5.1. I-Gain 45
5.1.1. Result 45
5.1.2. Discussion 50
5.2. Roughness 51
5.2.1. Result 51
5.2.2. Discussion 58
5.3. Contact Angle 60
5.3.1. Result 60
5.3.2. Discussion 67
6. Conclusion and Further Recommendation 69
6.1. Conclusion 69
6.2. Further Recommendations 70
References 71
Appendix A 73
Oil – Water separation velocity 73
Appendix B 75
Contact Angle 75
Appendix C 81
Roughness 81

List of Figures

Figure 1.1 Horizontal Three Phase Separator [2] 1
Figure 2.1Three phase separator with Droplet-Droplet coalescence, Droplet - interface Coalescence and Dense-Packed Zone 3
Figure 2.2 Surface tension and Contact Angle [9] 9
Figure 2.3 Sputter [18] 11
Figure 3.1 Picture of Lab setup Oil - Water Separation 14
Figure 3.2 Sketch of Oil-Water Separation Experiment 15
Figure 3.3 Sketch of the Crude Oil - Water separation 15
Figure 3.4 Picture of the light used for oil water separation 16
Figure 3.5 Picture of the 1.2*0.5 cm vessel used in the crude oil – water separation experiments. 17
Figure 3.6 Picture of the handheld mixer used to mix the to liquids in these experiments 18
Figure 3.7 Picture of camera used for the oil – water separation experiments 19
Figure 3.8 Picture of the holder used to visiolize the droplet sizes 20
Figure 3.9 Picture of the different samples of enhanced surfaces 21
Figure 3.10 Picture of the AFM Nanosurf 24
Figure 3.11 Figure 3.11: Picture of the setup used to measure the contact angle of the enhanced surfaces 25
Figure 3.12 Picture of the camera used to measure the contact angel of the glass 26
Figure 3.13 Picture showing the ImageJ software. The contact angle of a water droplet on the ITO surface sputtered for 10 min 27
Figure 4.1 Sketch of the separation velocity 29
Figure 4.2 Graph showing the separation velocity of SA-2 for different mixing times, with error bars, when moving 0,4 cm from approximately the same start- to endpoint. 30
Figure 4.3 Graph showing the size of a droplet with terminal velocity equal to the average separation velocity of the different mixtures in crude oil. 31
Figure 4.4 Graph showing the change in the visible height of crude oil and water mixture 32
Figure 4.5 Graph showing the change in the visible height for one experiment with mixing times from 5 to 60 seconds 33
Figure 4.6 Pictures showing the separation of crude oil – water when mixed for 45 seconds. Each picture represent 1 minute. The first picture, is right after the mixing stopped, and the last picture 17 minutes later. 35
Figure 4.7 Picture of droplets in crude oil-water mixture, mixing time was 20 seconds. 35
Figure 4.8 35
Figure 4.9 Picture of holes in the dense-packed zone 37
Figure 4.10 Graph showing the average separation velocity Exxol and water, with error bars. 39
Figure 4.11 Graph showing the droplet diameter with terminal velocity equal to the average separation velocity. 40
Figure 4.12 Graph showing the movement of the interface, for Exxol-Water mixture at different mixing times for one sample of experiments 41
Figure 4.13 Pictures showing the separation of Exxol – water mixed for 45 seconds. Each picture is 1 second. 43
Figure 5.1 Graph showing the root mean squared roughness of aluminum sample sputtered for 15 minutes, for different I-Gain values 45
Figure 5.2 Topography and amplitude of aluminum sputtered for 15 min, with I-Gain = 0 46
Figure 5.3 Topography and amplitude of aluminum sputtered for 15 min, with I-Gain = 200 46
Figure 5.4 Topography and amplitude of aluminum sputtered for 15 min, with I-Gain = 500 47

Figure 5.5 Topography and amplitude of aluminum sputtered for 15 min, with I-Gain = 1000..... 47
Figure 5.6 Topography and amplitude of aluminum sputtered for 15 min, with I-Gain = 4000..... 48
Figure 5.7 Topography and amplitude of aluminum sputtered for 15 min, with I-Gain = 8000..... 48
Figure 5.8 Topography and amplitude of aluminum sputtered for 15 min, with I-Gain = 10000..... 49
Figure 5.9 Topography and amplitude of aluminum sputtered for 15 min, with I-Gain = 20000..... 49
Figure 5.10 Graph showing the root mean squared roughness of the sputtered surfaces versus sputtered time..... 51
Figure 5.11 Bar graph showing the difference in roughness between the sputtered surface area and clean glass area from the same sample. 52
Figure 5.12 Topography and amplitude of Aluminum sputtered for 5 minutes..... 53
Figure 5.13 Topography and amplitude of Aluminum sputtered for 10 minutes..... 53
Figure 5.14 Topography and amplitude of Aluminum sputtered for 15 minutes..... 54
Figure 5.15Topography and amplitude of Aluminum sputtered for 20 minutes..... 54
Figure 5.16 Topography and amplitude of Aluminum sputtered for 30 minutes..... 55
Figure 5.17 Topography and amplitude of Aluminum sputtered for 45 minutes..... 55
Figure 5.18 Topography and amplitude of ITO sputtered for 10 minutes..... 56
Figure 5.19 Topography and amplitude of ITO sputtered for 20 minutes..... 56
Figure 5.20 Topography and amplitude of ITOsputtered for 30 minutes..... 57
Figure 5.21 Picture of ITO 30, showing a common problem with the measurement with the AFM.... 59
Figure 6.2 Graph of the average contact angles with water at different surfaces 60
Figure 6.3 Bar graph showing the difference between the average contact angle of water droplets on a sputtered area and a glass area on the same sample. 61
Figure 6.4 Aluminum sputtered 5 min: Contact angle: 71° 62
Figure 6.5 Aluminum sputtered 10min: Contact angle: 62° 62
Figure 6.6 Aluminum sputtered 15 min: Contact angle 60° 63
Figure 6.7 Aluminum sputtered 20 min: Contact angle: 59° 63
Figure 6.8 Aluminum sputtered 30 min: Contact angle: 74° 64
Figure 6.9 Aluminum sputtered 45 min: Contact angle: 82° 64
Figure 6.10 ITO sputtered 10 min: Contact angle: 80° 65
Figure 6.11 ITO sputtered 20 min: Contact angle 42° 65
Figure 6.12 ITO sputtered 30 min: Contact angle: 90° 66
Figure 6.13 Picture of crude oil on the ITO 30 surface..... 68

List of Tables

Table 3Table of the average contact angles with water at different surfaces, with the error given as the standard deviation. 60

List of Symbols

Symbol	Description	Unit
d	Diameter	[m]
g	Gravitation acceleration	$[\frac{m}{s^2}]$
V	Velocity	$[\frac{m}{s}]$
Re	Reynolds Number	[-]
K	Proportionality factor	[-]
R	Radius	[m]
F	Force	[N]
h	Film height	[m]
t	Time	[s]
C_w	Friction Coefficient	[-]
Ar	Archimedes number	[-]
K_{HR}	Hadamard-Rybczynski factor	[-]
La	Laplace number	[-]
H	Hamaker Coefficient	[N * m]
w	Work	[J]
r	Roughness factor	[-]
f	Fraction of wetted area	[-]
S	Roughness	[nm]

Greek symbols	Description	Unit
ρ	Density	$[\frac{kg}{m^3}]$
μ	Dynamic Viscosity	[Pa*s]
γ	Surface tension	$[\frac{N}{m}]$
ε	Volume Fraction	[-]

ϕ	Sauder Diameter	[m]
Δ	Difference	[-]
τ	Coalescence time	[s]
θ	Contact angle	[°]

Subscript	**Description**
0	Initial
c	Continuous Phase
∞	Infinite extended
s	Sedimentation
d	Dispersed phase
b	Between two drops
P	Dense-packed Zone
i	At the interface
a	Out of contact area
f	At contact area
v	Asymmetrical
py	Variable dense-packed zone
t	Terminal
critical	Critical
spher	Spherical particle
ideal	Ideal smooth surface
SG	Solid - Gas
SL	Solid - Liquid
LG	Liquid – Gas
CB	Cassie-Baxter
q	Root mean squared

1. Introduction

1.1. Background

Separators are an important part of the oil processing. The fluids extracted from a well, is a mixture of oil, gas and water. There are a lot of water in an oil well, especially a matured well. In fact, because the most used methods of retrieving oil involve injection water into the well, matured wells can have a water amount up to 80 – 90 % [1].To separate this water from the oil, large separators are used. To increase the efficiency of these separators, and reduce the size, it is important to quantify how long it takes the disperse phase to separate.

The gravitational separator is the most common separator. It rely on the difference in density to separate the different phases.

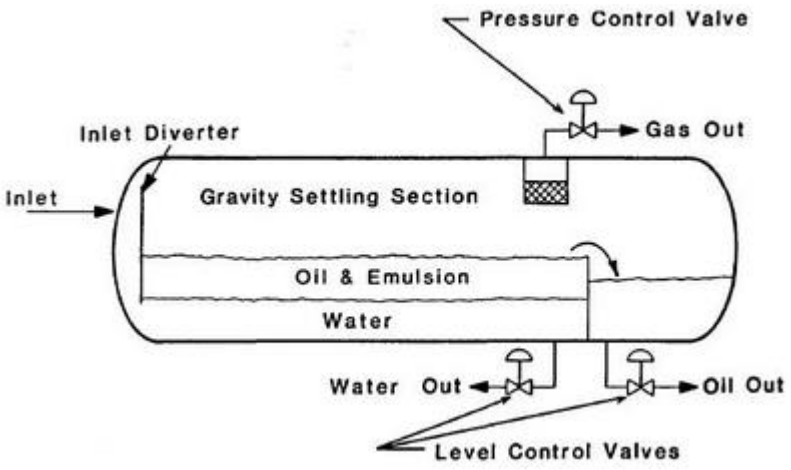

Figure 1.1 Horizontal Three Phase Separator [2]

To increase the efficiency of gravitational separators it is important to understand the underlying physics of the separation process. To get this knowledge the physical properties and hydrodynamic properties of the droplets in the mixture are important. Both the settling velocity of a droplet and the coalescence time between two droplets, and the droplets and its interface are important. It depends on the properties of the oil as well as the size of the droplets. Since many of the effects in the settling process is non-quantifiable, experimental work is important to reliable predict the separation process. [3]

When conducting a crude oil-water separation experiment, there is problem with the visibility. The oil interaction with the test cell makes the separation process hard to track. This is due to the high wettability between oil and glass. To improve the quality of the experiments, the structure of the glass surface needs to change. In studies of wettability, there has been a lot of focus on hydrophobic surfaces, and superhydrophobic surfaces. These surfaces are usually also highly oleophilic. This could

be of use in oil-water separation [4], however, they are not useful for experiments where the vision of the droplets are important.

1.2. Objective

The main objective in this thesis is to investigate two-phase batch separation of crude oil and water with a near infrared high speed camera. Furthermore, the possibility of controlling the wettability of the glass surface of the test cell using nano-enhanced surfaces, was evaluated.

1.3. Scope of Work

In this thesis, the oil-water separation will be investigated in a small vessel in order to get visual access with near infrared camera. A sample of crude oil and produced water, and Exxol D80 and distilled water will be used during the experiments. All the experiments are preformed at ambient condition.

The experiments related to improving the wettability of the glass surface were limited to the use of aluminum and Indium Tin Oxide (ITO).

1.4. Thesis Structure

The thesis is divided 6 into chapters. Chapter 2 is a literature review, focusing on the coalescence, terminal velocity, wettability and basic theory of some of the equipment. In chapter 3, there is a description of the setup of the experiments and the methodology, as well as an error analysis. Chapter four is the results and discussion of the oil – water separation part of the thesis. Chapter 5 is the results and discussion for the nano-enhanced surface. Finally, chapter 6 is the conclusion followed by a recommendation to further studies.

2. Theory

When two immiscible liquids are mixed, droplets form. The droplets with the highest density will fall due to gravity. The velocity of the droplets will increase until reaching its peak, the terminal velocity. The droplets fall until it reaches its interface, or another droplet. Once the droplet comes in contact with an other droplet or its interface, they will interact until the interfacial film rupture and the droplet coalescence. The time this takes is called the coalescence time. For a mixture, several of droplets will form on the interface, if the velocity of the coalescence of these droplets are slower the velocity of the falling droplets, they will accumulate and form a layer of droplets, called the dense-packed zone.

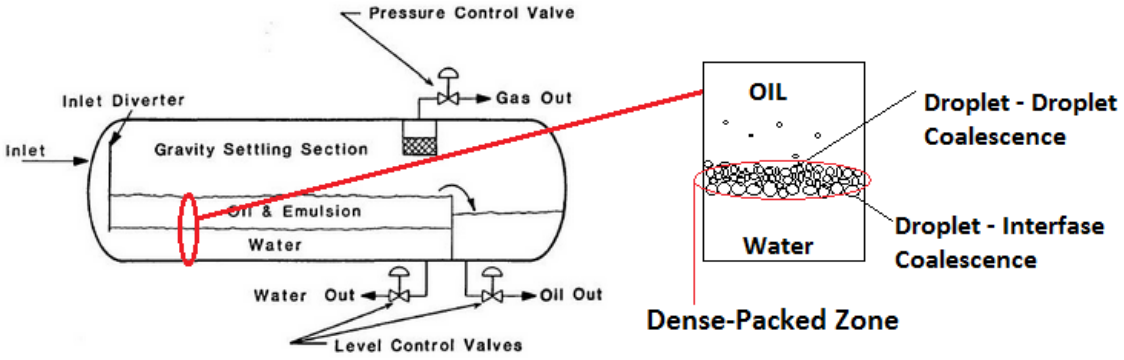

Figure 2.1Three phase separator with Droplet-Droplet coalescence, Droplet - interface Coalescence and Dense-Packed Zone

2.1. Coalescence

When a droplet come in contact with its interface or another droplet, they will interact, and after a given time, the two will emerge. According to Tom Frising et. al[5], who in 2006 wrote a review of the current coalescence literature, most agree that the coalescence mechanics have three stages, the approach and collision of the droplets, or the droplets and the interface. The drainage of the interface between the two. Lastly, there is a destabilization of the film, by the Van der Wall and other intermolecular forces. This leads to the rupture of the film. Of these stages, it is the drainage of the interface that is the time determining factor [3].

The interface can act in three different ways. Immobile, partially mobile and mobile. The interface can be assumed immobile if the viscosity of the droplet is very high or if the fluid in the continuous phase has sufficient numbers of surfactants, which is the case in crude oil systems [5].

The approaching velocity for an immobile interface can be written as:

$$-\frac{dh}{dt} = \frac{2h^3F}{3\pi\mu_c R_f^4} \qquad (2.1)$$

$$F \cong \pi R_f^2 \left(\frac{2\gamma}{R}\right) \qquad (2.2)$$

$$-\frac{dh}{dt} \cong \frac{8\pi\gamma^2 h^3}{3\mu_c R^2 F} \qquad (2.3)$$

γ is the interfacial tension, and R is the droplet radius, h is the film thickness, μ_c is the viscosity in the continuous phase and F is the approach force.

If F is constant:

$$\frac{1}{h^2} - \frac{1}{h_0^2} \cong \frac{16\pi\gamma^2}{3\mu_c R^2 F} t \qquad (2.4)$$

Where h_0 is the initial film thickness and t is the drainage time.

2.1.1. Modeling

There are two main ways of modeling the coalescence problem in a liquid-liquid separator. Models that concentrate on the sedimentation of the droplet, and the coalescence with the interface. These models are called Sedimentation-based models. The other model concentrate on the coalescence between two droplets, and are called Coalescence-based model. For experiments with small droplets, <1mm, a coalescence based model is usually used. [5]

M. Henscke et. al [6], created a coalescence-based model for characterizing the coalescence problem, using one coalescence parameter. However, this model does not consider surfactants.

In Henschkes model there is almost no droplet-droplet coalescence in the sedimentation zone. This only happens in the dense-paked zone. To estimate the droplets size, the sedimentation velocity, v_s, for the drop swarm is important. The v_s follows a linear slope and can be found from the experimental sedimentation curve. Then, to model the sedimentation of the drop swarms, Henschke et. al used [6, 5]:

$$Re_s = \frac{3q\varepsilon_0}{C_w \xi (1-\varepsilon_0)} \left[\left(1 + Ar \frac{C_w \xi (1-\varepsilon_0)^3}{54 q^2 \varepsilon_0^2} \right)^{0,5} - 1 \right] \qquad (2.5)$$

where;

$$Re_s = \frac{\rho_c v_s \phi_0}{\mu_c} \qquad (2.6)$$

$$Ar = \frac{\rho_{co} \Delta\rho g \phi_0^3}{\mu_c^2} \qquad (2.7)$$

$$\xi = 5 K_{HR}^{-3/2} \left(\frac{\varepsilon_0}{1-\varepsilon_0} \right)^{0,45} \qquad (2.8)$$

$$K_{HR} = \frac{3(\mu_c + \mu_d)}{2\mu_c + 3\mu_d} \qquad (2.9)$$

$$q = \frac{1-\varepsilon_0}{2\varepsilon_0 K_{HR}} \exp\left(\frac{2,5\varepsilon_0}{1-0,61\varepsilon_0} \right) \qquad (2.10)$$

$$C_w = \frac{Ar}{6Re_\infty^2} - \frac{3}{K_{HR} Re_\infty} \qquad (2.11)$$

Where Re_s is the Reynolds number for the sedimentation, Ar is the Archimedes number and for this model to be valid the $Ar > 1$, ε_0 is the initial value of the volume fraction of the dispersed phase and has to be; $0,06 < \varepsilon_0 < 0,55$ in this model, ρ_c is the density in the continuous phase, ϕ_0 is the initial Sauter diameter, which is the average initial droplet diameter. ξ and q are defined by their equations and K_{HR} is the Hadamard-Rybczynski factor.

For finding the Re_∞, which is the Reynolds number in an infinite expanding fluid, Henschke et al. uses:

$$Re_\infty = \frac{\rho_c v_{s,\infty} \phi_0}{\mu_c} = 9{,}72[(1 + 0{,}01Ar)^{\frac{4}{7}} - 1] \qquad (2.12)$$

Furthermore, for calculating the height of the dense-packed zone Henschkes et. al uses the coalescence velocity given by:

$$\frac{dh_d}{dt} = \frac{2\varepsilon_i \phi_i}{3\tau_i} \qquad (2.13)$$

Where τ_i is the droplet – interface coalescence time, and ϕ_i is the average diameter of the droplets at it interface. ε_i should be close to 1.

By taking the droplet – droplet coalescence time, τ_b, into account, the drop growth in the dense-packed zone can be calculated from

$$\frac{d\phi(h,t)}{dt} = \frac{\phi(h,t)}{6\tau_b} \qquad (2.14)$$

Then by looking at the dense-packed zone over time, 0 < t < t', the height is given by

$$h_p = \frac{(h_0 - v_s t)\varepsilon_0 - (1-\varepsilon_0)h_d}{\varepsilon_{P,0} - \varepsilon_0} \qquad (2.15)$$

$$\varepsilon_{P,0} = \frac{1}{2}(\varepsilon_i + \varepsilon_0) \qquad (2.16)$$

where $\varepsilon_{P,0}$ is representing the average volume fraction in the dense-packed zone.

When there is no free sedimentation, the equation becomes:

$$h_p = \frac{h_0\varepsilon_0 - h_d}{\varepsilon_P} \qquad (2.17)$$

where

$$\varepsilon_P = \varepsilon_i - \exp(-C_1 t - C_2) \qquad (2.18)$$

$$C_1 = \left.\frac{\left(v_s - \frac{dh_d}{dt}\right)\varepsilon_{P,0}^2 + \frac{dh_d}{dt}\varepsilon_{P,0}}{(h_d - h_0\varepsilon_0)(\varepsilon_i - \varepsilon_{P,0})}\right|_{t=t'} \qquad (2.19)$$

$$C_2 = -C_1 t' - \ln(\varepsilon_i - \varepsilon_{P,0}) \qquad (2.20)$$

In the dense-packed zone the droplets touch each other and the dispersed phase fraction is then close to unity, $\varepsilon_i = 1$

For the coalescence time Henscke arrive at:

$$\tau = -\frac{(6\pi)^{7/6}\mu_c r_a^{7/3}}{4\sigma^{5/6} r_{f,t} r_v^* H^{1/6}} \qquad (2.21)$$

$r_{f,t}$ and r_a is from the deformation of the droplets where:

$$r_{f,t} = 0{,}030\phi\sqrt{1 - \frac{4{,}7}{4{,}7+La}} \qquad (2.22)$$

$$r_a = 0{,}5\sqrt{1 - \frac{4{,}7}{4{,}7+La}} \qquad (2.23)$$

$$La = (\frac{\Delta\rho g}{\sigma})^{0{,}6} h_{py}^{0{,}2}\phi \qquad (2.24)$$

La is a modified Laplace number. It is representing the ratio between the hydrostatic pressure and the interfacial tension.

$h_{py}$is the drop-packed height.

The H, which is the Hamaker coefficient, is an unknown. It can be found experimentally, however, Henschke et. al, uses a fixed value of $1 * 10^{-20}\ [N\ m]$ for all systems. Stating that since it has the exponent$\frac{1}{6}$, it does not affect the coalescence time much.

The r_v^* is an asymmetry parameter, it is then the only variable in the equation. It is calculated using a settling curve. It is not affected by a change in the geometry of the experiment.

2.2. Terminal Velocity

The terminal velocity is the velocity when the gravity and the sum of drags and buoyancy forces is in equilibrium. When a drop enters a fluid with lower density, the gravitation force will accelerate the drop until those forces are equal.

For low Reynolds numbers stokes' law is used to calculate the terminal velocity[7]:

$$V_t = \frac{gd^2(\rho_{spher} - \rho)}{18\mu} \qquad (2.25)$$

Where: V_t is the terminal velocity of the droplet, ρ_{spher} is the density, d is the diameter, μ is the dynamic viscosity of the fluid, g is the gravitational force and ρ is the density of the fluid.

2.3. Wetting

Wetting is a balance between adhesive forces and cohesive forces. The adhesive forces works between the solid surface and the liquid droplet, and the cohesive forces works within the liquid. If the adhesive forces are the dominate force, the wettability will be high. With higher cohesive forces the wettability will be low. With low wettability, the liquid will form as a droplet on top of the solid surface.

2.3.1. Surface Energy

The surface energy, γ, is given by the work required to create a new surface, divided by the area of the new surface[8]:

$$\gamma = \frac{\delta w}{\delta A} \qquad (2.26)$$

For fluids the surface energy is referred to as surface tension. By assuming the area is extending $\delta A = l\delta x$. The work is then given by $\delta w = \gamma l \delta x$, and if the extension is driven by a force, F_{ext}, then $\delta w = F_{ext}\delta x$ and the surface tension equation become:

$$\gamma = \frac{F_{ext}}{l} \qquad (2.27)$$

The surface tension can also be given by the force working on both sides of a fluid in interaction with a solid. Where[24]:

$$\gamma = \frac{F_s}{2l} \qquad (2.28)$$

where l is the length of the solid.

2.3.2. Contact Angle

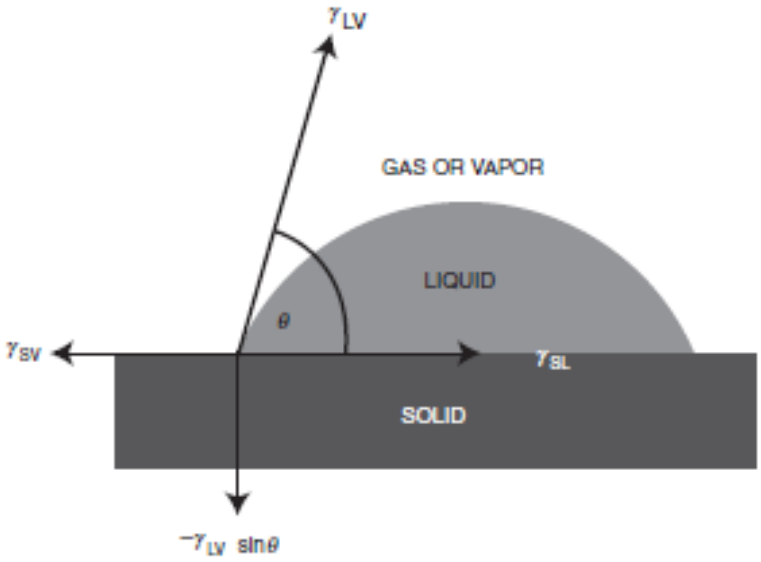

Figure 2.2 Surface tension and Contact Angle [9]

The contact angle is where the interface of the solid, liquid and gas meets. Depending on the adhesive and cohesive forces, the contact angle could be from 0 – 180°. Where as 0°means full wettability and 180° would be perfect non-wettability.

For ideal smooth solid surfaces the contact angle can be given by the three surface tensions that are working on the interfaces: solid-liquid, liquid-gas and solid-gas.

The contact angle of an ideal smooth surface is given by the Young-Dupré equation[10]:

$$cos\theta_{ideal} = (\frac{\gamma_{SG}-\gamma_{SL}}{\gamma_{LG}}) \qquad (2.29)$$

Which is the force balance between the three different phases. By increasing or decreasing the cohesive or adhesive forces, the balance will shift. This will change the contact angle of the droplet.

For surfaces that are not smooth, the roughness has to be included. By adding a roughness factor r.

Wenzel equation[11]:

$$cos\theta = r\left(\frac{\gamma_{SG}-\gamma_{SL}}{\gamma_{LG}}\right) = rcos\theta_0 \qquad (2.30)$$

Where: $$r = \frac{actual\ surface}{geometric\ surface} \qquad (2.31)$$

The geometrical surface is measured in the plane of the interface, and the actual surface includes the roughness. Which means that for solid surfaces the actual surface will be larger than the geometric surface. For smooth surfaces the r=1, which means that this is a more general equation, working for both ideal smooth and rough surfaces.

However, this equation assume a homogeneous surface, with no gas pockets. For measuring the contact angle of heterogeneous surfaces, where there can be gas pockets, Cassie-Baxter equation could be used [12, 13]:

$$cos\theta_{CB} = r_f f cos\theta_{ideal} + f - 1 \qquad (2.32)$$

Where f is the fraction of the area of the solid that is wetted. And r_f is the roughness ratio of the wet area. With f=1 and $r_{frac} = r$ this equation becomes the Wenzel equation

2.4. Hydrophobic and Oleophobic surface

A surface is considered hydrophobic or oleophobic if the contact angle between the solid surface and the liquid is larger than 90°. To achieve a super hydrophobic surface the contact angle has be larger than 150. [14]

Both the chemical composition and the geometrical structure of the surface is important when creating a hydrophobic or oleophobic surface [4]. The surface energy of the surface has to be low and the roughness high. Although, for creating transparent surface, a high roughness will increase the light scattering.[15] To create an oleophobic surface the surface energy has to be very low. To decrease the surface energy the surfaces could be modified with flourchemicals and flouropolymers. [4]

The roughness can be increased in many different ways. However, the methods used can be summarized into two main categories. The top-down approach, and the bottom up approach. As the names indicates the top-down methods increase the roughness by modifying the surface with tools that carve, mold or machining bulk materials. In the bottom up method, on the other hand, small components are used to design complex objects on the surface. [16

2.4.1. Sputtering

By bombarding a solid surface with energetic particles, surface atoms are removed. This is called sputtering. [17] The atoms from this surface, called the target, is deposit on another solid surface, called the substrate. The atoms forms a thin film on the substrate.

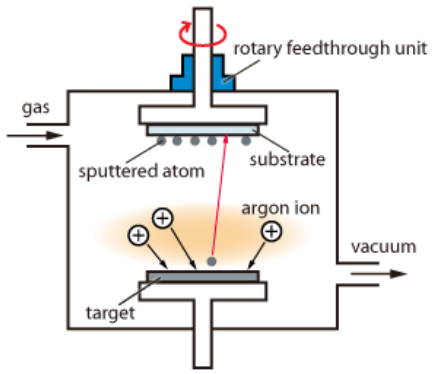

Figure 2.3 Sputter [18]

In this thesis, aluminum and ITO was used as targets, and a glass slide as the substrate. Argon atoms was used as high energetic particles. The thickness of the film depend on the amount of time the sputter is used, and the power used in the sputtering.

2.4.2. Atomic Force Microscope

An AFM uses a probe that is attached to a cantilever to measure the topography of a surface. The probe is lowered down close to the surface, and uses the interaction of forces between the tip and the surface. This force is held constant but the deflection of the flexible cantilever is monitored, and is used to plot the topography [20].

There are different modes to create a picture. In the AFM Nanosurf, both a static mode and a dynamic mode could be used.

In the static mode the probe was held constant close to the surface and followed the surface topography.

The dynamic mode the probe is tapping the surface of the sample. The cantilever is oscillating up and down, and uses the in the amplitude of this oscillation, as it gets close to the surface to measure the surface.

The roughness used in this thesis is the root mean square roughness , S_q, over the whole area measured. It is given by the equation[21]:

$$S_q = \sqrt{\frac{1}{MN}\sum_0^{M-1}\sum_0^{N-1}(z(x_M, y_N))^2} \qquad (2.33)$$

where z is the change in height in x,y plan.

The setpoint is the working point for the Z-controller. In the dynamic mode, which is used in this thesis, it is the relative cantilever vibration amplitude. This means that the setpoint is realtaive to the operative amplitude, and by increasing the setpoint the tip is moved closer to the surface. It is given as a percentage of the operating amplitude, and will move closer to the surface until the vibrating amplitude is decreased to the setpoint.

The error signal can be controlled by three different parameters; The P-Gain, I-Gain and the D-Gain. These control the strength of the z-controllers reaction. P-gain is proportional to the error signal, the I-Gain is proportional to the integral of the error signal and the D-Gain is proportional to the derivative of the error signal. The I-Gain is the main contributor to the topography. Increasing the I-Gain decreases the error signal over time.

3. Experimental Work

The work in this thesis was divided into two main activities. The first one was focused on the investigation of the batch separation process of oil and water. The second was related to the evaluation of the use of nano-enhanced surfaces for controlling the wettability of the glass surface. The latter experiment is critical to improve the experiments related to the visualization of the oil-water separation.

There were three different experiments preformed in this thesis;

1. Oil-water separation: The oil-water separation was done by mixing crude oil and water, and Exxol D80 and water. The separation time was measured by using a near infrared camera.
2. Surface enhancement: The surface enhancement part was conducted in a clean-room, by using a sputtering technic, and measured by an atomic force microscope.
3. Measurement of the contact angle: The contact angles on the surfaces was measured by planting a single droplet on the surface, then take a picture of the droplet and measure the angle by using a computer software.

3.1. Experimental Setup for Oil – Water Separation

The setup used in the experimental study of water and oil separation in this thesis consist of the following components:

- Goldeye P-008 SWR Cool camera
- ThorsLabs SLS201/M near infrared light
- LB1761 lens focal length: 25.4mm
- BIospec mixer
- vessel containing oil and water

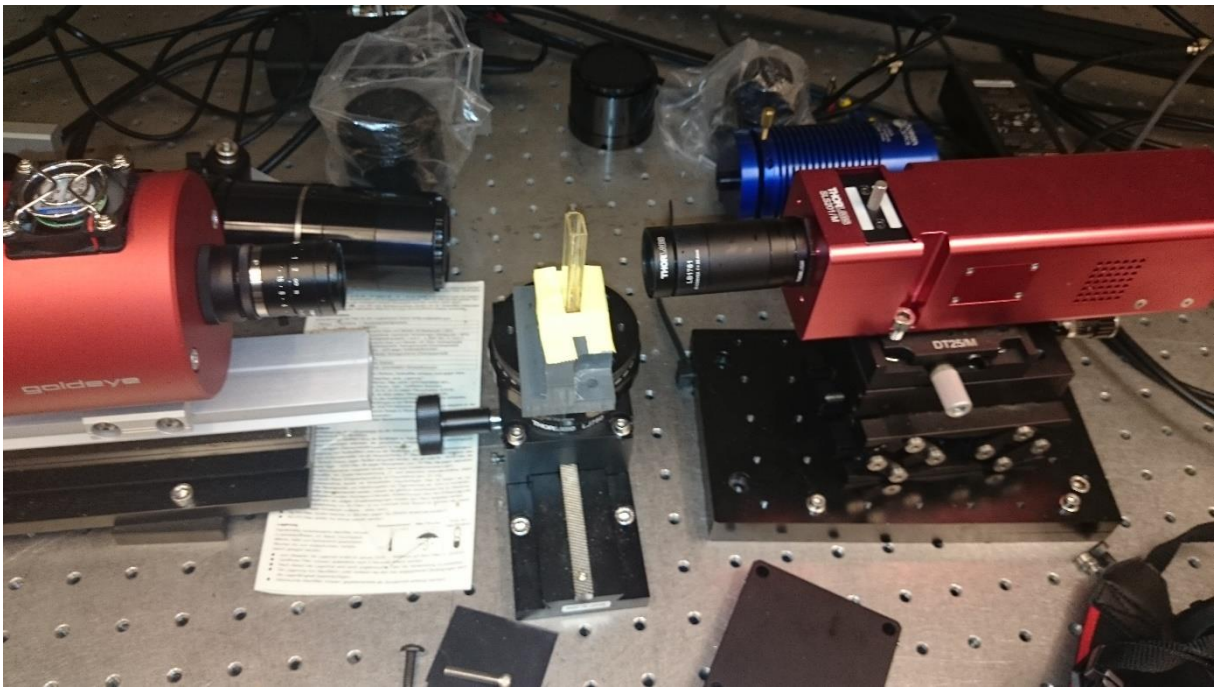

Figure 3.1 Picture of Lab setup Oil - Water Separation

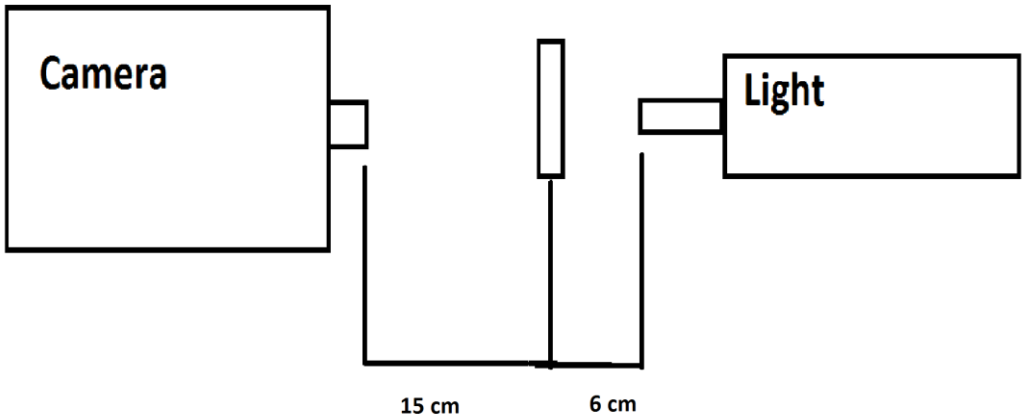

Figure 3.2 Sketch of Oil-Water Separation Experiment

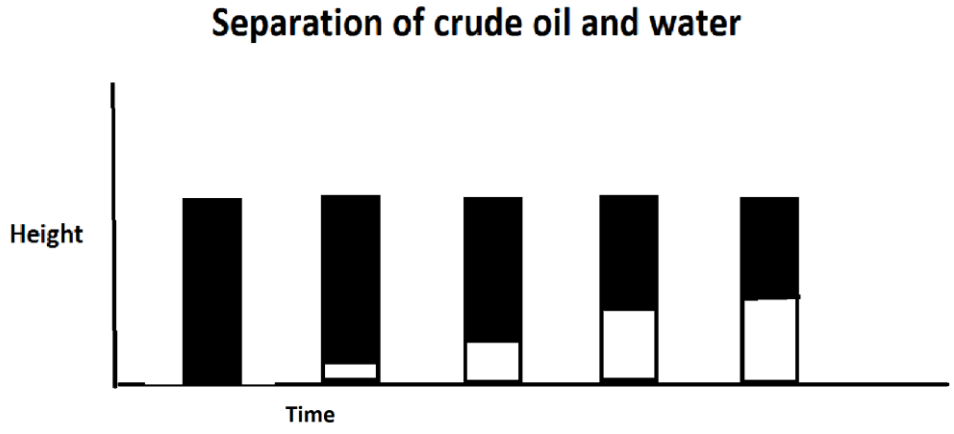

Figure 3.3 Sketch of the Crude Oil - Water separation

3.1.1. Procedure

For measuring the oil – water separation, first the vessel was filled with water and oil. Depending on the size of the vessel different amount of liquid was used. However, it was always the same amount of oil and water in the vessel. The vessel is then placed on a small lift between the camera and the light. The height of the vessel was changed so that the interface was placed in the middle of the picture. The framerate of the camera was chosen based on the oil in the experiment. For crude oil, a framerate of 0.1 frames per second (fps) was used, and for the Exxol D80, 1 fps was used.

To perform the mixing, first the stopwatch was started. Then, by using a handheld mixer, the liquids was mixed for the amount of time that was desired.

3.1.2. Light

The light used in these experiments was mounted, but it could be moved in every direction. The lens used had a focal length of 25.4mm. The light could, however, not pierce through the crude oil in the vessel. Therefore, it was not possible to see the droplet formation in area with large amount of crude oil. Additionally, the light was too bright for clear water, and the Exxol D80 – water mixture. So to reduce the intensity of the light, different technics was tried. Both different kinds of paper in front of the light, and diffusers. However, the best results were achieved with a band pass filter and a diffuser in front of the light. The band pass filter used had a center wave value(CWI) of 1000 nm and full with half maximum (FWI) of 10 nm.

Figure 3.4 Picture of the light used for oil water separation

3.1.3. Vessel

In these experiments, two different vessels was used. A small 1.2 × 0.5 cm vessel and a larger 2.8 × 0.7 cm vessel. Both were glass vessels. Due to the size difference there were different amounts of liquids in the vessels. For the small vessel 0.8 ml of oil and water was used, while the larger had 30 ml of both oil and water. The larger vessel was made after the smaller, which was first used, broke. There were some problems with leakage from the large vessel. However, it was improved, to minimize this problem.

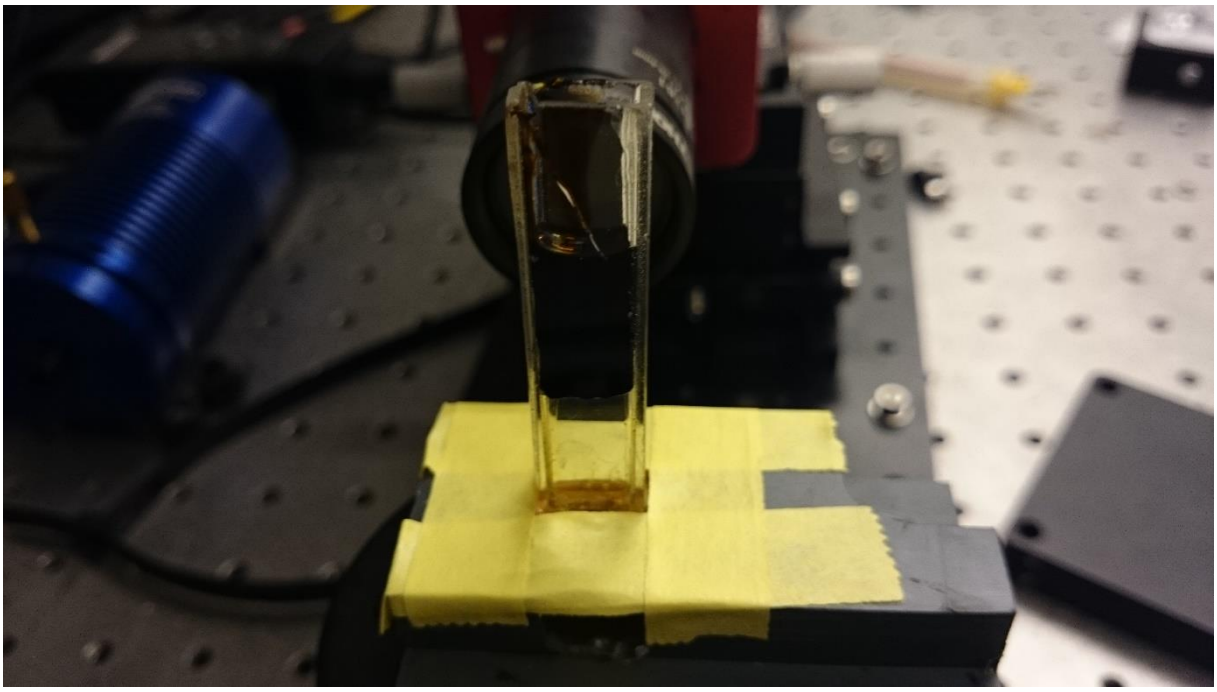

*Figure 3.5 Picture of the 1.2*0.5 cm vessel used in the crude oil – water separation experiments.*

3.1.4. Mixer

With the handheld mixer there was some problems with holding it straight and not move it to much. The reason this is important is that any difference in movement, could ether improve or worsen the mixing. Both way, there would be differences from experiment to experiment, and it would be hard to reenact.

At earlier stages there were also experiments were the oil and water was mixed in an other vessel. However, with this procedure there were losses, of both oil and water, which makes it hard to predict the fraction of the liquids in the mixture. For the experiments with Exxol D80 and water, the separation usually happened before the mixture was moved from the mixing vessel to the vessel used in the measurements. Therefore, it was not possible to measure the rate of the separation.

There are only data from mixing inside the measurement vessel in this thesis.

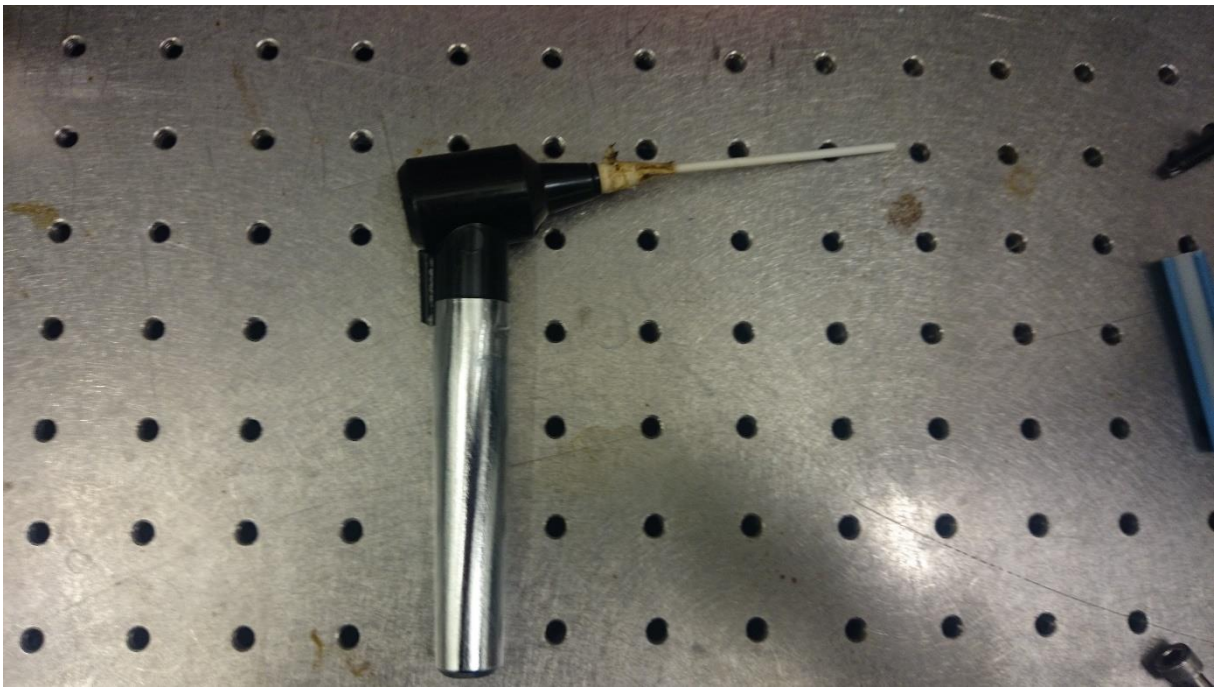

Figure 3.6 Picture of the handheld mixer used to mix the to liquids in these experiments

3.1.5. Camera

The camera used was a Goldeye P-008 SWR Cool camera. The camera could only be moved in horizontal direction, and by doing so, it changed the focus of the camera. This meant that with every change of the distance between the camera and the vessel, the pixel size of the vessel had to be measured.

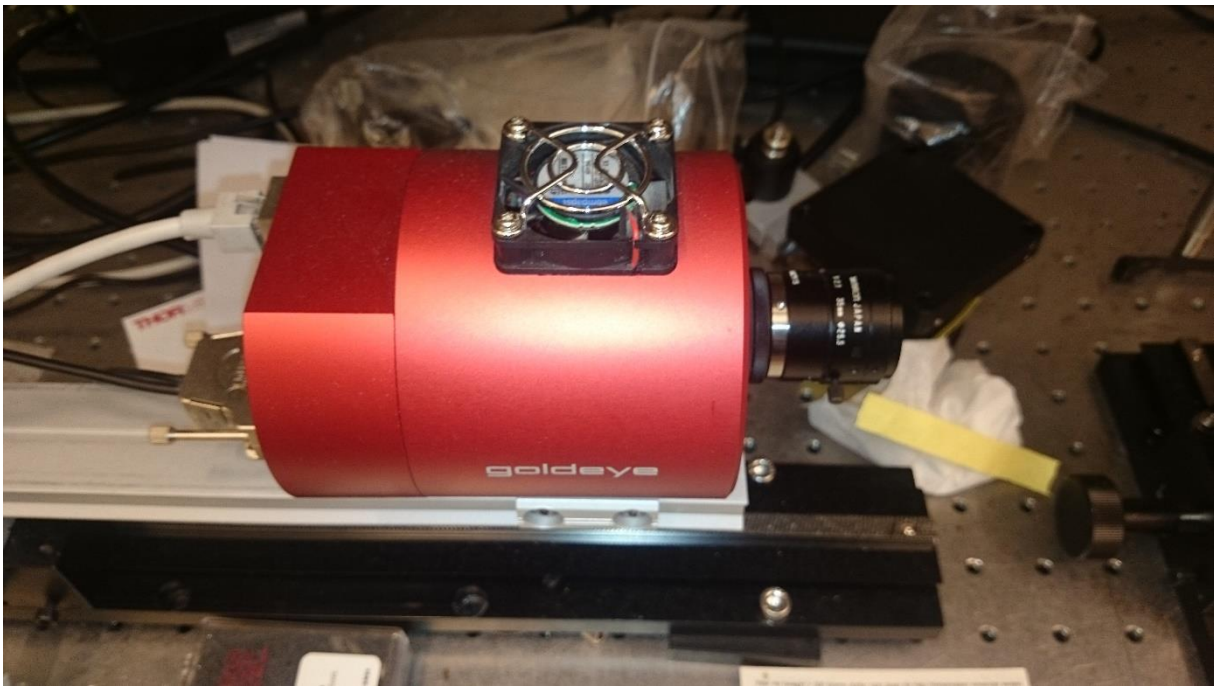

Figure 3.7 Picture of camera used for the oil – water separation experiments

3.1.6. Droplet size measuring

A Droplet of the mixture was placed on a glass slide in front of the camera. The class slide was mounted on a holder with a needle to compare the size. The diameter of the needle was 0.78 mm. This method did, however, have some problems. In some cases the mixture was too dark, even though there was only used a small amount of the mixture. Often the mixture would touch the needle, and follow the needle. Both made it hard to accurately measure the droplet size.

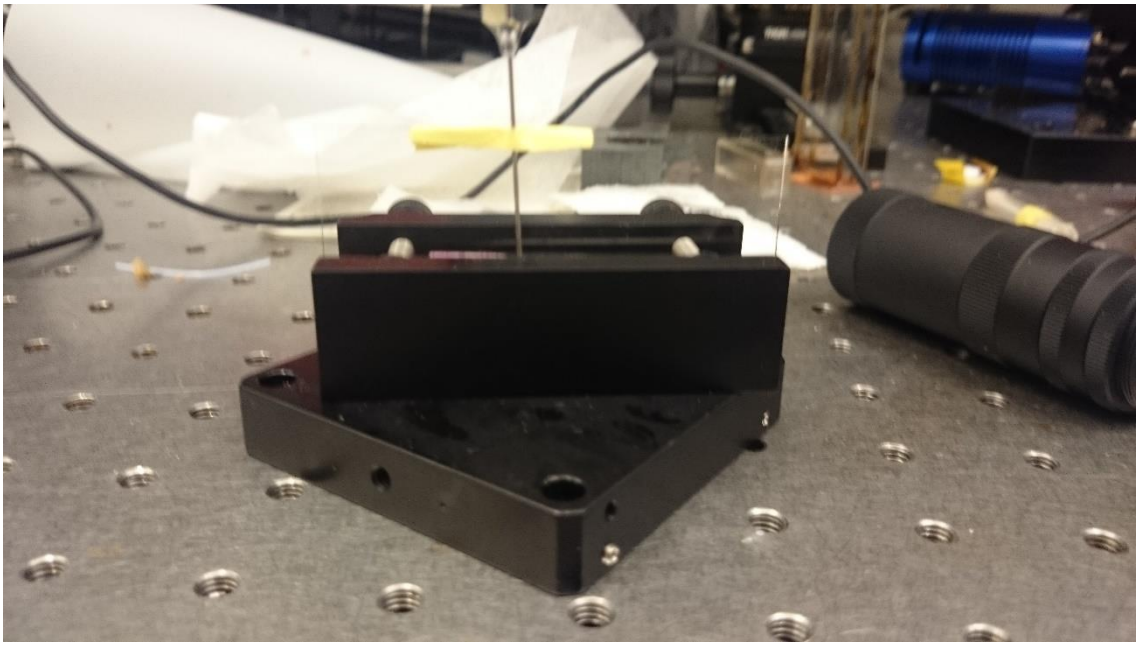

Figure 3.8 Picture of the holder used to visiolize the droplet sizes

3.2. Enhanced Surface

For creating an enhanced surface for controlling the wettability the following equipment was used:

- AJA sputter and evaporator
- AFM Nanosurf

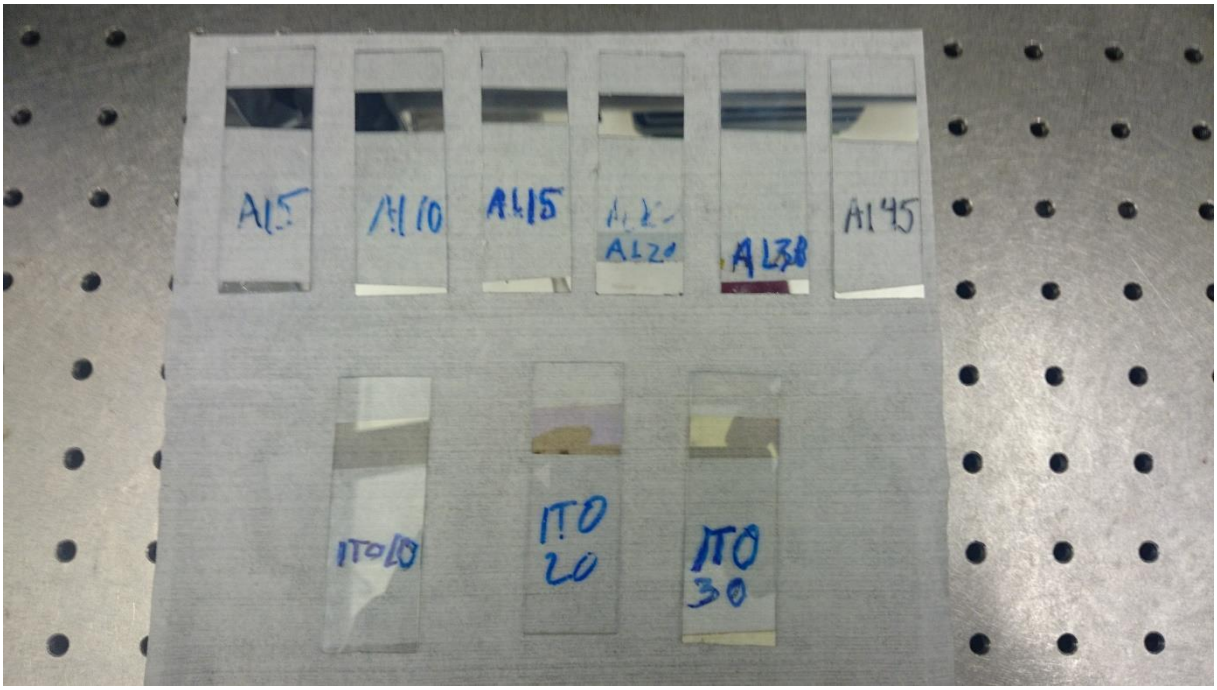

Figure 3.9 Picture of the different samples of enhanced surfaces

3.2.1. Procedure

The surface samples was created and investigated in a clean room. A glass slide was washed with Aceton, Ethanol, Iso-Propanol, water and then air-dried. This was to make sure the glass was totally cleaned before the sputtering. Then the sample was covered by heat resisting tape, so that only a part of the sample would be covered by the target in the sputter. In this way the difference between the roughness of the glass by itself and the new surface could be measured, as well as the difference in the contact angle.

3.2.2. Sputter

AJA sputter and evaporator was used to deposit the different targets on glass samples. The glass slide was placed on top of a silicon wafer and mounted to a disk, and placed in a small chamber. The main chamber is held at vacuum, and a smaller “waiting chamber” is used when the sample is inserted. The sample is inserted to the main chamber once there is vacuum in the smaller chamber. Before the sputter deposition of the target, the glass is sputtered by Bias at 20 W for 2 minutes. This is to, further, clean the glass. When this is over, the sputter deposition can start. Depending on what substance you want on the glass, different parameter should be chosen.

For Aluminum, only argon should be used in the sputtering. Oxygen in the chamber will create an aluminum oxide. The power to preserve the plasma in the sputter could be from 200 W to 400 W. In this thesis 300 W was the power used. This was chosen because it was desired that the power was at a high uniform level, and with 400 W, the actual measured power was at 337 W. With 300 W the measured value was also at 300, and it was stable throughout different depositions. The deposition lasted from 5 to 45 minutes.

To deposit ITO on a substrate, heating enhance the deposition. To achieve best results, the chamber was heated to 150 C. When heating an object in the chamber, the object has to be rotating to get a uniform heating. For ITO there was used a mixture of both oxygen and argon, with 97,5 % argon and 2,5 % oxygen. The power was set to 150 W, which is the maximum power for ITO deposition, and the deposition lasted from 10 to 30 minutes.

3.2.3. Atomic Force Microscope

To measure the roughness of the sample, the AFM is places an active motion controller then wired up to a computer to get a picture of the needle, and the measurements. To control the distance from the AFM to the sample, there are three screws used to lower it down. This is done on eyesight. There can of course be some problems in making this level, however, the control program can fix small mistakes in the alignment, by adjusting the slope.

In these experiments, an Acl-a tip with dynamic force was used. To set the different parameters of the program, an Auto set button, helps. To set the Free Amplitude Vibration the height difference of the sample have to be assumed. After some trial and error, it was assumed that the height difference was between 3.1 – 6.2 nm. This was chosen because it created the least amount of noise and slopes in the topography. When assuming a larger difference, the picture created was high on both sides, with a valley in the center. This happened, no matter were on the surface the AFM scanned. By assuming the height difference of the sample to be around 3.1 – 6.2 nm, the Auto set chooses the Free amplitude vibration to be at 59.97 mV.

Different setpoints were also tested. However, there were no clear difference, except when increased a lot, up to 76 %. Around this point the topography changed dramatically, however, the center topography went from a “valley” to a “hill”, and seemingly less correct. Therefore, 55%, was used, which was the recommended from the software.

The other parameter that was of interest was the I-Gain. The I-Gain is the integral of the error signal and the dominant contributor to the topography measurement. [21] To see how the I-Gain affected the measurement, several experiments on an aluminum surface that had been sputtered for 15 minutes was done. An I-Gain of 4000 was chosen because it created a clear topography without too much noise.

The AFM was set to scan 256 points per line, the time it was set to use on each line was 2 seconds. With these settings a good picture of the surface was created.

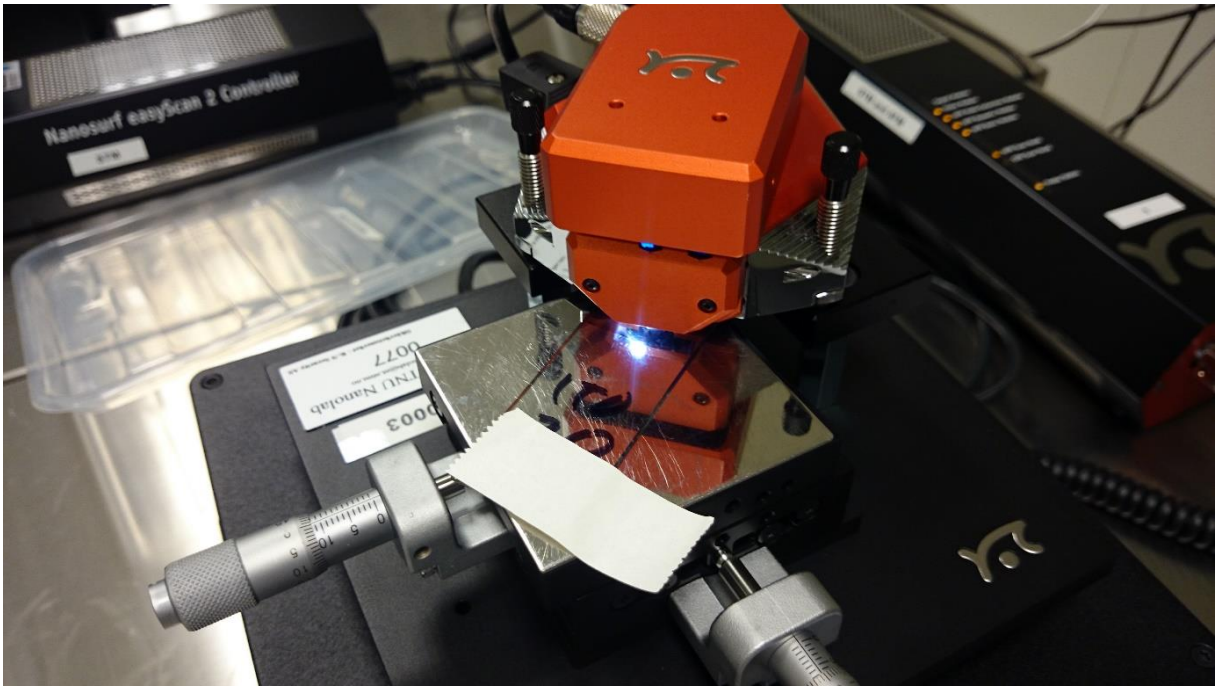

Figure 3.10 Picture of the AFM Nanosurf

3.3. Experimental Setup for Measuring Contact Angle

For measuring the contact angle of the liquids these components was used:

- ThorLabs DCC1545M camera
- Chemyx NanoJet syringe control
- BD Plastipak 3.0ml needle

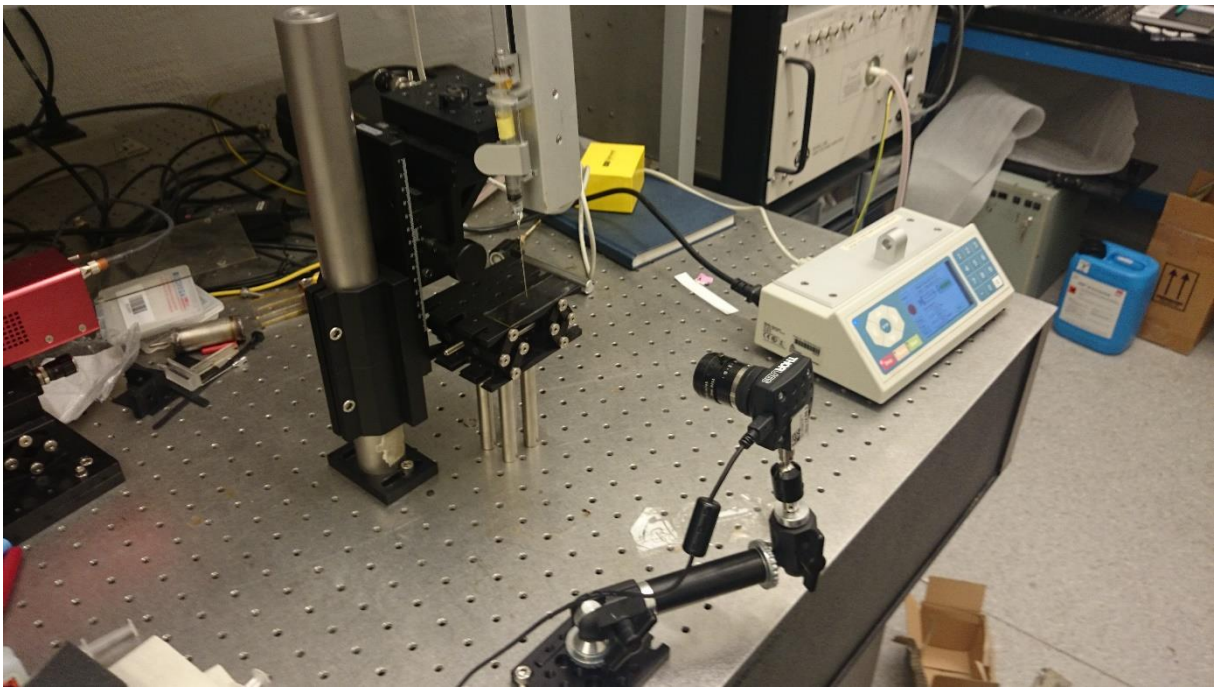

Figure 3.11 Figure 3.11: Picture of the setup used to measure the contact angle of the enhanced surfaces

3.3.1. Procedure

To measure the contact angle on the different surfaces, one drop of ether oil or water was dropped on the sample surfaces that was placed on a table in front of a camera. It is not always easy to get the correct contact angle. The lights might in some cases make it very difficult to see the exact shape of the angle between the surface and droplet. Also, a small change in ether of the three points that was set manually, had a big impact on the contact angle measured. This could lead to some errors in the measurements.

3.3.2. Camera

The camera used for the measuring of the contact angle, was a black and white Thor laboratories camera. It was mounted on a flexible arm that could be moved in any direction making sure the glass sample was leveled with the camera.

Figure 3.12 Picture of the camera used to measure the contact angel of the glass

3.3.3. Syringe Controller

In the beginning of the experiment the droplets on the surfaces was constructed manually. However, due to the problems of controlling the force inflicted on the syringe, they usually were of different size. To address this problem, a system with an automatic syringe pusher was installed and it created droplets of approximately same size. The syringe controller was set at a constant rate of 0.01 ml/s.

3.3.4. Computer tool for measurement

To measure the contact of the droplets a program called ImageJ was used. In this program you can zoom into the droplet and measure the contact angle by setting three points, one in the middle of the droplet, one in the edge of the droplet, and the final one follow the tangent of the angle between the droplet and the surface. Then the program automatically calculates the angle.

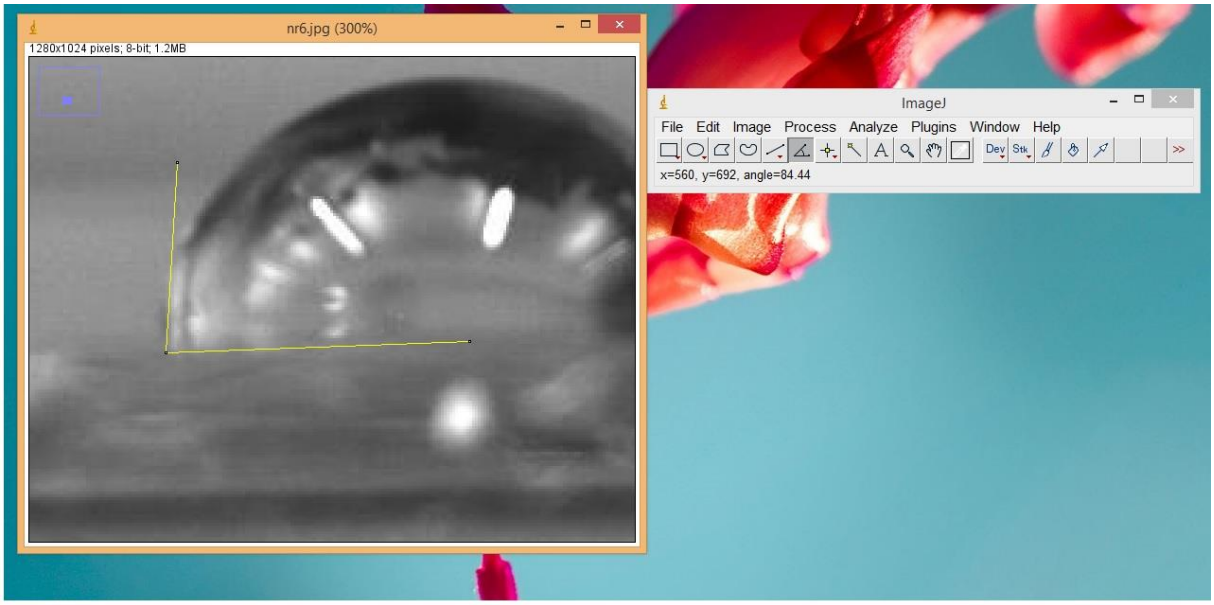

Figure 3.13 Picture showing the ImageJ software. The contact angle of a water droplet on the ITO surface sputtered for 10 min

3.4. Error Analyses

3.4.1. Oil and Water Separation

To measure the rate of the separation of the water and oil, the change in the interface was measured by using the Microsoft program Paint. The pixels was measured on eyesight with an accuracy of ±1 pixel. The needle used for droplet visualization was 0,78 mm with and error of 0,02 mm. The larger vessel was measured to be 2,793 cm with an error of 0,03 mm. The smaller vessel was measured to be 1,201 cm with an error of 0,03 mm. When measuring the separation velocity, or the position of the interface was never completely straight. Therefore, it will be some small differences, approximately ±5 pixel difference in the samples.

3.4.2. Enhanced Surface

The different samples were conducted at different times. There were reported problems with the ITO target. Were the quality of the sputtering did vary.

3.4.3. Contact Angle

The contact angle was measured by using a program called ImageJ. The angle is found by the user, with an accuracy of ±3 degrees. In addition, the order of the experiments differed. In some samples the contact angle of oil were tested before water and others the other way around. This was done because it was more efficient; however, if the sample was not cleaned properly there could be traces of oil still on the sample, which could affect the results.

4. Oil – Water separation

The oil used for the separation experiments are both SA-2 crude oil and Exxol D80, a processed oil. There are two different sized vessels used for the experiment. Where the data for Exxol is from a larger vessel then used for SA-2.

4.1. Crude Oil and Water

4.1.1. Results

Average Separation velocity

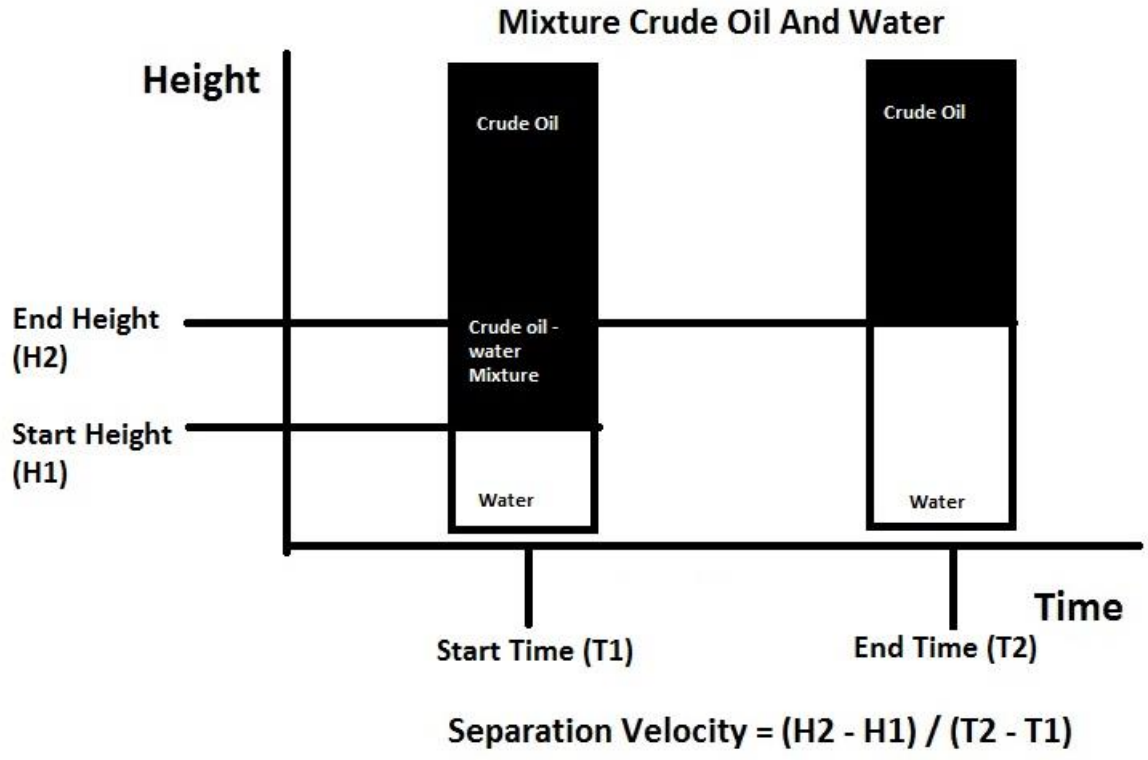

Figure 4.1 Sketch of the separation velocity

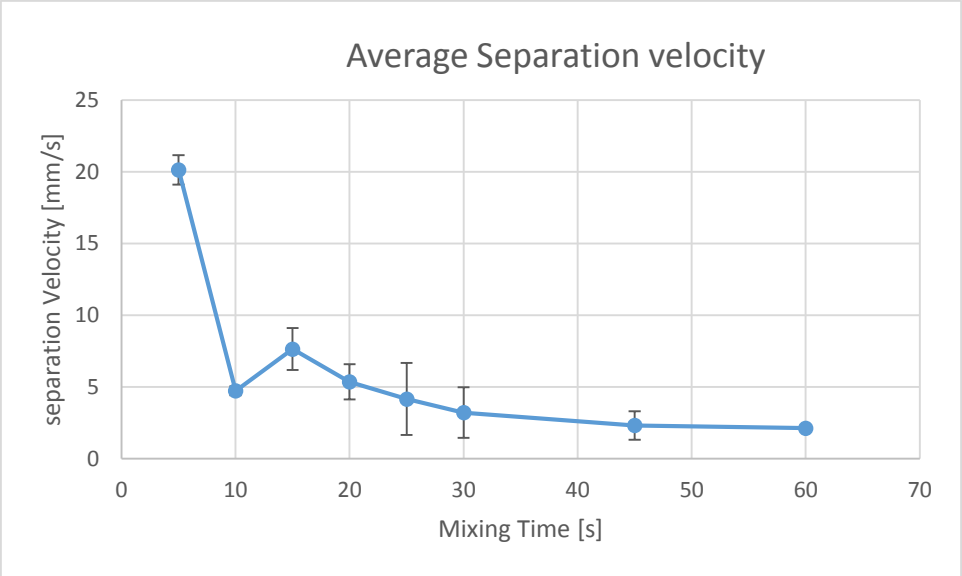

Figure 4.2 Graph showing the separation velocity of SA-2 for different mixing times, with error bars, when moving 0,4 cm from approximately the same start- to endpoint.

This graph shows the motion of the interface. It is calculated by measuring the change in the interface of from a start point to an end point, by using pictures taken of the mixture every 10 second. The starting point for this velocity is in a place where there were droplet – interface coalescence for all mixing times.

With a mixing time of only 5 seconds the velocity of the separation is very high, around 20 [mm/s], but decreases quickly when the mixing time increases. The velocity of the separation when mixed for 10 seconds is lower than the velocity for mixing times 15 -20 but higher 25 seconds. However, the velocities of all of these mixtures are in the same area. From 25 to 30 seconds the velocity decreases a lot, but seems like settling for 30 – 60 seconds.

Compared with terminal velocity

In a previous study, the teminal velocity of water droplets in SA-2 crude oil, with water droplets from 50 µm to 200µm [22]. The terminal velocity of a droplet in SA-2 crude oil was correlated by the following equation:

$$V_t = 10.1 * 10^{-6} d^2 + 0.000292d$$

Where d is the diameter of the water droplet in µm and V_t is the terminal velocity in [mm/s].

By using the average separation velocity as the terminal velocity, the diameter of the droplets is given by this graph:

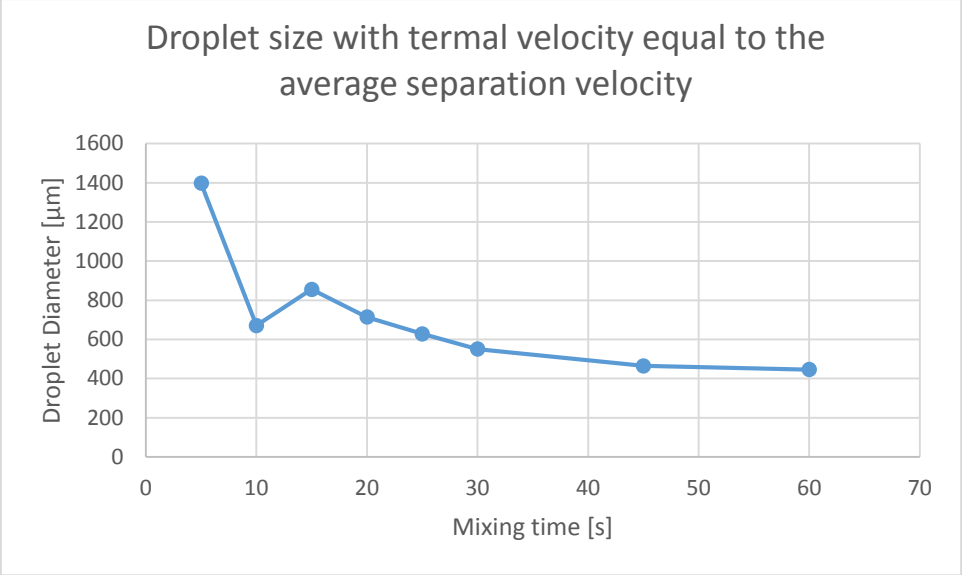

Figure 4.3 Graph showing the size of a droplet with terminal velocity equal to the average separation velocity of the different mixtures in crude oil.

This graph gives a visualization of the velocities of the separation. Where the velocity of the droplet – interface coalescence for the mixture, is identical to the terminal velocity of a single water droplet dispersed in crude oil. For the mixture mixed for 5 seconds the corresponding droplet diameter is 1400 [µm], for the mixture mixed for 60 seconds the corresponding diameter is 445 [µm].

Change in height

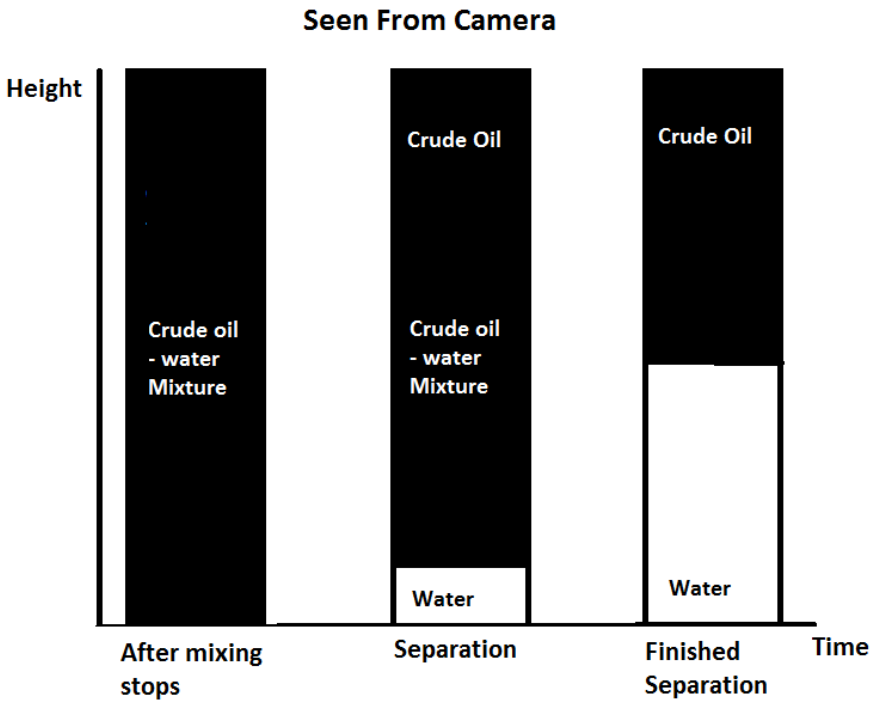

Figure 4.4 Graph showing the change in the visible height of crude oil and water mixture

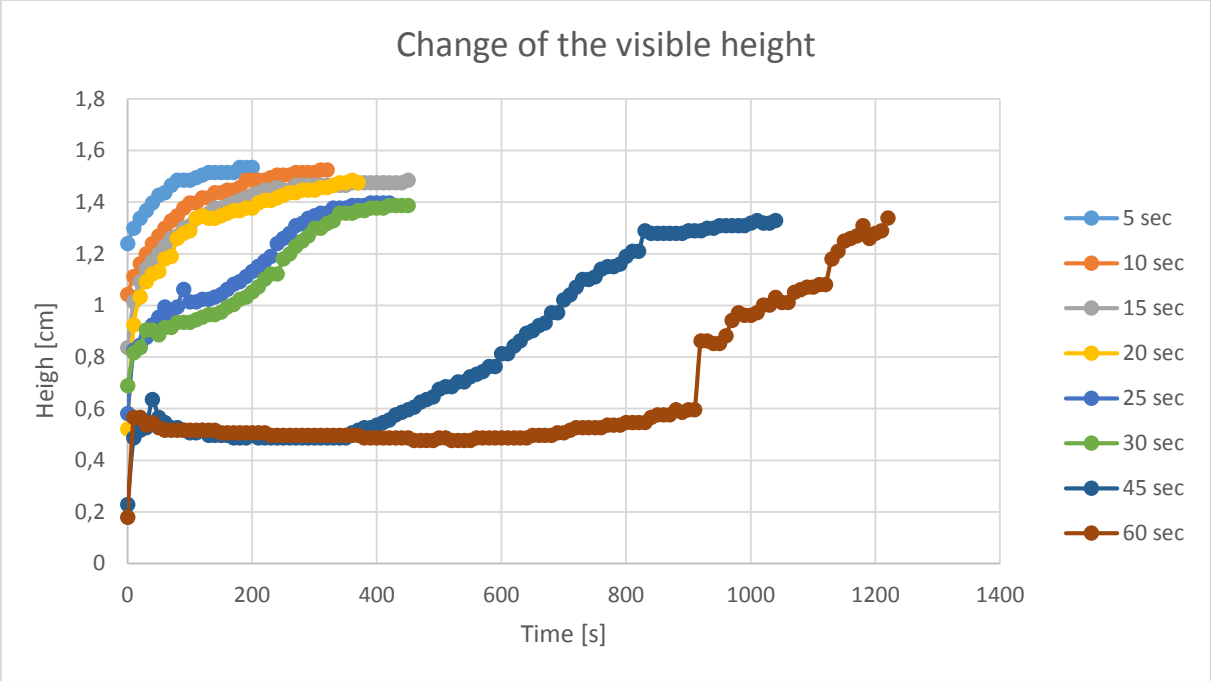

Figure 4.5 Graph showing the change in the visible height for one experiment with mixing times from 5 to 60 seconds.

This is a graph of the movement of the interface over time, after the separation has started. The pictures is taken every 10 seconds, and the height different is measured by the pixel difference from picture to picture.

Separation sequence for crude oil and water

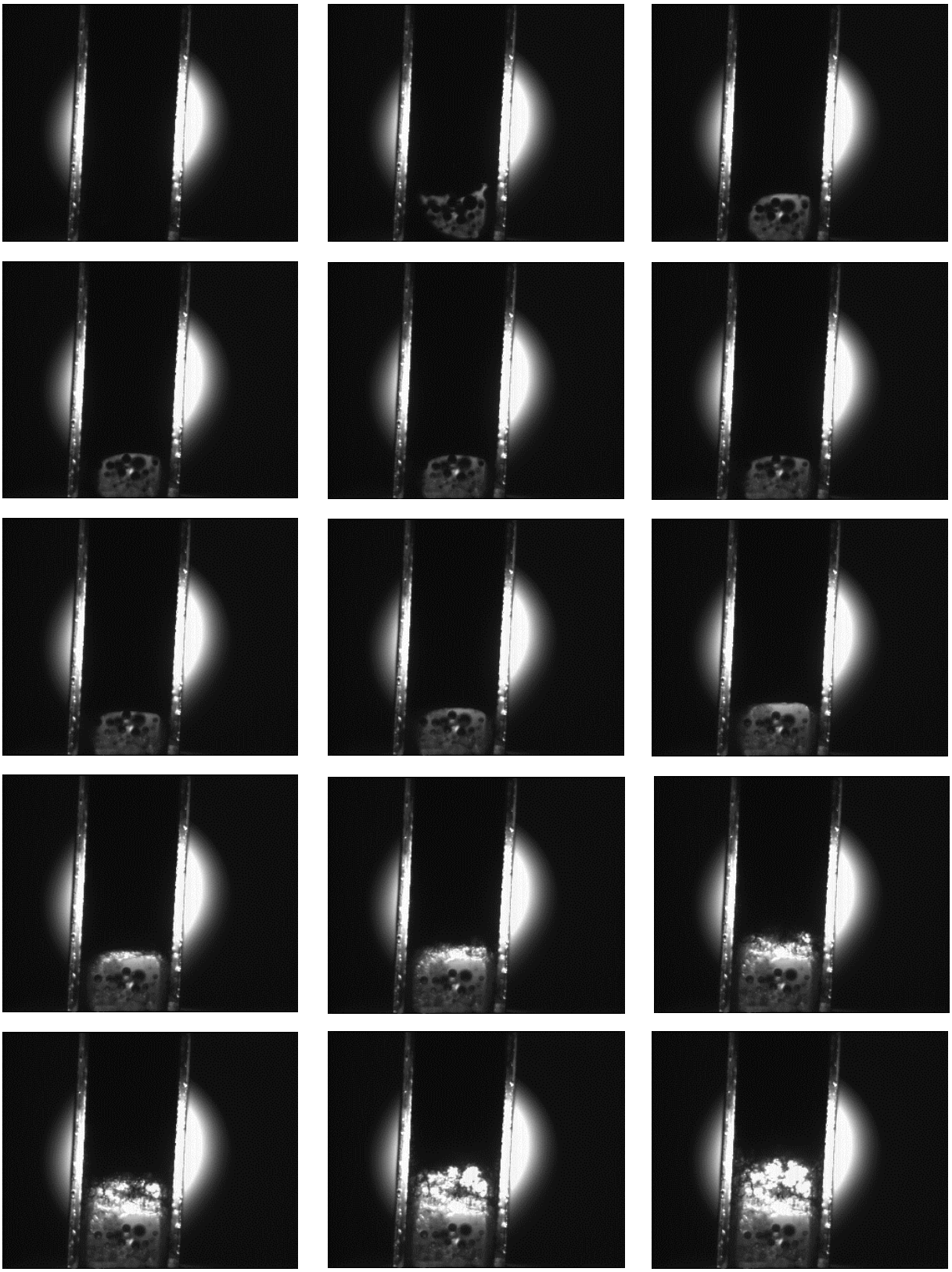

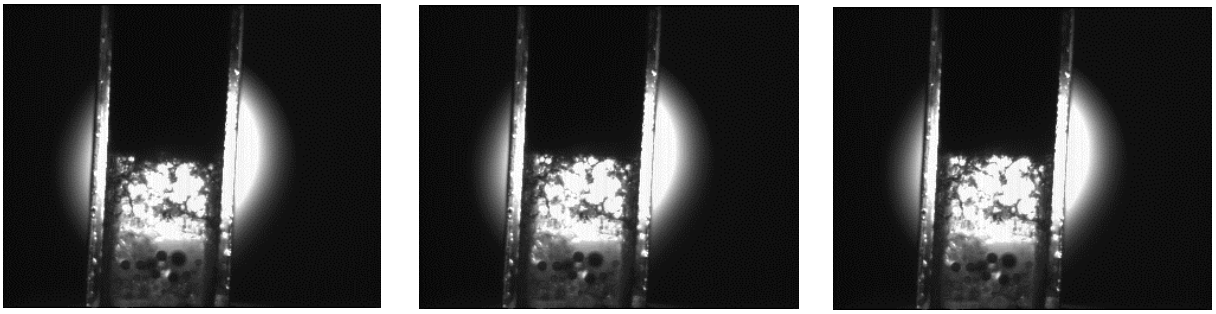

Figure 4.6 Pictures showing the separation of crude oil – water when mixed for 45 seconds. Each picture represent 1 minute. The first picture, is right after the mixing stopped, and the last picture 17 minutes later.

This sequence of picture shows the mechanics of the SA-2 – water separation. First, there is a relatively rapid separation, before there is a stall. Due to the darkness of the oil, it is not possible to see the separation in sections of the vessel with large amounts of oil. Therefore, it is not possible to see the sedimentation in the oil zone.

Visualizing the droplet size

Crude oil and water was mixed for 20 seconds before a small droplet of the mixture was placed on a glass slide in front of the camera. The droplet sizes could then be visualized.

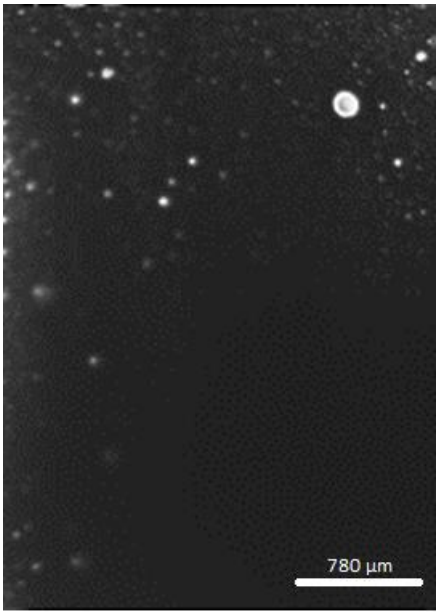

Figure 4.7 Picture of droplets in crude oil-water mixture, mixing time was 20 seconds.

This picture shows the droplet sizes in a 20 second mixture, soon after the mixing had stopped. In the 20 second mixture the droplet sizes varied from 260 µm to approximately 15 µm.

4.1.2. Discussion

The separation velocity for the mixtures decreases with mixing time. This velocity is given by the droplet size on the interface, and the droplet - interface coalescence time. As expected, it shows that the increase in mixing time decreases the droplet size forming on the interface. The difference in the velocity also decreases with mixing time, and it is almost equal for 45 and 60 seconds mixing. This could indicate that the droplet coalescing with the interface in the 45 – 60 seconds mixtures, are approximately the same size.

Comparing the separation velocity to the terminal velocity of a single droplet, the diameter of the droplets was calculated to be from 1400 [µm] at 5 seconds mixing time, and 445 [µm] at 60 seconds. This indicates that the hindering of the settling velocity due to the neighbor droplets, plays an important role in the separation process. Further studies are required to quantify this hindering factor, and its dependence on the droplet size distribution. Improving the visualization of the test cell is a critical step in this direction.

When looking at the graph for the visible height, for 45 – 60 seconds mixing, there are several minutes where there is no visible change in the height. This is the dense-packed zone. Here the droplets start to coalescence with each other. In the beginning, it seems like there are only droplet-droplet coalescence, and therefore, the dense-packed zone does not decrease in size. Visibly it seems like the separation has stopped. The droplet-droplet coalescence increases the droplets size until it coalescence with the interface. When the droplet-interface coalescence start, the height of the dense-packed zone decreases with the speed of the separation velocity. The dense-packed zone in the 60 seconds mixture last significantly longer than in the 45 seconds mixture. This indicates that the initial droplet size created by the 60 seconds mixture are smaller than in the 45 seconds mixture. Therefore, there is more droplet - droplet coalescence in the 60 seconds mixture, which increases the separation time.

This stall only happened when mixed for 45 and 60 seconds. For mixing times below this, the sedimentation never completely stops. This indicate that for smaller mixing times, there are droplets that have a sufficient size to rapid coalesce with the interface, without having to increase its size with droplet-droplet coalescence.

There is a leap in height for the mixture, mixed for 60 seconds. The reason for this leap is how the separation is visualized in the dense-packed zone. Where there are formed small pockets where there are vision, and these pockets increase with time. This behavior could be caused by the oil interaction with the glass surface. Where the oil sticks to the glass, due to the high wettability.

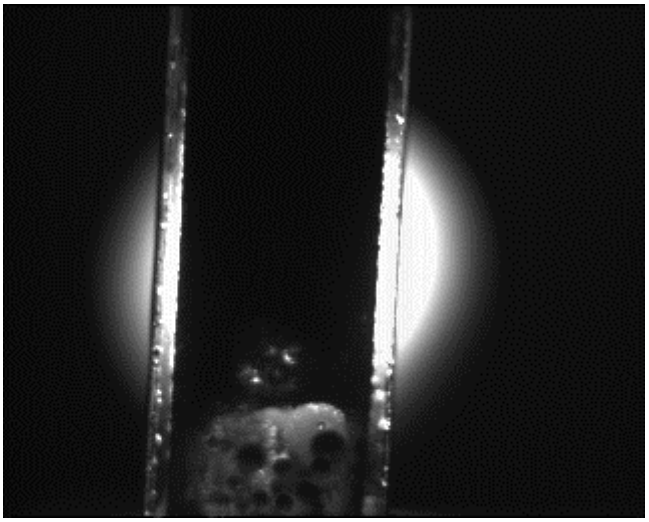

Figure 4.9 Picture of holes in the dense-packed zone

In the pictures showing the separation sequence of a 45 seconds mixture, there is an initial, rapid separation. This separation correspond to the separation in the sedimentation zone. According to Heischke et. al [6] is this a place where there is almost no droplet interaction and coalescence. Therefore, it is only the buoyancy, drag and gravitational forces that determine the separation rate in this zone.

The coalescence time of the droplets in the dense-packed zone and the interaction of the crude oil with the glass surface was a major problem in this thesis. In many experiments, there were no visible separation even hours after the experiment started. This was a problem especially for large mixing times, or with vertical movement in the mixing. For shorter mixing times, there were problems with creating a mixture. Often, it was ether no mixing, or a mixture with very high separation time. In addition, using larger vessel with crude oil – water mixture, was problematic. It made it harder to mix the two liquids, and when mixed the separation time was very high.

To get a vision on the droplet sizes in the mixture first the imaging was magnified by using a longer lens on the camera. However, the oil was too thick too get a vision. Since the light could not pierce through the oil, there was not possible to see the droplet size, or even, the separation. Therefore, the droplets inside a small portion of the mixture was visualized. The droplet sizes varied from 260 µm to around 15 µm. However, to see the droplets in the 15 µm range, the picture had to be enlarged. This caused it to be diffused, which is problematic when the diameter of the droplet seen, was in the 5 pixel range. Many of the droplets in the visualization was approximately 15 µm. What it shows, however, is that the droplets in a crude – oil water mixture can be very small.

Since the needle used in the visualization has a cylindrical shape, it is hard to get both the needle and the droplet in focus. The small difference from the needle to the glass surface caused some diffusion in some pictures. The could be countered by using a larger droplet. However, with a too thick droplet, it was not possible to see through the oil. The fact that even the amount of oil used in this experiments, some times was too thick to get a vision, shows that the light source has to be modified, to have any change of seeing trough the crude oil – water mixture.

There was a hypothesis that the mixing process of the two fluids were the problem. That mixing the two fluids in a small vessel increased the interaction between the glass surface and the oil. Therefore, made the separation harder to see. In an attempt to see if this was the case, the crude oil

–water was mixed in a separate larger vessel. This did, however, not increase the visibility of the separation. The mixing in a separate vessel did, it seemed, increase the separation time. This could be because the mixing improved, and created a smaller initial droplet size, than when mixed in the small vessel.

4.2. Exxol D80 and Water

4.2.1. Result

Average separation velocity

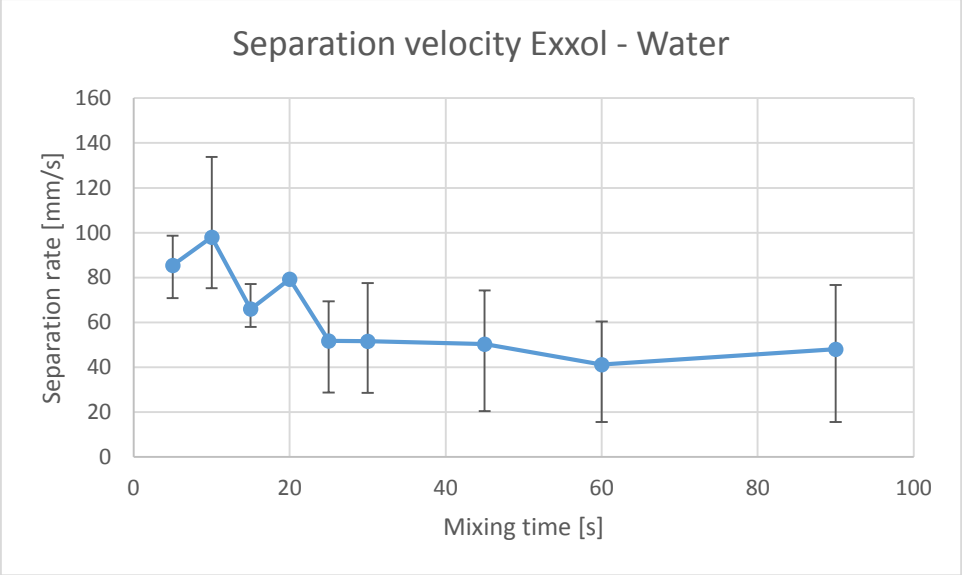

Figure 4.10 Graph showing the average separation velocity Exxol and water, with error bars.

This is a graph showing the average separation velocity of Exxol – water mixture with different mixing times. The velocity is measured by tracking the height difference of the interface over time.

Compared with Terminal Velocity

A previous study correlated an equation for the terminal velocity for water droplets in Exxol D80[22]:

$$V_t = 5.4 * 10^{-5} d^2 + 0.0011d$$

where d is diameter of the water droplet given in µm and V_t is in [mm/s]

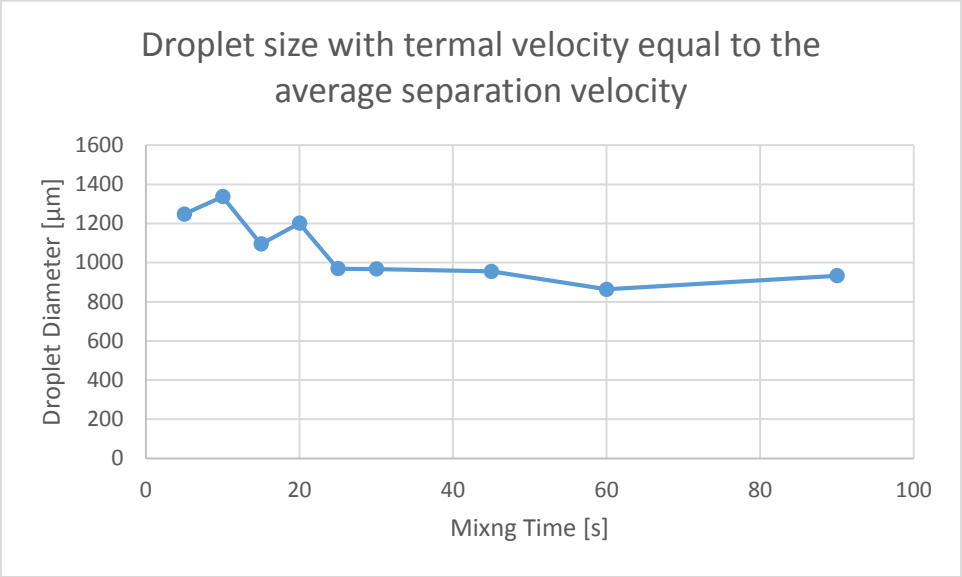

Figure 4.11 Graph showing the droplet diameter with terminal velocity equal to the average separation velocity.

This graph shows the size of a water droplet with terminal velocity equal to the separation velocity. The diameters vary from 1340 µm for the separation velocity at 10 seconds to 860 µm for the separation velocity at 60 seconds.

Change in height

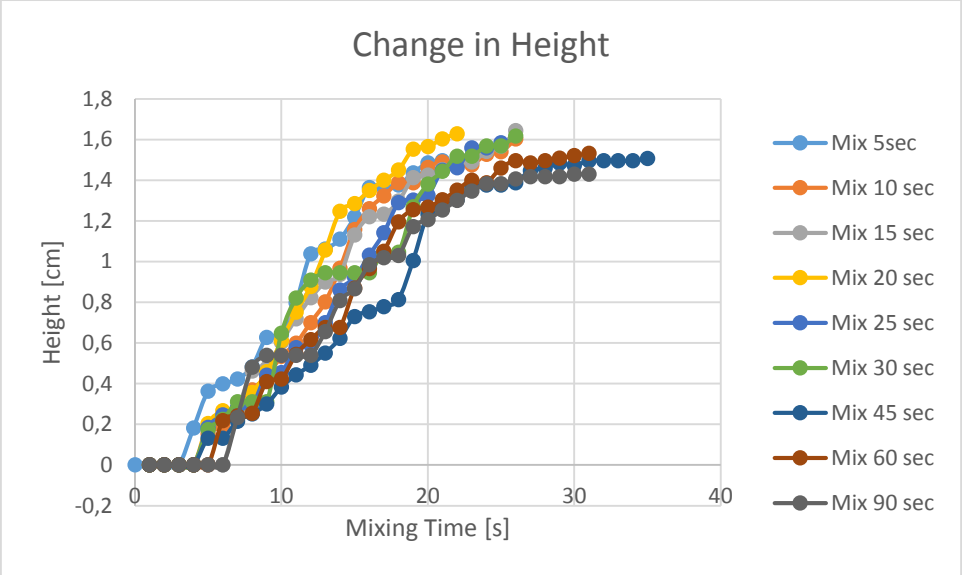

Figure 4.12 Graph showing the movement of the interface, for Exxol-Water mixture at different mixing times for one sample of experiments

This graph shows the movement of the interface, for the Exxol – water mixture. The starting time is immediately after the separation stoppe. To measure the height, the camera took 1 picture every second.

Exxol – water separation sequence

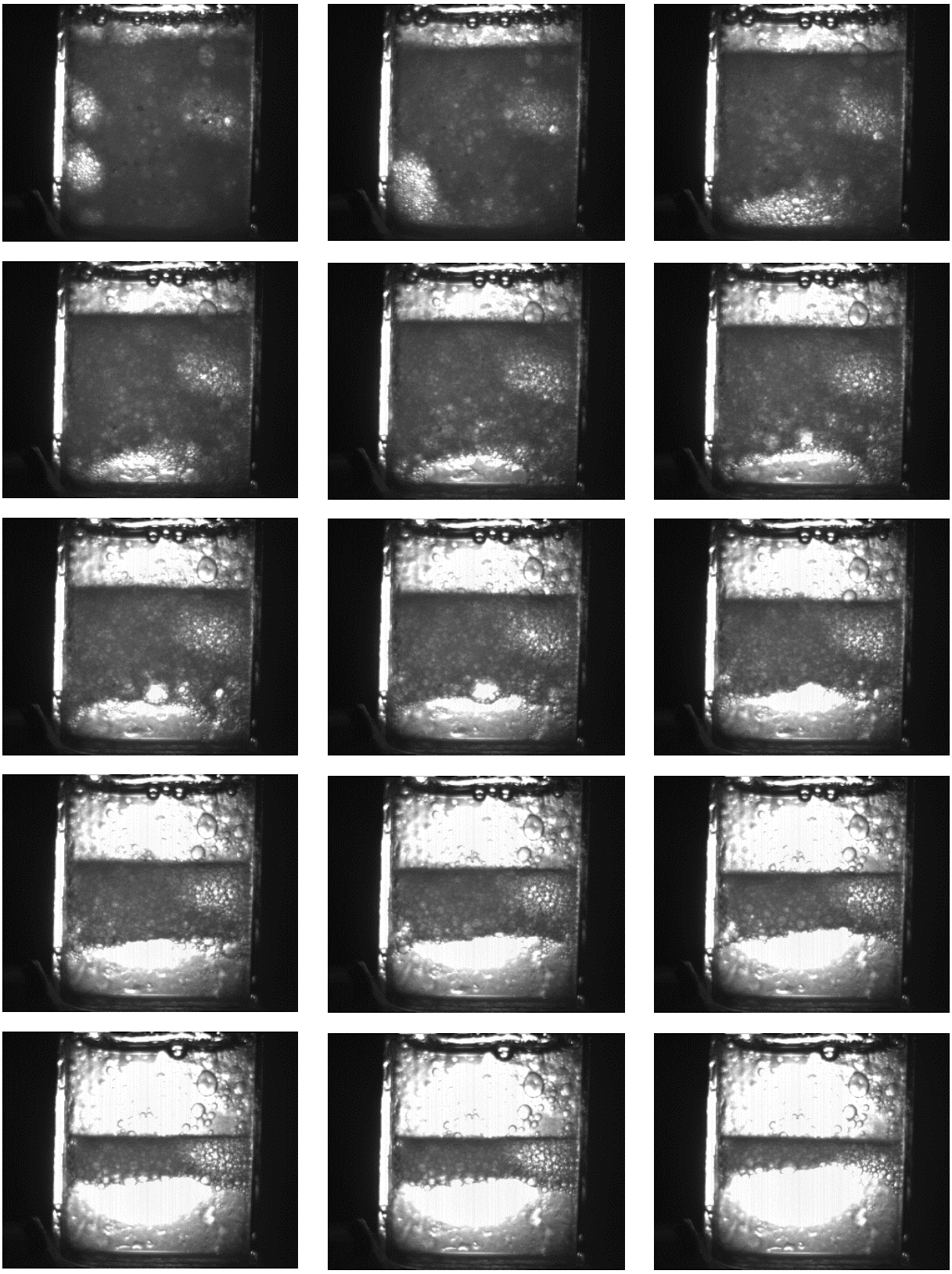

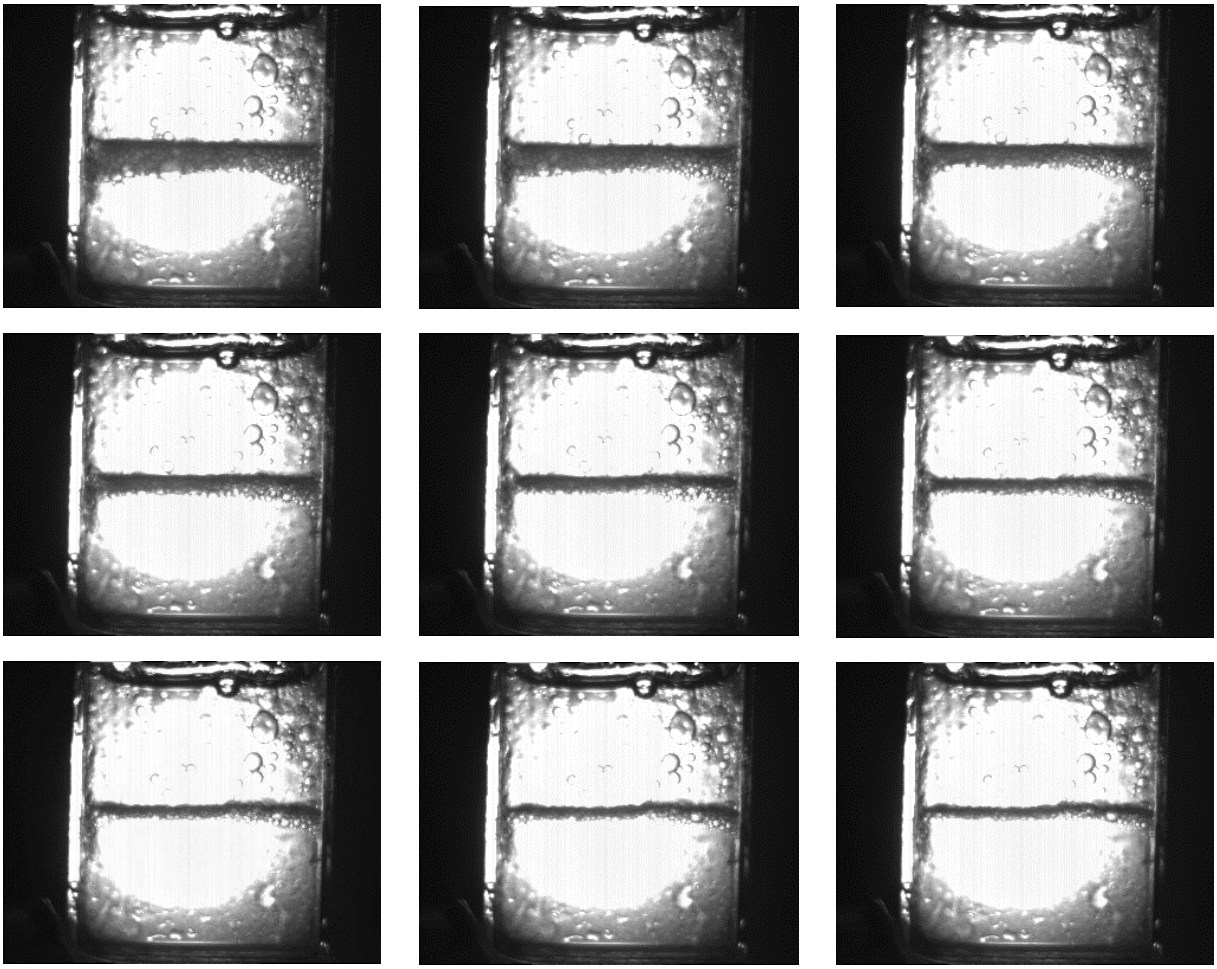

Figure 4.13 Pictures showing the separation of Exxol – water mixed for 45 seconds. Each picture is 1 second.

The first picture in this sequence, is taken right after the mixing had stopped. Each picture represent 1 second.

4.2.2. Discussion

The separation velocity of the mixture of Exxol – water decreases with mixing time. From 5 seconds mixing time to 20 seconds the velocity vary, but at a higher rate. From 25 seconds mixing time the average separation velocity is nearly constant. This can indicate that the Exxol – water mixture is fully mixed at 25 seconds, and the increase in mixing time after this does not decrease the initial droplet size, and therefore, does not affect the separation time.

The average separation velocity of Exxol D80 – water mixture is equal to the terminal velocity of a single water droplet dispersed in Exxol D80, with different water droplet diameter corresponding to different mixing times. The largest correstponding diameter is at 10 seconds mixing time and 1340 µm. The smallest corresponding diameter is at 60 seconds mixing time and is 860 µm. As for the crude oil – water separation, the settling velocity is hindered by neighbor droplets.

The error in separation velocity are at times significant. There are some possibilities for human error, and some possible properties changes. In addition, the order in which the experiments took place, can have affected the velocities. Especially for the larger mixing times there was a clear difference when the order changed. When the experiments started with the shorter mixing times, the velocity of the separation for the longer mixing times increased, compared to when starting with the longer. This could be caused be temperature differences. Where the temperature of the mixture could increase with the mixing, and therefore decrease the viscosity of the oil. However, this was not the case for the shorter mixing times.

The picture sequence shows the separation for Exxol – water mixture. Due to the Exxol being a transparent oil, the whole process is visible. Although, in many experiments the droplets interaction with the surface, made it difficult to see the separation. Especially right after the mixing was finished.

After the mixing stops, the whole area is seemingly a dense-packed zone. However, in contrary to the crude oil, the Exxol – water mixture does not have a zone where there is only droplet – droplet coalescence. The droplet – interface coalescence continues throughout the whole experiment. However, there is clearly also droplet – droplet coalescence. Some of the droplets near the interface clearly increases in size before coalescence.

For all the mixing times, there is a high initial velocity, however, for the larger mixing times, this initial velocity slows down much earlier.

The experiments with Exxol – water mixture took place in a larger vessel than the SA-2 crude oil – water mixture. This could affect the size of the initial droplets. Since it required more mixing when the amount of liquid increases. However, when the crude oil – water mixture was tried in the larger vessel, the separation velocity decreased a lot. In addition, when compared to the crude oil – water, the Exxol – water mixture separates quickly. This is because of the difference in the properties of these oils. The main reason is the viscosity, which is an important parameter for the coalescence time. Exxol has lower viscosity than crude oil. Therefore, for droplets of the same size, the coalescence in Exxol will be much quicker than in crude oil.

5. Enhanced surface

In this section both the results used for choosing the setting of the AFM software, and the actual results of the measurements is presented. Then the wettability of the surfaces was tested. The roughness is given as the root mean squared roughness of the whole area that was measured.

5.1. I-Gain

Before measuring the roughness of the different surfaces, the correct parameter had to be set in the software. There were problems with the scanned topography. Where the surface was not straight. To address this problem, different values for the I-Gain was tested. This is the parameter that affect the topography the most [17]. The sample of aluminum sputtered for 15 minutes, was measured with the AFM for different I-Gains.

5.1.1. Result

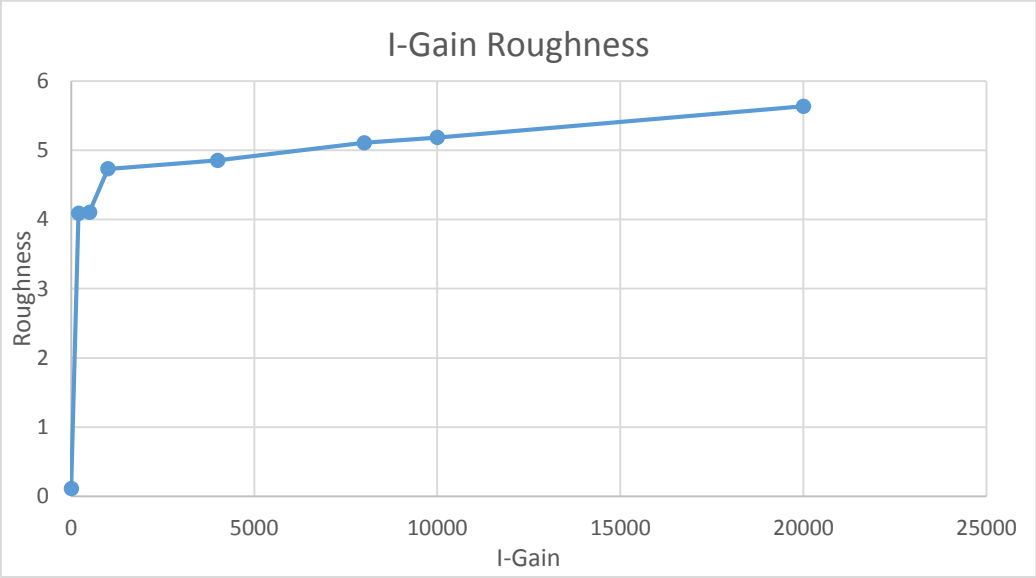

Figure 5.1 Graph showing the root mean squared roughness of aluminum sample sputtered for 15 minutes, for different I-Gain values

Pictures showing the topography and amplitudes of Aluminum surface, sputtered for 15 minutes, with different I-Gain

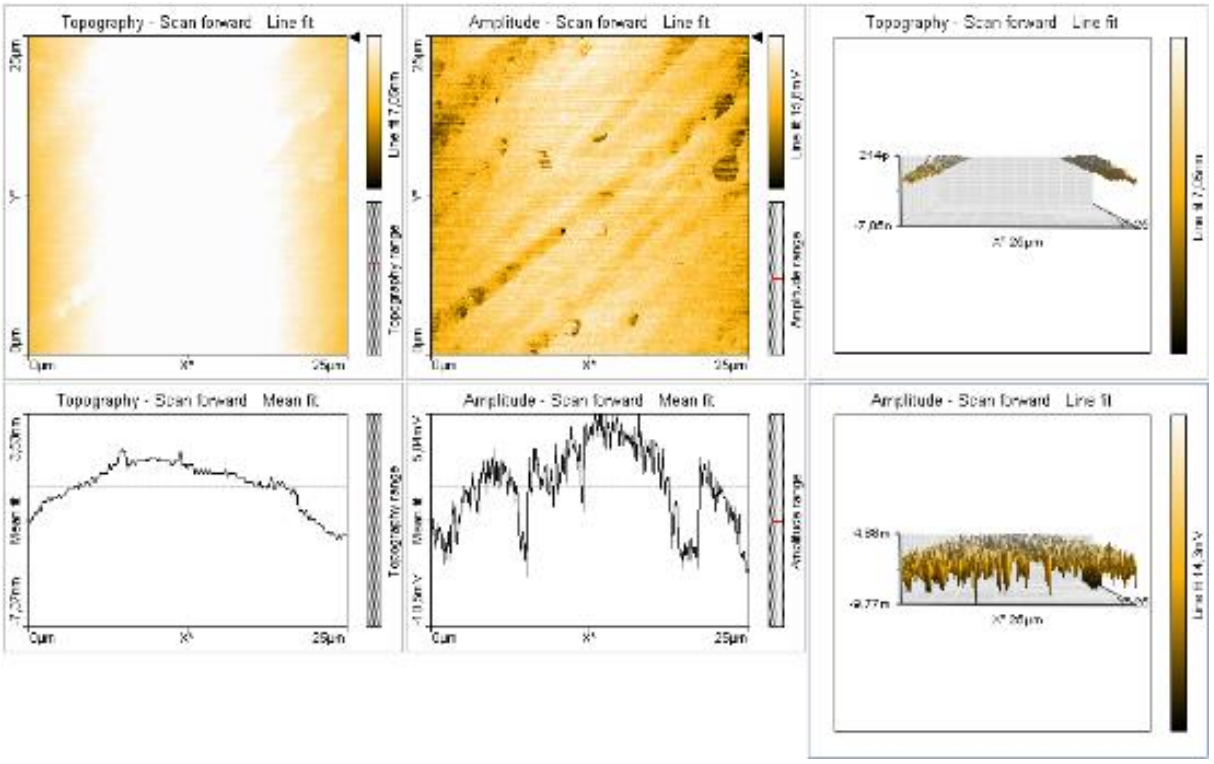

Figure 5.2 Topography and amplitude of aluminum sputtered for 15 min, with I-Gain = 0

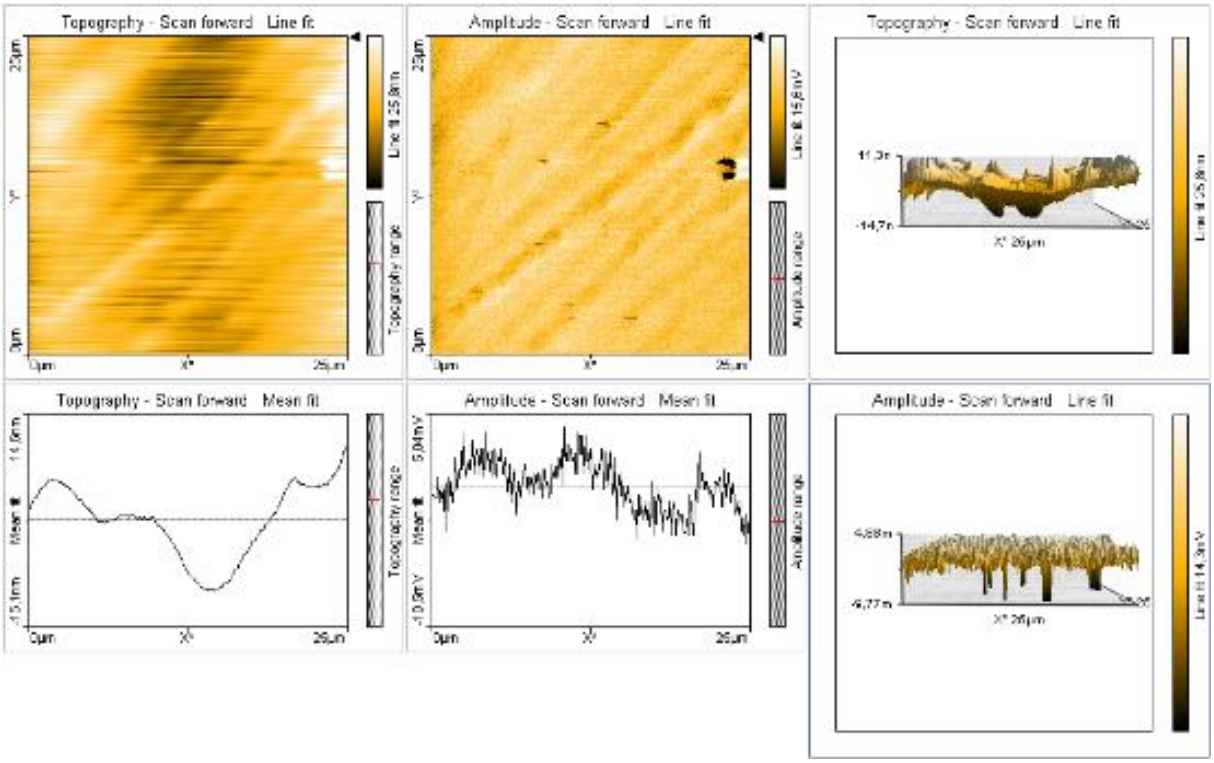

Figure 5.3 Topography and amplitude of aluminum sputtered for 15 min, with I-Gain = 200

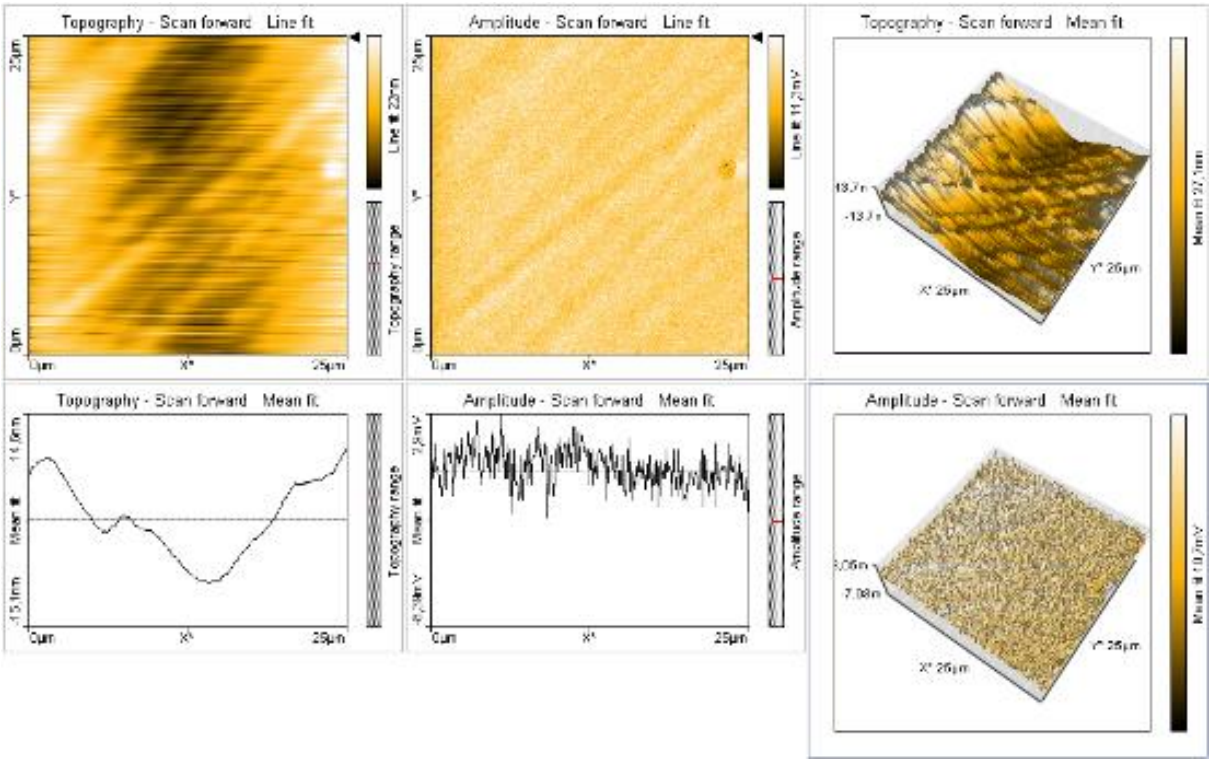

Figure 5.4 Topography and amplitude of aluminum sputtered for 15 min, with I-Gain = 500

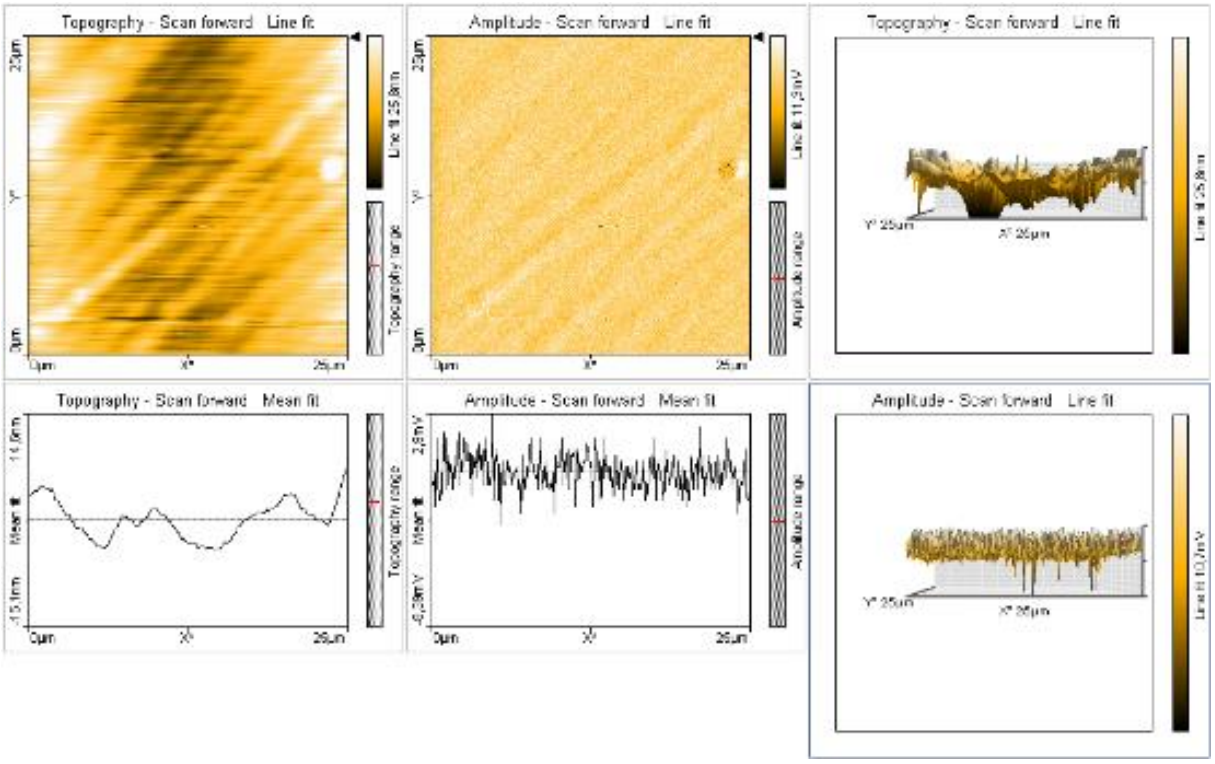

Figure 5.5 Topography and amplitude of aluminum sputtered for 15 min, with I-Gain = 1000

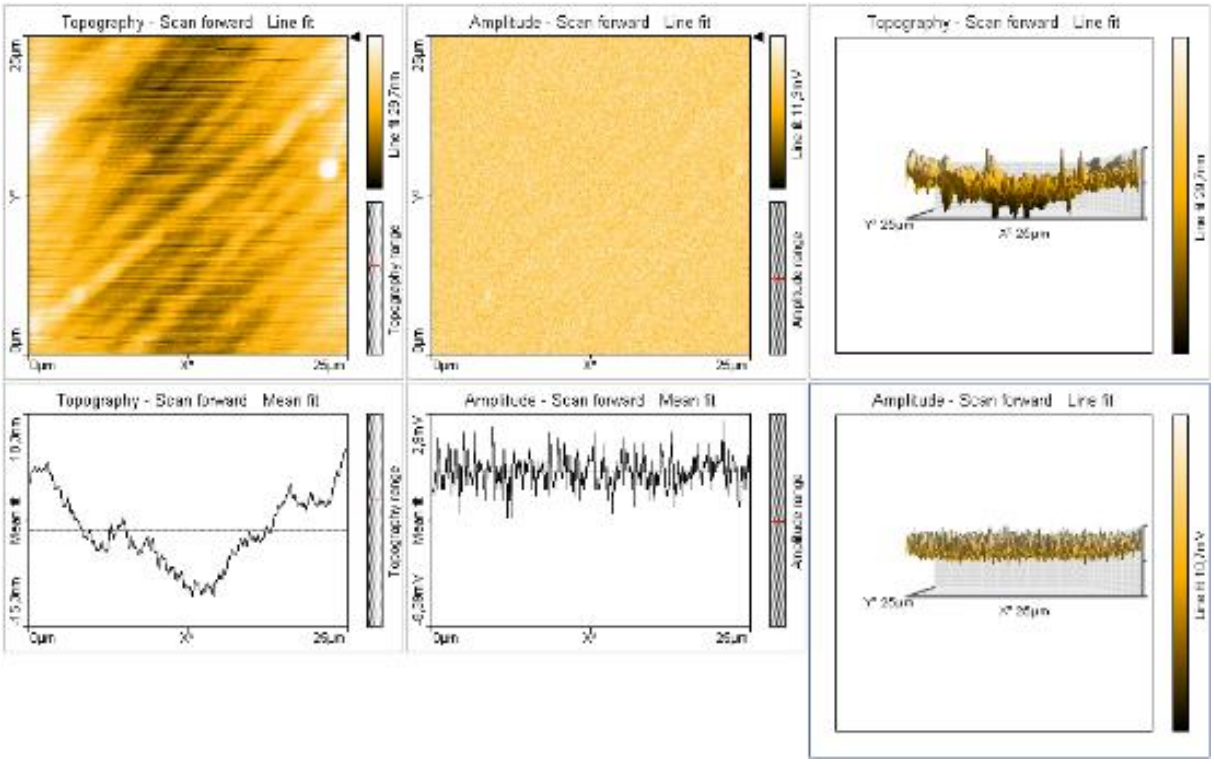

Figure 5.6 Topography and amplitude of aluminum sputtered for 15 min, with I-Gain = 4000

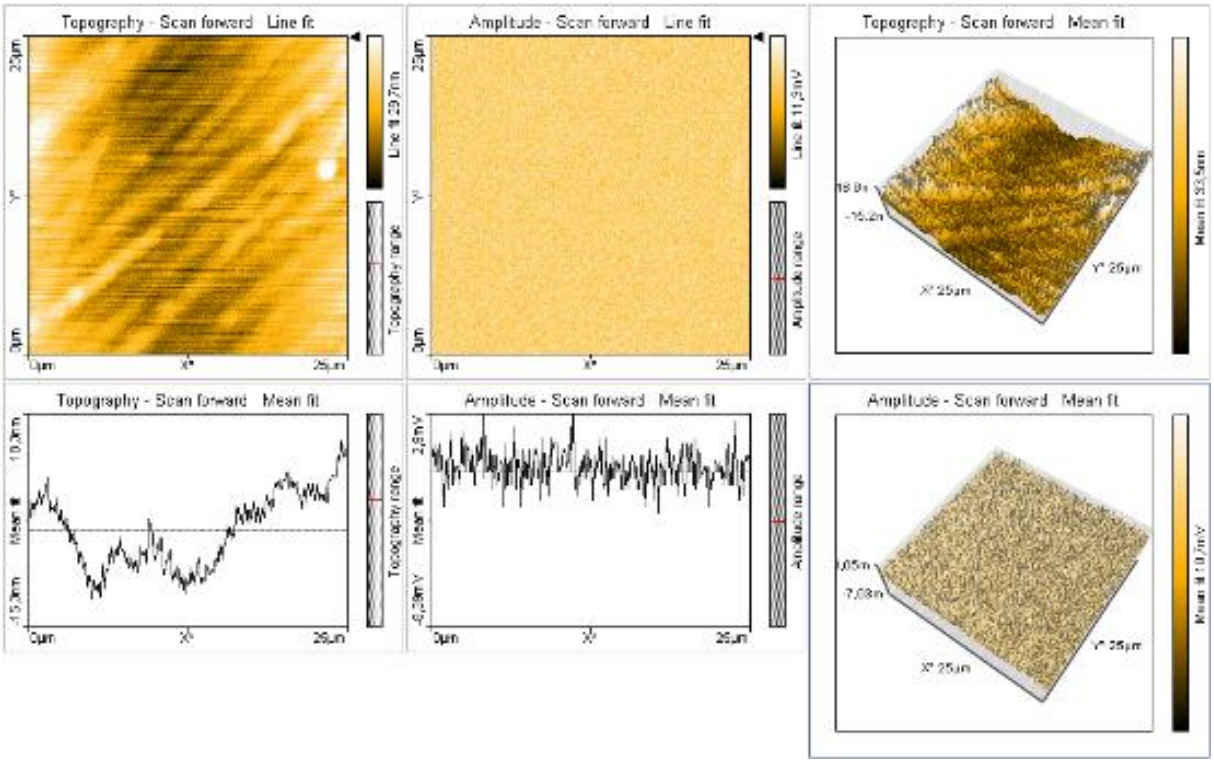

Figure 5.7 Topography and amplitude of aluminum sputtered for 15 min, with I-Gain = 8000

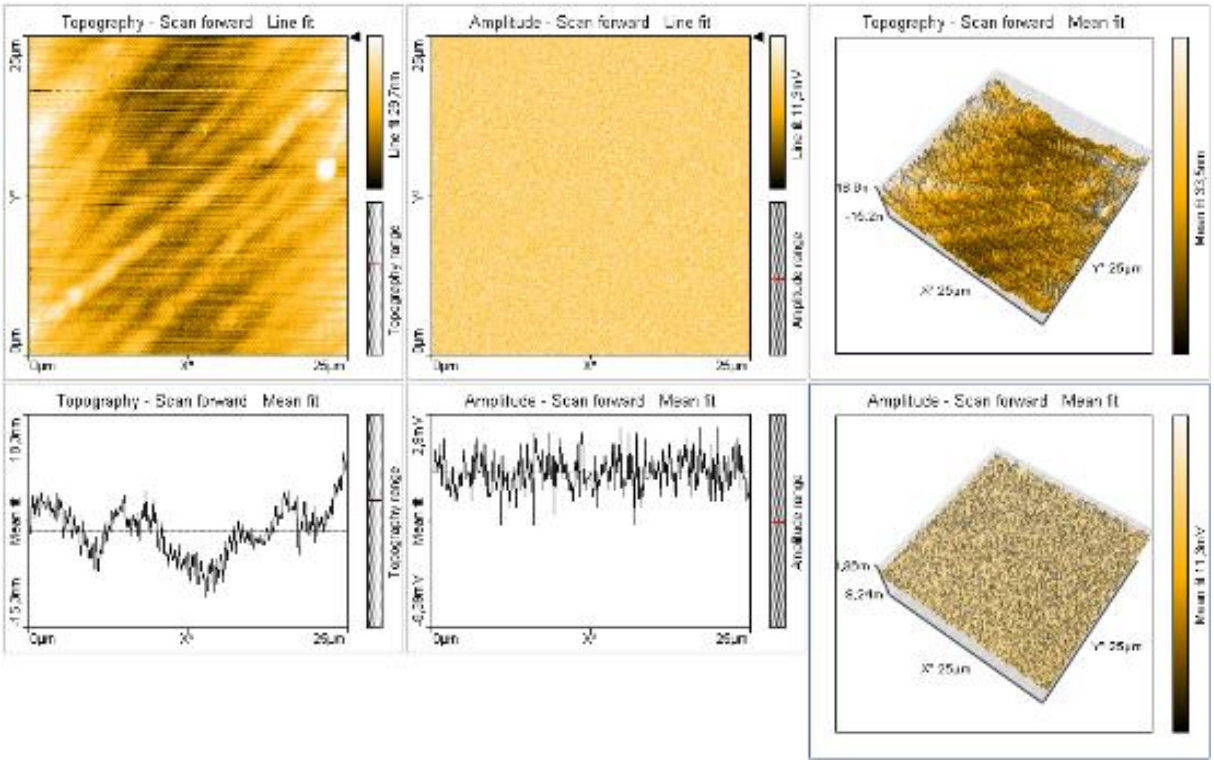

Figure 5.8 Topography and amplitude of aluminum sputtered for 15 min, with I-Gain = 10000

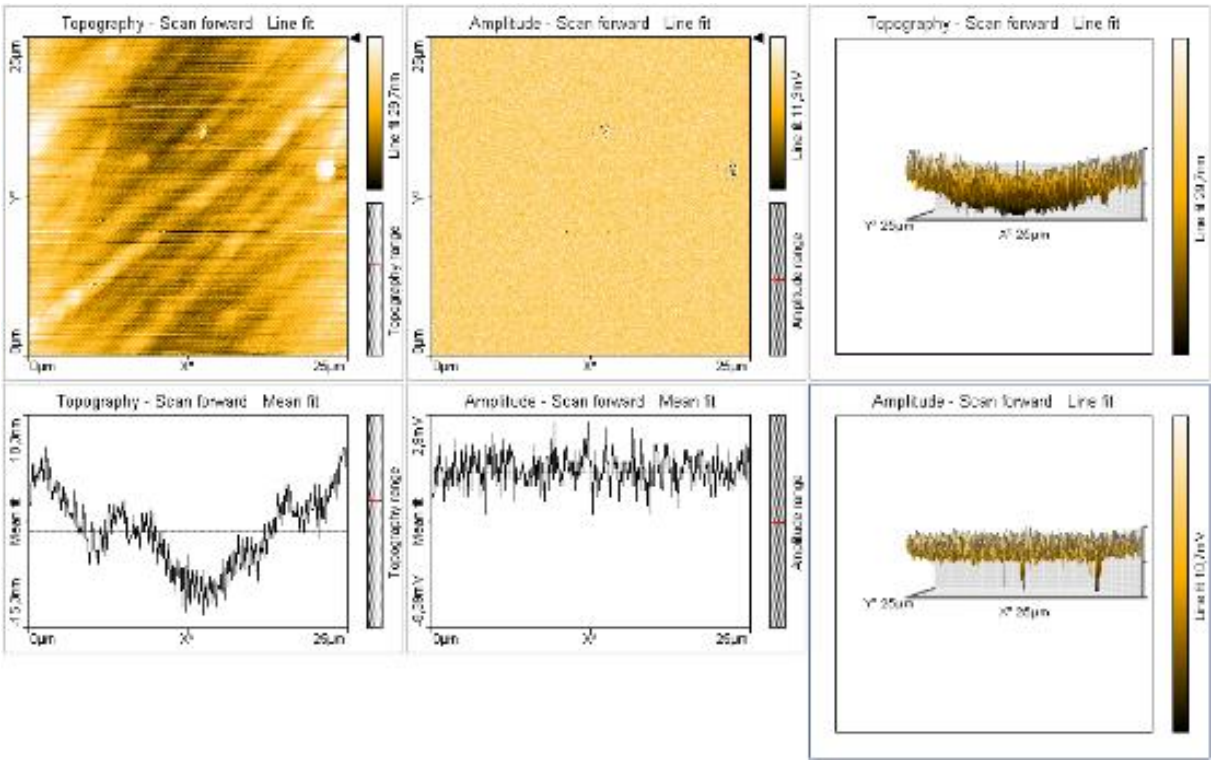

Figure 5.9 Topography and amplitude of aluminum sputtered for 15 min, with I-Gain = 20000

5.1.2. Discussion

Changing the I-Gain does affect the roughness measured by the AFM. For I-Gain 0, the measurement of the surface is not accurate, some of the surface is not measured, and therefore the roughness is very low. Also for I-Gain 200 – 500 the surface roughness is low, although almost identical. There is a rapid increase in roughness measured from I-Gain 500 to I-Gain 1000. From I-Gain 1000 there is a nearly linear increase in the roughness.

As, seen in the picture, the I-Gain = 0 is not possible to use. When is increased to 200 and 500, there is a clear picture of the scanned surface. However, for I-Gain = 200 the image was defused. For I-Gain= 500 the topography is clearer, and when increased to 1000 and further, the scanned picture of the topography are similar.

Since increasing the I-Gain decreases the error signal over time, the increase in I-Gain decreases the correction of the scanning from the AFM. This leads to an increase in the noise, and for I-Gain 8000 and up this noise is very clear in the topography lines. An I-Gain of 4000 was used in the rest of the result. Snce this gave an accurate topography without too much noise in the results.

5.2. Roughness

The I-Gain was set to 4000 in the measurements. For both aluminum, ITO and the glass results. The roughness given are the root mean squared roughness of the area measured.

5.2.1. Result

Figure 5.10 Graph showing the root mean squared roughness of the sputtered surfaces versus sputtered time.

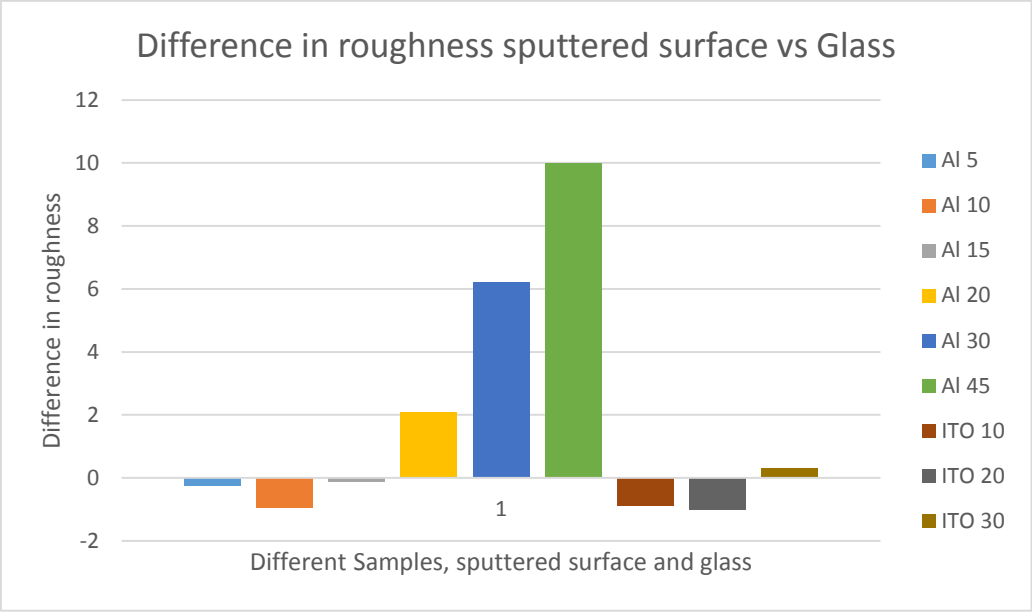

Figure 5.11 Bar graph showing the difference in roughness between the sputtered surface area and clean glass area from the same sample.

Result from the AFM

Aluminum:

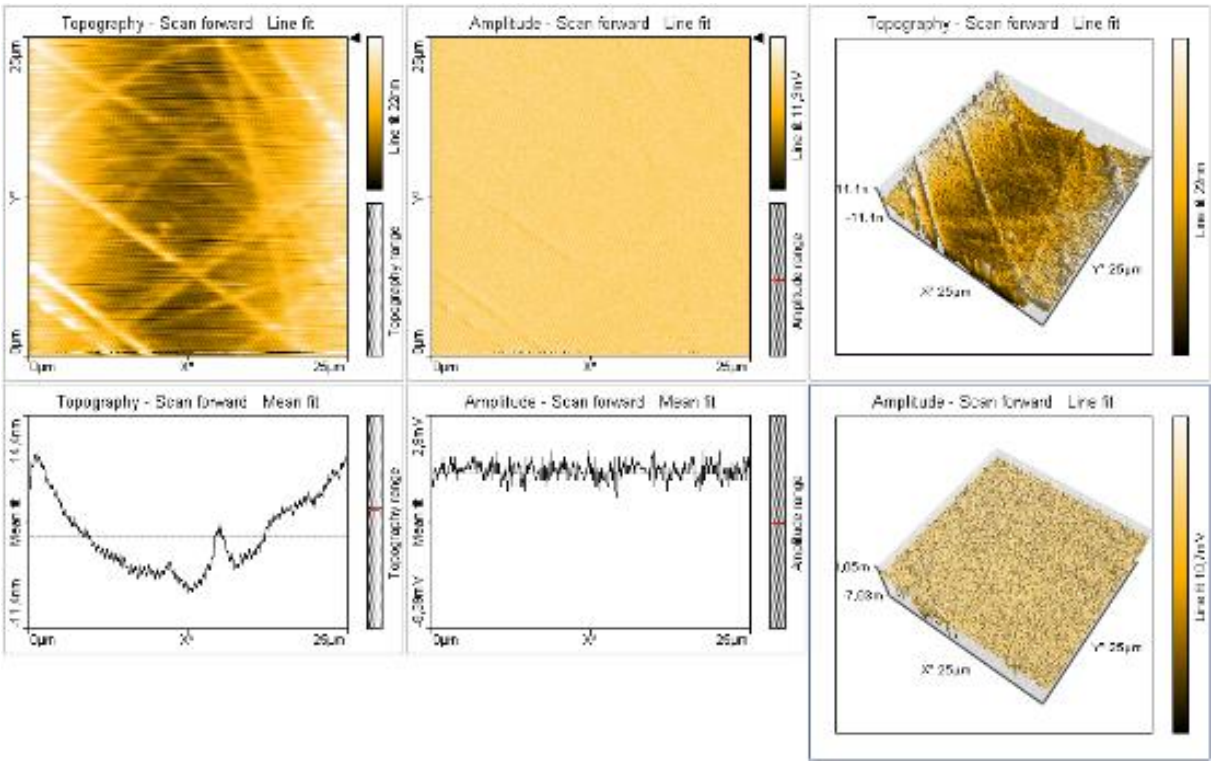

Figure 5.12 Topography and amplitude of Aluminum sputtered for 5 minutes

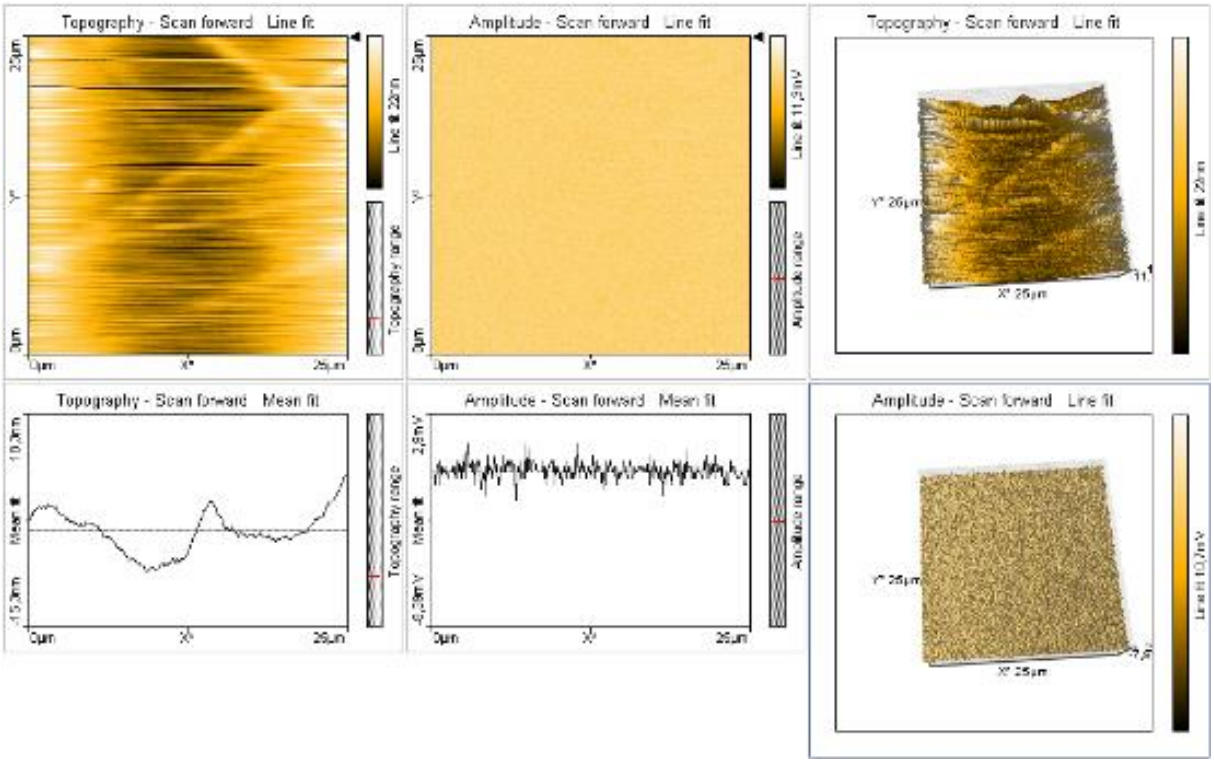

Figure 5.13 Topography and amplitude of Aluminum sputtered for 10 minutes

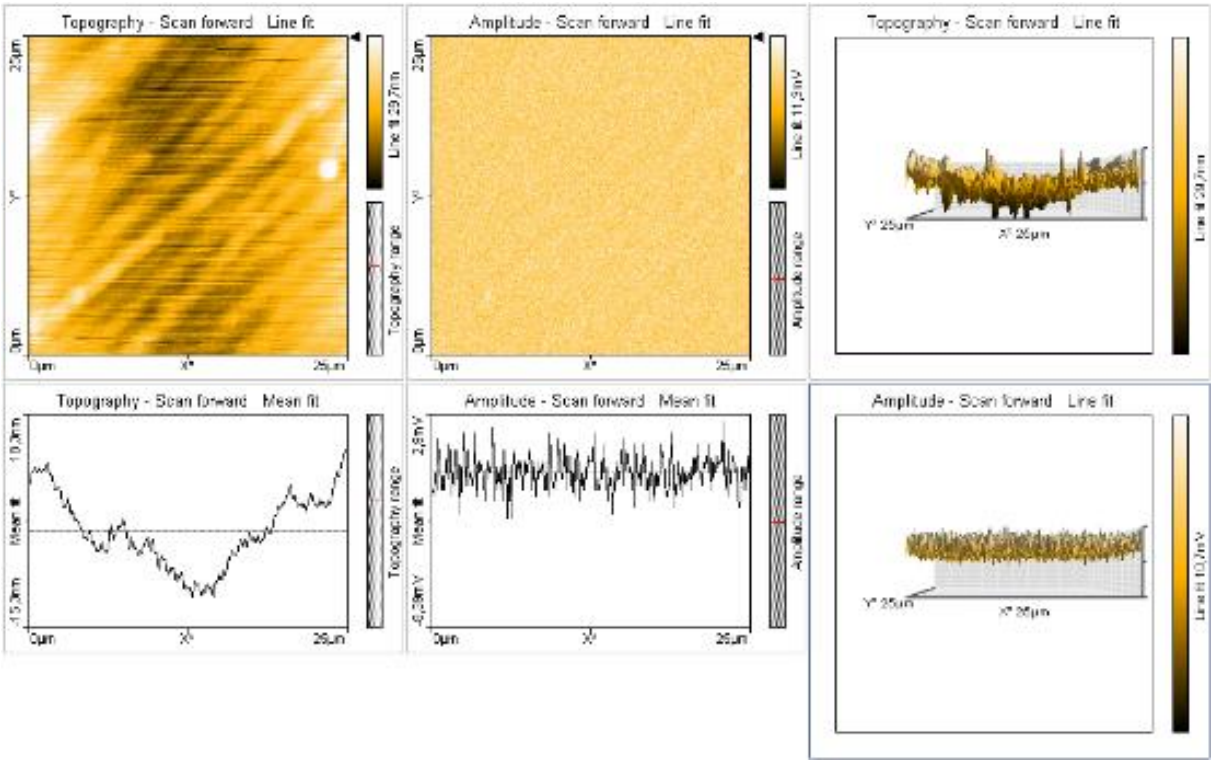

Figure 5.14 Topography and amplitude of Aluminum sputtered for 15 minutes

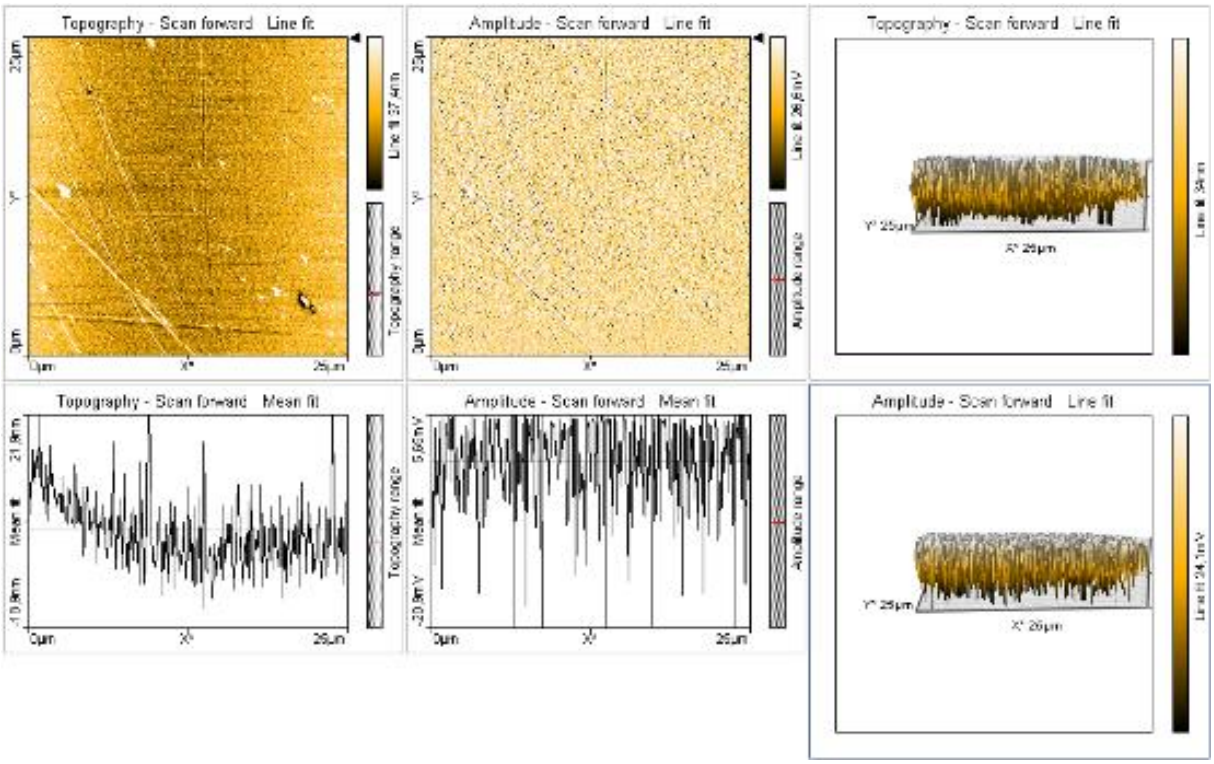

Figure 5.15Topography and amplitude of Aluminum sputtered for 20 minutes

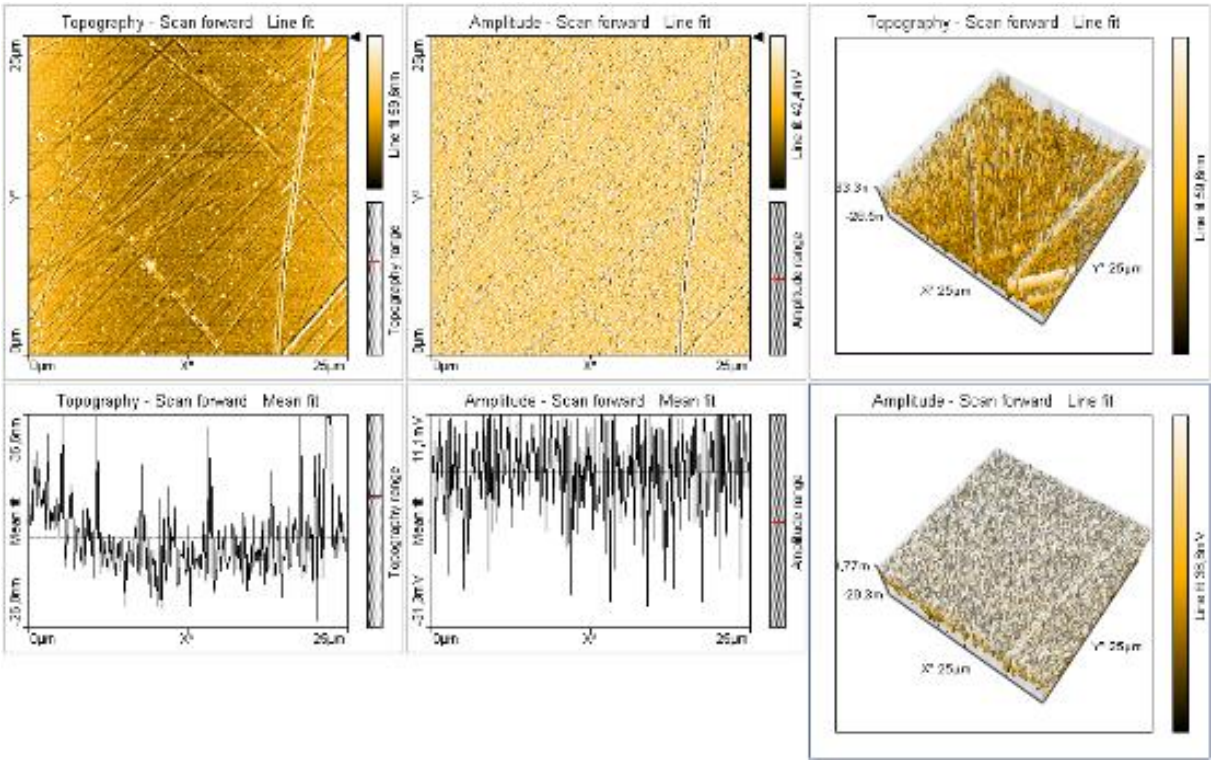

Figure 5.16 Topography and amplitude of Aluminum sputtered for 30 minutes

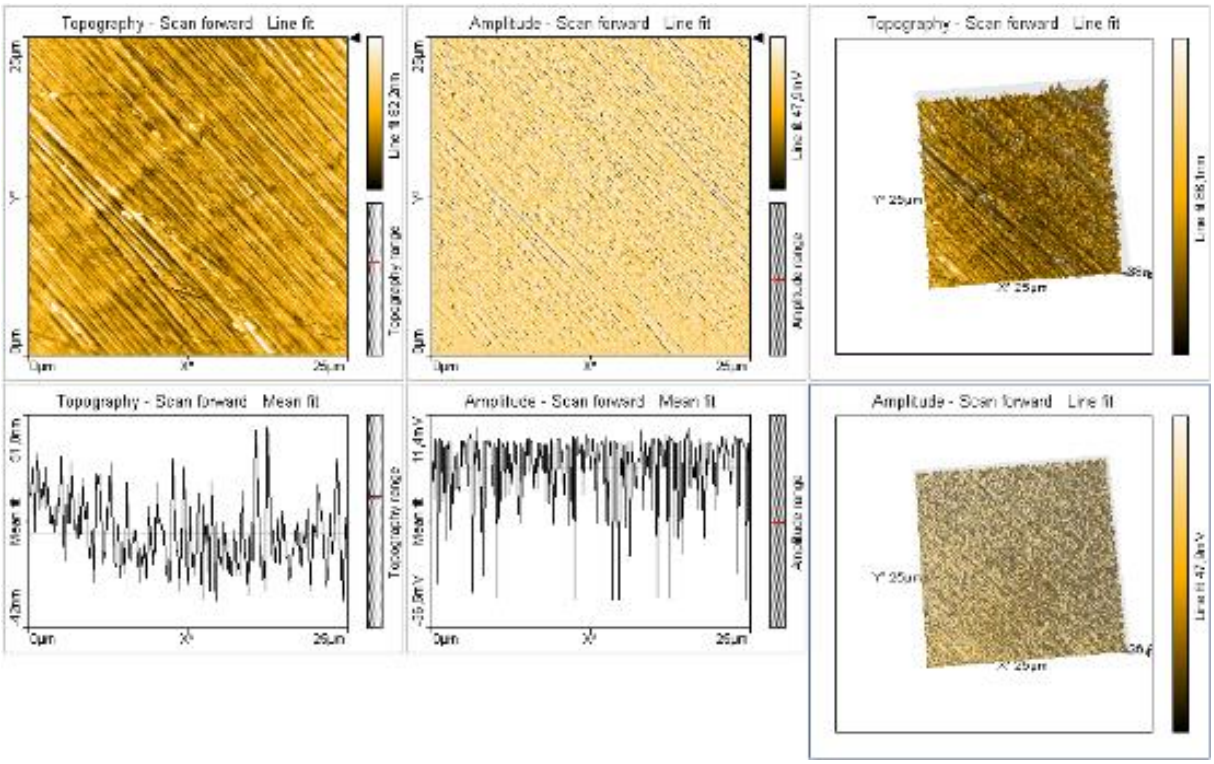

Figure 5.17 Topography and amplitude of Aluminum sputtered for 45 minutes

ITO:

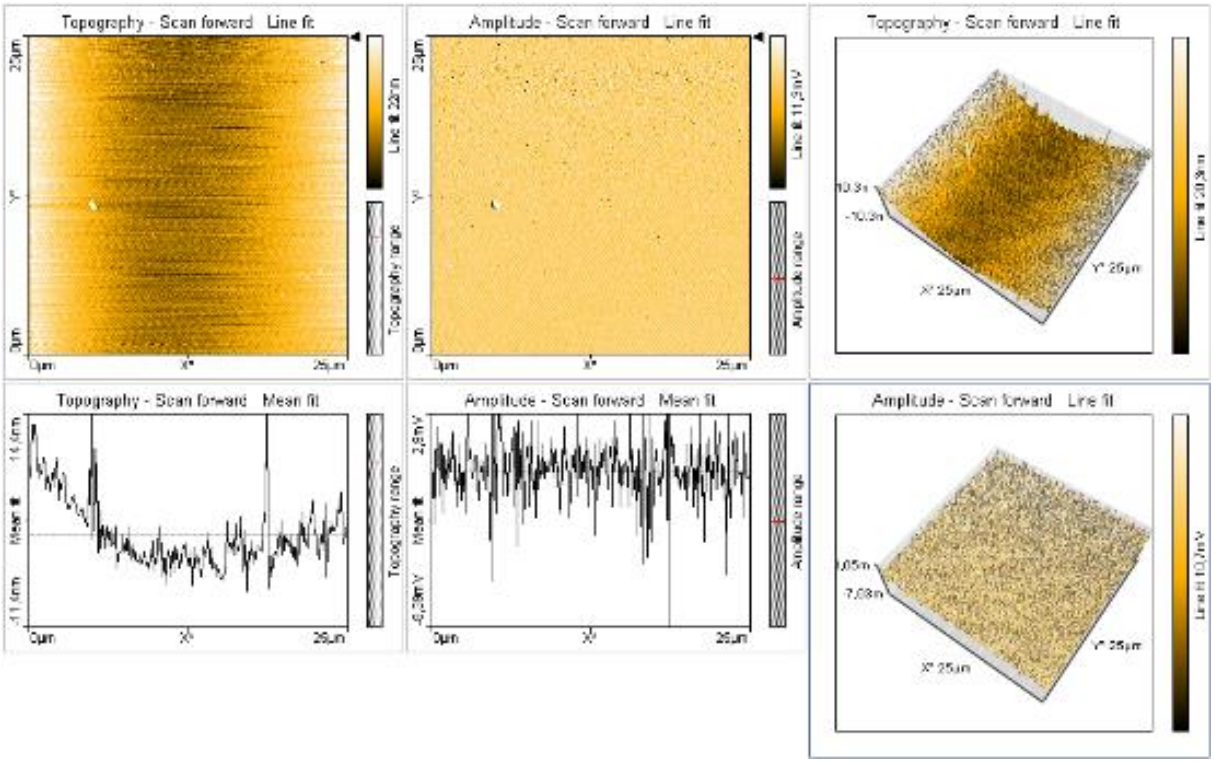

Figure 5.18 Topography and amplitude of ITO sputtered for 10 minutes

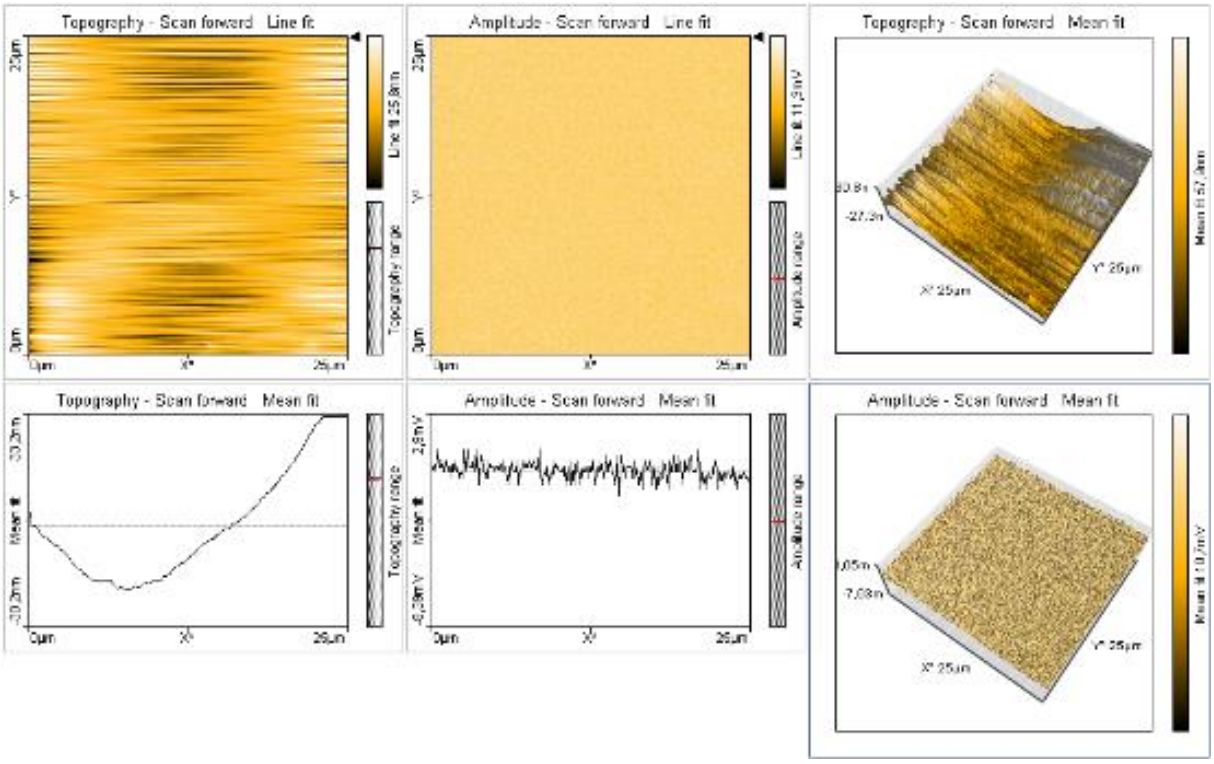

Figure 5.19 Topography and amplitude of ITO sputtered for 20 minutes

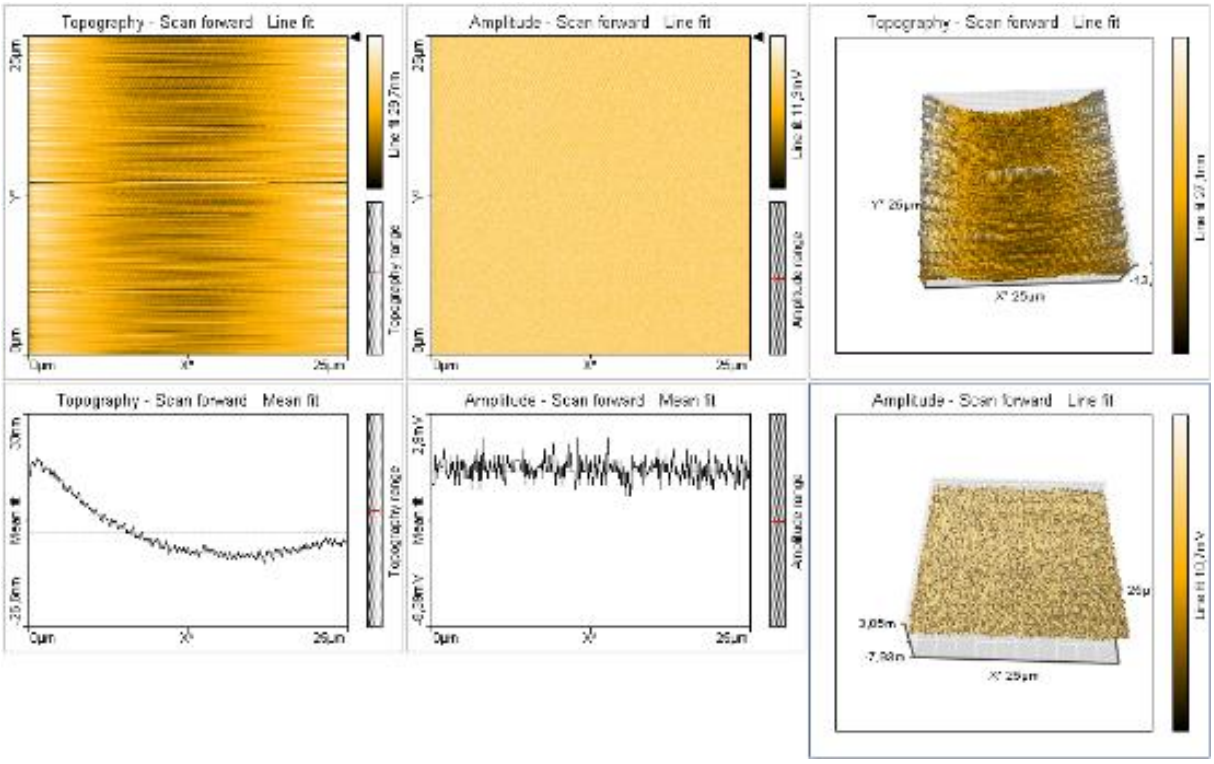

Figure 5.20 Topography and amplitude of ITOsputtered for 30 minutes

5.2.2. Discussion

The surfaces of aluminum and ITO react differently with increase in sputter time. For ITO there is almost no difference in the roughness between the samples in this thesis. The roughness measured on the ITO surfaces, was almost identical with the roughness measured of the clean glass surface from the same sample. For aluminum, on the other hand, this is only true for the shorter sputter times. From 5 minutes – 15 minutes sputtering the roughness is almost constant and in line with the glass surface. However, when increasing the sputter time to 20 minutes, and further, the roughness of the sample increases.

Since sputtering is a process where atoms are moved from one surface and placed on another, as a thin film, it does not necessarily increase the roughness. The atoms can form an even layer and even decrease the roughness of the sample used. Although the roughness of the aluminum surfaces increases with sputter time it is unclear if this trend will continue with further increase or if it will stall, with longer sputter times.

The thickness of the surfaces is not measured, since the tool on the sputter used for this was not functioning. However, with increase in the sputter time, the surface thickness should also increase. This is not beneficial for an oil – water separation experiment, where vision is important. To increase the roughness without increasing the thickness, it could be more beneficial to modify the surface with other technics. Although increase in roughness, can increase the light scattering.

Aluminum is not transparent, even when sputtered for short amounts of time. Therefore, it is not suitable for experiments where vision is important, and cannot be used in the oil – water separation experiments. ITO, on the other hand, is transparent. Therefore, it could be used in further studies.

Since ITO is transparent there are some difficulties in the measurement of the roughness. The tip of the AFM is lowered by the user, which relies on the reflection from the surface to stop the immersion. With transparent surfaces this reflection is hard to see, and therefore, the automatic approach of the tip might have to be used at an earlier time. If not done so, the tip might crash with the surface, and damage both. Using the automatic approach is much more time consuming, then relying on reflection. Also in the sputtering process is ITO a more time consuming. Since the sputtering should happen at 150°C, both the heating of the chamber, but especially the cooling of the sample, takes time.

The topography scanned by the AFM vary a lot for the different surfaces. For the short sputter times with aluminum and with the ITO, the measured topography is defused. and seemingly smooth. For the measurement of the aluminum, this changes when sputtered for 20 -45 minutes, where there are clear lines.

In general, there was many problems with the measurement of the surfaces with the AFM. It often sketched a sudden large height or valley in the middle of the sample. These instabilities in the sample affected the roughness greatly. This was a major problem in the experiments, and happened more often than not. This could happen because there was a tiny scratch on the surface, causing the height difference to increase a lot, very sudden. To prevent this and get an accurate measurement of the average surface, a camera, placed near the tip of the of the AFM, was used to decide the area that was scanned. With this approach, there is a higher possibility for a good result; however, there could still be problems.

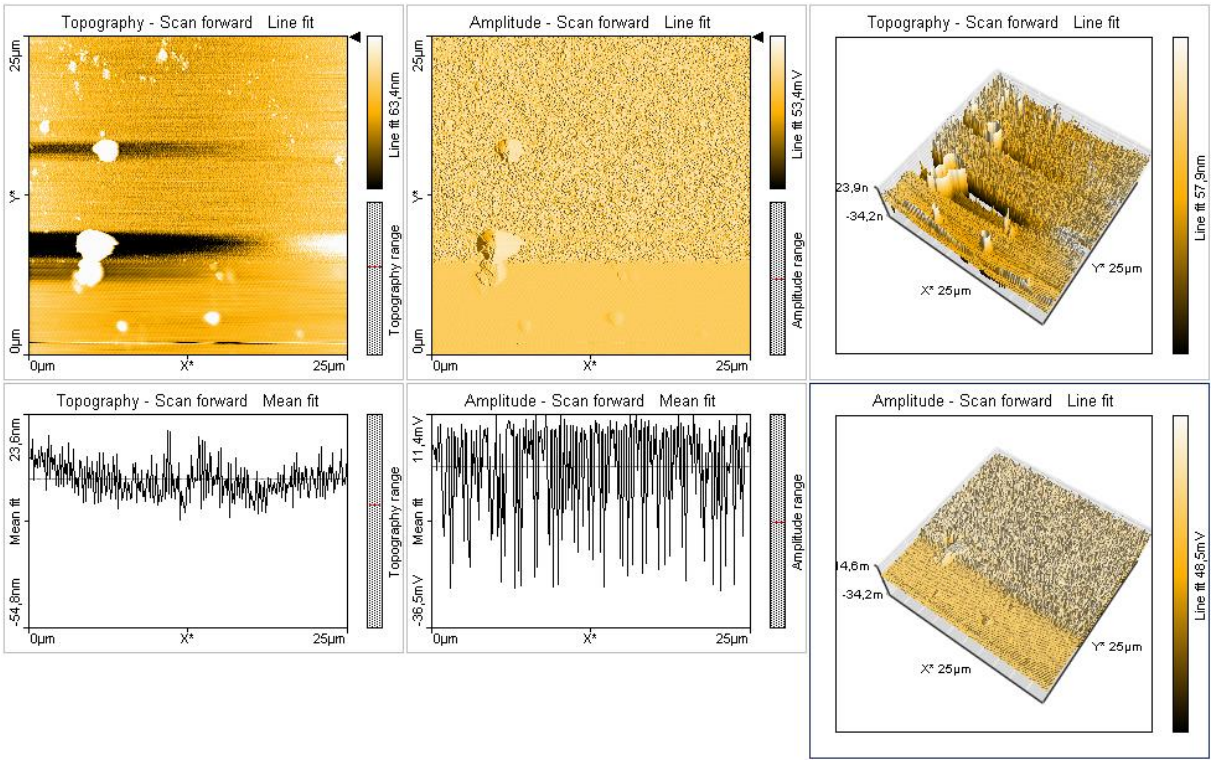

Figure 5.21 Picture of ITO 30, showing a common problem with the measurement with the AFM

5.3. Contact Angle

The contact angle of all the samples were tested. On both the sputtered surface and the clean glass surface. The liquid used was crude oil and water from the same oil well. However, the contact angle of the oil was approximately 0° on all surfaces in this thesis. Therefore, only the water contact angles are included in these results.

5.3.1. Result

The average contact angle values are calculated after doing the experiments 10 different times on all the surfaces.

Table 1Table of the average contact angles with water at different surfaces, with the error given as the standard deviation.

	5	**10**	**15**	**20**	**30**	**45**
Al	70° (± 4°)	66° (± 6°)	61° (± 4°)	59° (± 3°)	74° (± 6°)	83° (± 6°)
ITO		81° (± 6°)		42° (± 4°)	91° (± 6°)	

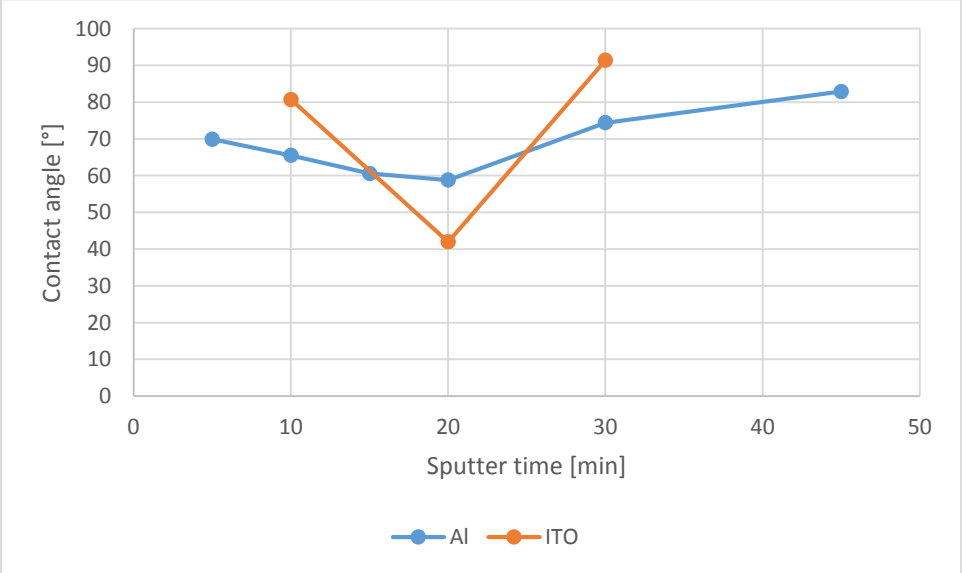

Figure 5.22 Graph of the average contact angles with water at different surfaces

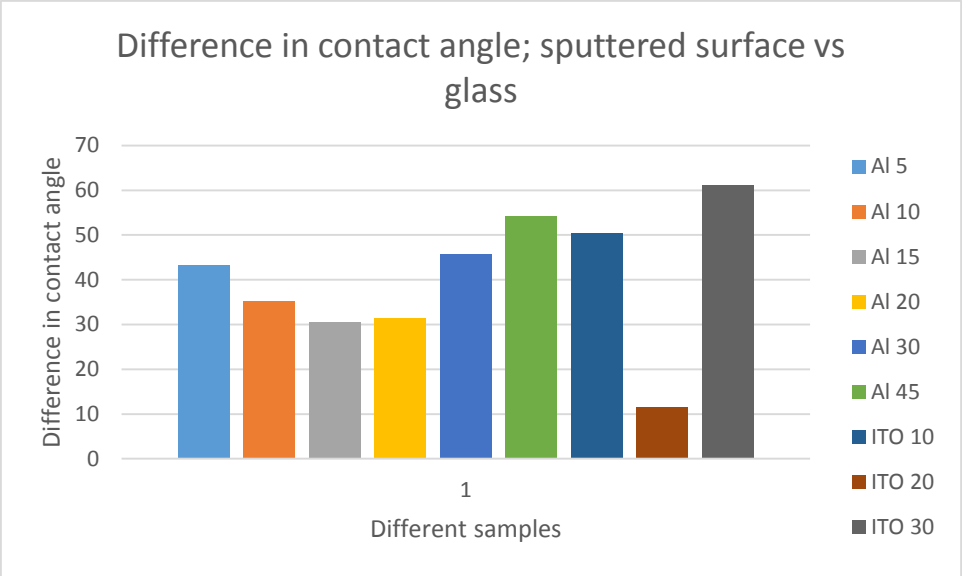

Figure 5.23 Bar graph showing the difference between the average contact angle of water droplets on a sputtered area and a glass area on the same sample.

Pictures of the contact angle of water on enhanced surface

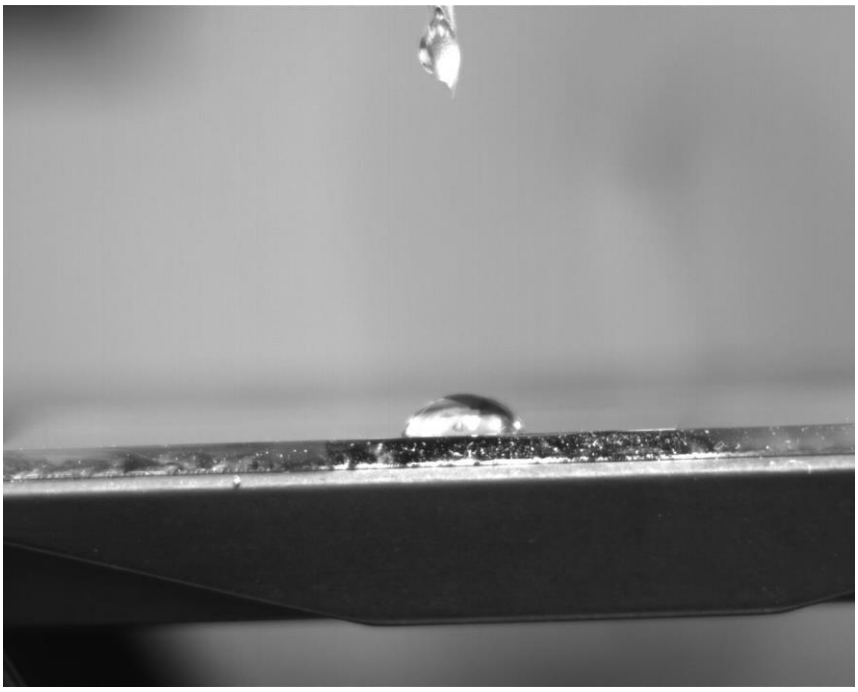

Figure 5.24 Aluminum sputtered 5 min: Contact angle: 71°

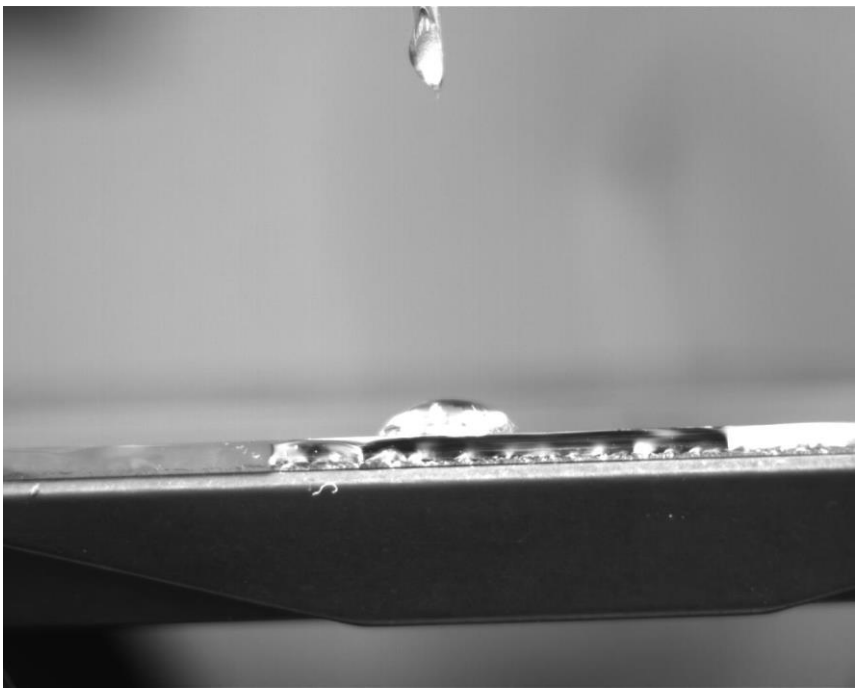

Figure 5.25 Aluminum sputtered 10min: Contact angle: 62°

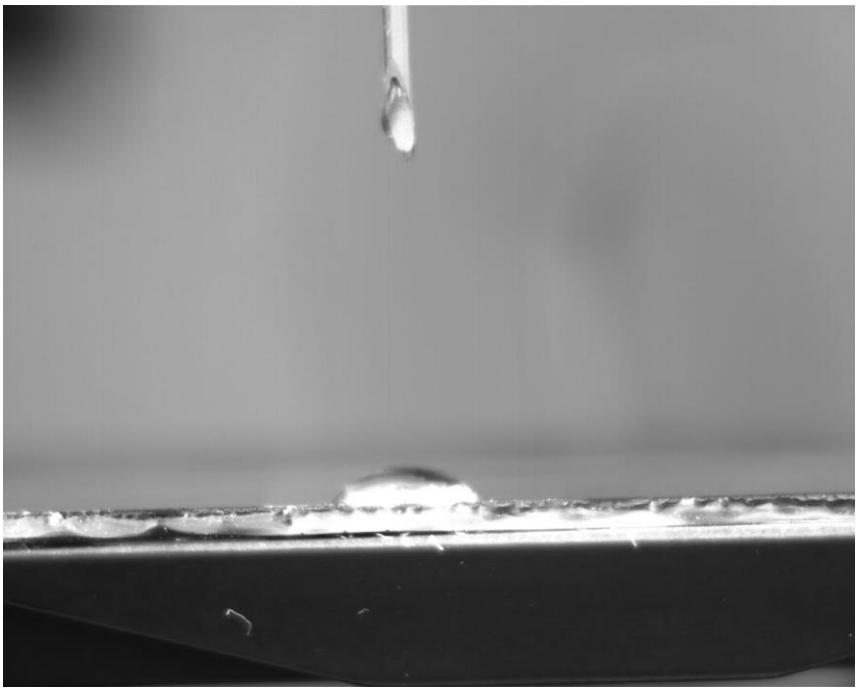

Figure 5.26 Aluminum sputtered 15 min: Contact angle 60°

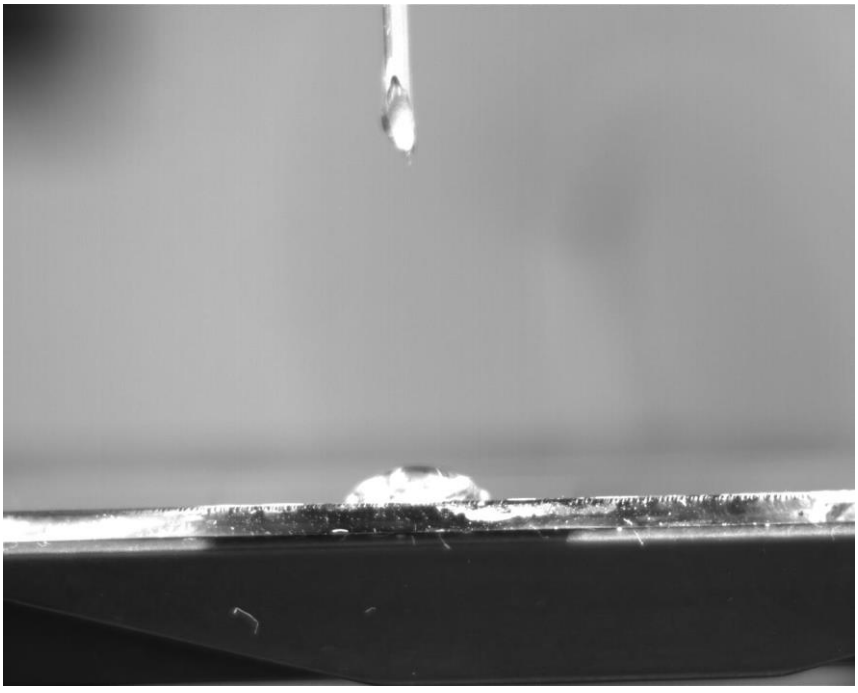

Figure 5.27 Aluminum sputtered 20 min: Contact angle: 59°

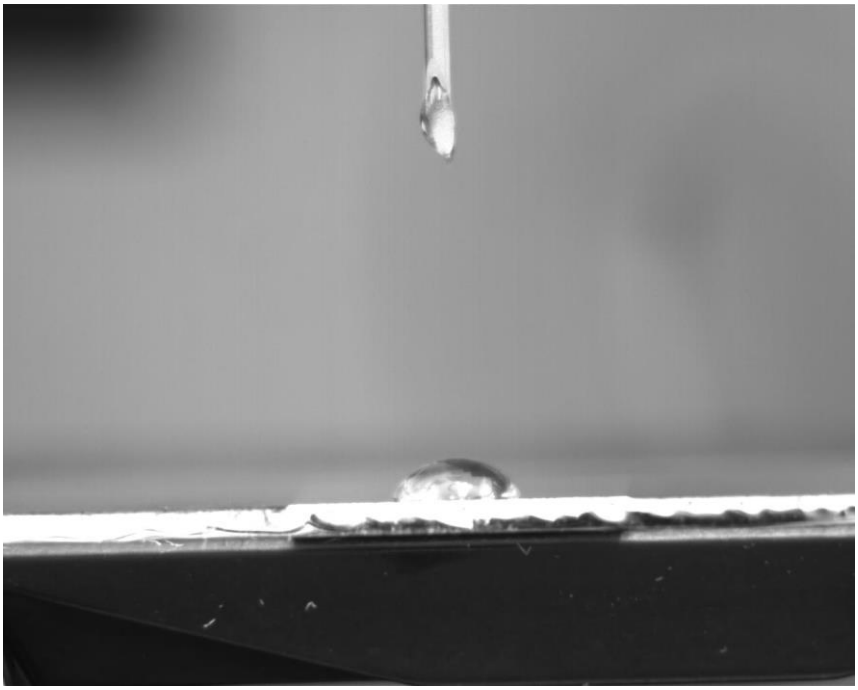

Figure 5.28 Aluminum sputtered 30 min: Contact angle: 74°

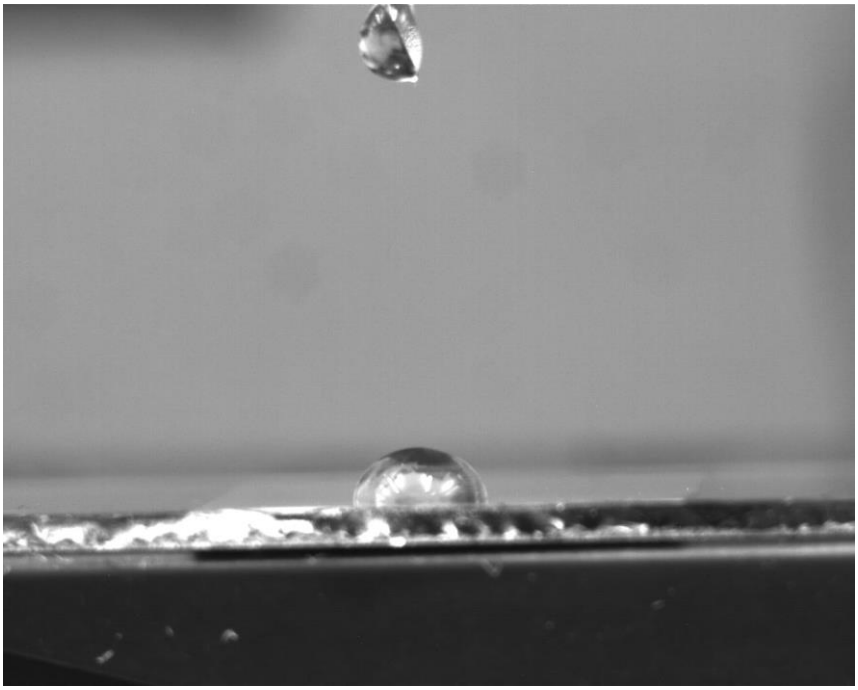

Figure 5.29 Aluminum sputtered 45 min: Contact angle: 82°

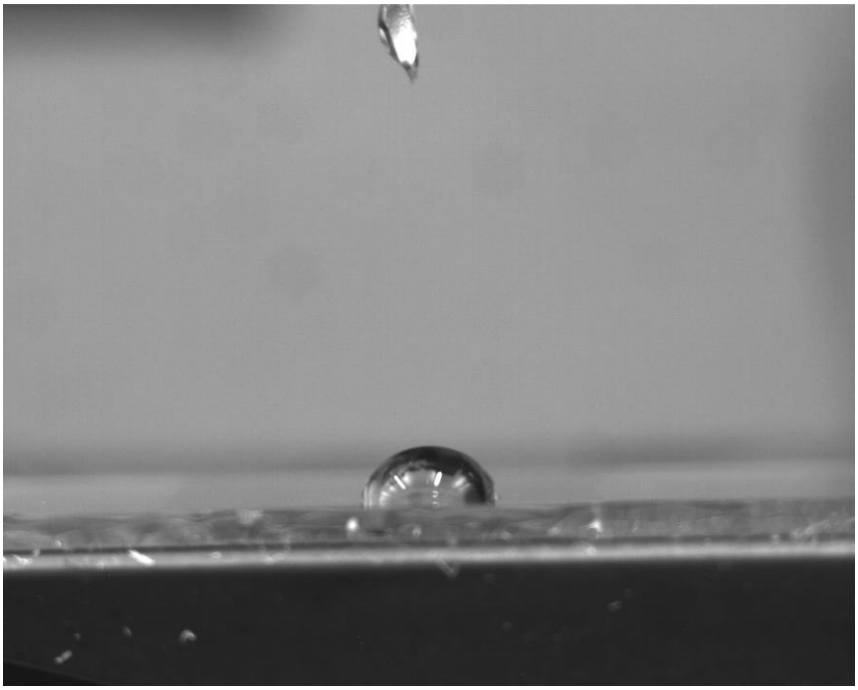

Figure 5.30 ITO sputtered 10 min: Contact angle: 80°

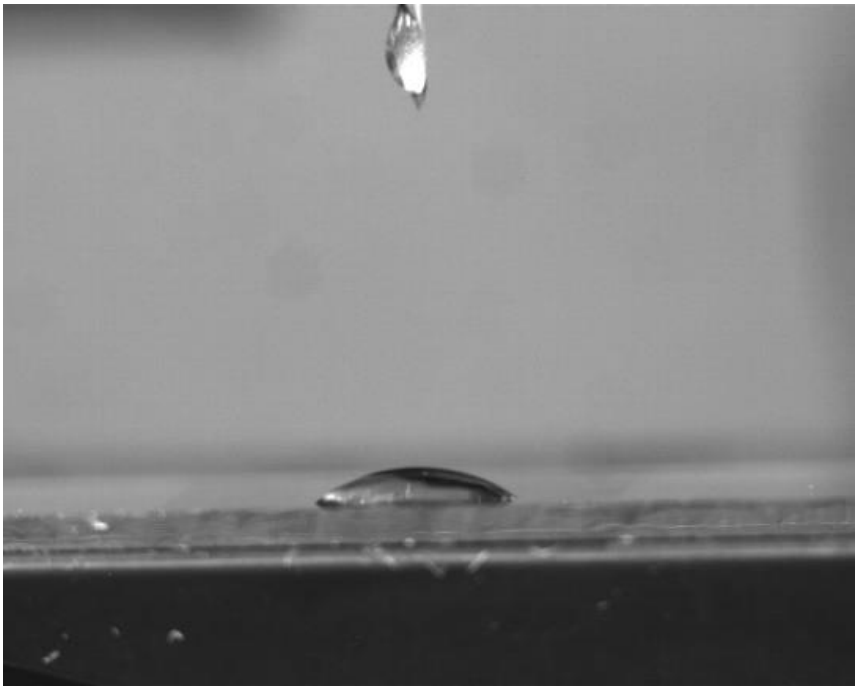

Figure 5.31 ITO sputtered 20 min: Contact angle 42°

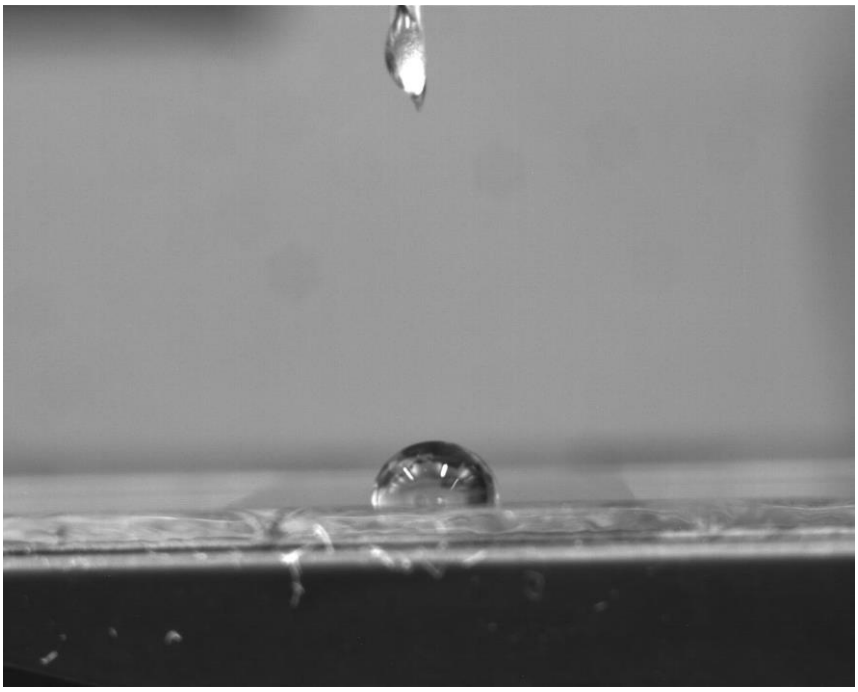

Figure 5.32 ITO sputtered 30 min: Contact angle: 90°

5.3.2. Discussion

The contact angle of both the aluminum and the ITO decreases with sputter time, before increasing. The contact angle of the aluminum surfaces decreases from 5 minutes sputter time, to 20 minutes. The contact angle at 30 minutes is slightly higher than for 5 minutes, and for 45 minutes it is even higher. For ITO the contact angle when sputtered for 10 minutes is high. In line with the highest contact angel measured with aluminum surface. The ITO sputtered for 30 minutes are even higher, and is the only contact angle measured above 90°. However, ITO sputtered for 20 minutes has the lowest contact angle measured in these experiments, apart from the glass samples.

As discussed in the theory, the wettability of a surface depend on the balance of the cohesive and adhesive forces, and the roughness of the surface. Since is the same liquid, water, with approximately the same size, that is used in these experiments, it is the adhesive forces, or surface energy, and roughness that vary.

For the aluminum, the roughness of the samples is almost constant between 5 to 15 minutes sputtering time. At 20 the roughness has almost doubled. Therefore, by just looking at the roughness of the samples, aluminum sputtered for 20 minutes, should have a higher contact angle than aluminum sputtered for a shorter amount of time. The surface energy of aluminum is constant, and therefore the only different should be the roughness. However, increasing sputter time increases the thickness of the surface. This could play a part for the measuring of the contact angle.

The contact angle steadily decreases, from 5 to 15. Where the thickness increases, but the roughness remains the same. At 20 minutes sputter time, the roughness increases as well as the thickness, and the contact angle remains almost the same as for 15 minutes sputter time. It is possible that the surface behaves like a heterogeneous surfaces at low sputter times and increasingly more homogeneous, with increase in sputter time. Where the geometry of the surfaces at low sputter times allows small gas pocket, between the liquid and solid, but increasing the thickness, decreases this possibility. If so, then only when the roughness is high enough, at aluminum sputtered for 30 minutes, can it counter this behavior.

The highest measured contact angles are with the ITO. Even though the roughness of the surfaces was almost identical as the glass. This could mean that the surface energy of the ITO is low. At least lower than aluminum and glass. The interesting part is the very low contact angle for ITO sputtered for 20 minutes. The roughness of this sample is lower than the other ITO samples, which could explain some of the decrease in contact angle. However, it is not significantly lower. It has to be mention that that this sample was constructed at a different time than the two other ITO samples. There has been problems with the ITO target in AJA sputter and Evaporator, where the quality of the surfaces did vary. This might be the case for this sample.

In addition, the oliphobic properties of these surfaces were tested. However, the contact angle of the oil, with all these surfaces was approximately 0°. However, the low contact angle made it impossible to get accurate results for the contact angle. There were no difference between the surfaces. Since the cohesive forces of the oil, is much lower than for water, the adhesive forces from the surface has to be very low to create an oleophobic surface. Even though, a surface of ITO lowers the adhesive forces compared to clean glass or aluminum, the forces are still too strong to be able to change the wettability of crude oil. Previous studies [4, 14] has showed that the surfaces has to be covered by a layer that creates a low surface energy such as flurchemicals and fluorpolymer.

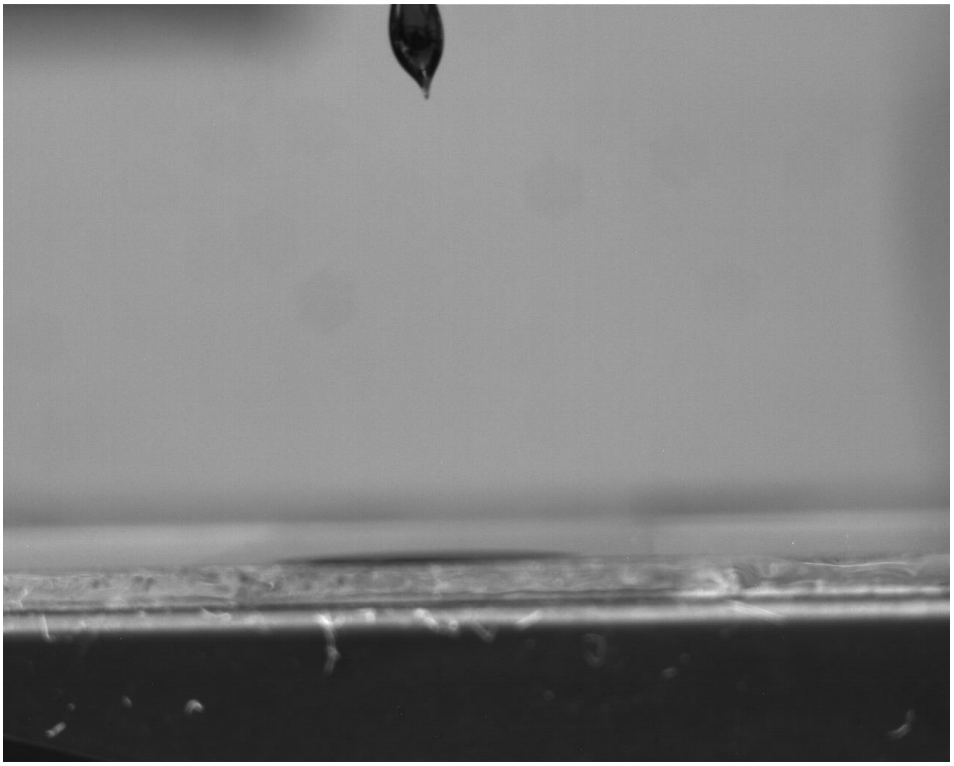

Figure 5.33 Picture of crude oil on the ITO 30 surface.

6. Conclusion and Further Recommendation

6.1. Conclusion

In this work two main research tasks were performed. The first one was related to the investigation of a batch separation process with oil – water. In this case the challenge was focused on using a near infrared high-speed camera for observing the separation process. The second task was related to the use of nano-enhanced surfaces for controlling the wettability of glass surface used for the visualization cell in order to improve the experiments related to oil-water separation.

In the oil – water separation experiments it was observed that the velocity of the droplet – interface coalescence for both Exxol and crude oil, decreases with mixing time. The crude oil separation velocity does at its highest correspond with the terminal velocity of a water droplet with diameter 1400 [µm] dispersed in crude oil. For its lowest it correspond to a water droplet diameter of 450 [µm]. This results indicates that the hindering effect of neighboring droplets is significantly affecting the dynamic of the separation process. Therefore, more experiments are required in this direction for quantifying the hindering factor. When mixed at for a long time the initial average diameter of the droplets in the mixture are very small. The droplets coalescence with each other in the dense-packed zone, and increasing their size before coalescence with the interface. This is a very slow process. Combined with the low visibility, due to the properties of the crude oil, and the interaction of the oil and the glass surface of the vessel, it is hard to get good results. For low mixing times, on the other hand, there are problems creating small droplets.

For Exxol the separation velocity is higher and correspond to the velocity of droplets in the range of 1340 [µm] to 860 [µm]. The velocity of this separation is nearly constant for mixing times 25 to 90 seconds. Which indicate that the increase in mixing after 25 seconds does not influence the initial droplet size. In the Exxol D80 – water mixture, there is a droplet – interface coalescence throughout the experiment.

For the nano-enhanced surface treatment task, only one surface in this thesis could be called hydrophobic. That is ITO sputtered for 30 minuets. However, it is just barley hydrophobic, with an average contact angle of 91°. The enhanced surfaces, did in all cases improve the hydrophobic properties of the glass sample, however, there was no change in the oleophobic properties. The roughness of all the surfaces used in this thesis was measured. For low sputter times with aluminum, and for all the ITO surfaces the roughness of the sputtered sample was almost identical to the glass surface. When aluminum was sputtered for 20 minutes, and further, to 45 minutes, the roughness increased. The roughness is important for the wettability of the surface, however, in this thesis other properties was equally important. It is suspected that it the surface energy of the ITO is lower than aluminum, furthermore, that the aluminum surface become more homogeneous with increase in thickness. Both these properties played an important part in the contact angel measured in this thesis. The ITO is transparent, and therefore, can be used as a surface for water – oil separation experiments.

6.2. Further Recommendations

There is a trend in the separation velocities for both crude oil – water mixtures, and Exxol D80 – water mixtures. However, there are not enough experiments to conclude. Therefore, it is recommended that more experiments, especially with crude oil – water mixture be conducted. In addition, the experiments in this thesis is all preformed at ambient condition. It can be interesting to see the influence temperature and pressure has on the oil – water separation.

To create an enhanced surface for oil – water separation experiments, it is recommended that the roughness of the surfaces are modified without increasing the thickness of the samples. There are many different methods to do so, for example, carving or molding.

An enhanced surface for oil – water separation experiments should be oliophobic. To create an oleophobic surface the surface energy has to be low. Flourchemicals and flouropolymers could be used for this. Furthermore, since the visibility of the experiments are vital, the surface has to be transparent.

References

1. J. Raisin. Electrocoalescence eau-huile Emulsion: Vers une efficacité critère. Fluids mechanics, Université de Grenoble, 2011.
2. www.oilngasseparator.info/oil-handling-surfacefacilities/oil-and-water-separation/horizontal-three-phase-separator-part-1.html 2009
3. W. Rommel, W.Teon and E. Blass. Hydrodynamic modeling of droplet coalecnence liquid-liquid interfaces, Separation science and technology 27:2, 129-159. 1992
4. R. V. Lakshmi, T. Bharathidasan, P. Bera, B. J. Basu. Fabrication of superhydrophobic and oleophobic sol-gel nanocomposite coating. Surface coatings technology 206, 3888-3894. 2012
5. T. Frising, C. Noïk and C. Dalmazzone. The Liquid/Liquid Sedimentation Process: From droplet Coalescence to technologically enhanced water/oil emulsion gravity separators: a review. 27:1035-1057. 2006
6. M. Henschke, L. H. Schlieper, A. Pfenning. Determination of a coalescence parameter from batch-settling experiments. Chemical Engineering Journal 85: 369-378. 2002.
7. R. Cusack. Rethink your liquid-liquid separations. Hydrocarbon processing 53-60. 2009
8. R. J. Hunter. Introduction to Modern Colloid Science. 132-134. 1993
9. www.surface-tension.org/article/60.html
10. M. Schoen. Fluid bridges confined between chemically nanopatterned solid substrates. Physical chemistry chemical physics. 10, 223-256. 2008.
11. R. N. Wenzel. Resistance of solid surfaces to wetting by water. Industrial and engineering chemistry. 28:8, 988-994. 1936
12. A. B. D. Cassie and S. Baxter. Wettability of porous surfaces. Trans. Faraday Soc. 40, 546-551. 1944
13. A. Marmur. Wetting on hydrophobic Rough Surface: To be heterogeneous or not to be? Lagmuir, 19: 8343-8348. 2003.
14. H. J. Lee and J. R. Owens. Motion of liquid droplets on a superhydrophobic oleophobic surface. J Matter sci, 46:69-76. 2011
15. Y. lin, K. Su, P. Tsai, F. Chuang, Y. Yang. Fabrication and characterization of transparent superhydrophilic/superhydrophobic silica nanoparticulate thin films. Thin solid films, 519 5450-5455. 2011
16. X. Li, D. Reinhoudt and M. Crego-Calama. What do we need for a superhydrophobic surface? A review on the recent progress in the preparation of superhydrophobic surfaces. Chem. Soc. Rev. 36: 1350-1368. 2007
17. R. Behrish, W. Eckstein. Sputtering by Particle bombardment. Topics appl. Physics 110, 1-20-2007
18. http://en.rigaku-mechatronics.com/case/sputtering-systems.html 2009
19. http://www.norfab.no/technologies/deposition/ntnu-nanolab/sputter-coater-and-thermal-evaporator/ 2015
20. H. Butt, B. Cappella, M. Kappl. Force measurments with the atopmic force microscope. Technique interpretation applications. Surface science reports. 59: 1-152. 2005
21. Operating Instructions, easyScan 2 AFM, SPM Software version 3.0
22. K. Sjursen. Water droplets Settling in Crude Oil: Effect of Neighbouring Droplets and Temperature. 2014
23. H. G. Polderman, J. S. Bouma and H. van der Poel. Design Rules for Dehydration Tanks and Separator Vessels. Society of Petroleum Engineers. 1997

24. T. C. Hobæk. Nanostructured PDMS surfaces with patterned wettability. 2011

Appendix A

Oil – Water separation velocity

Crude Oil – Water

Separation Velocity

Experiment 1

Mix Time	Pixel size		Change Pixel	Change cm	Time		Velocity
5	0,00983607		43	0,42295082	20		21,147541
10	0,00983607		41	0,40327869	80		5,04098361
15	0,00983607		44	0,43278689	70		6,18266979
20	0,00983607		42	0,41311475	100		4,13114754
25	0,00983607		39	0,38360656	230		1,6678546
30	0,00983607		40	0,39344262	270		1,4571949
45	0,00991736		39	0,38677686	290		1,33371331
60	0,00991736		43	0,42644628	220		1,93839219

Experiment 2

Mix Time	Pixel size		Change Pixel	Change cm	Time		Velocity
5	0,008		43	0,344	18		19,1111111
10	0,00847458		47	0,39830508	90		4,42561205
15	0,00847458		43	0,36440678	40		9,11016949
20	0,00840336		47	0,39495798	60		6,58263305
25	0,00833333		48	0,4	60		6,66666667
30	0,00847458		47	0,39830508	80		4,97881356
45	0,00826446		44	0,36363636	110		3,30578512
60	0,00813008		46	0,37398374	160		2,33739837

Exxol D80 – Water separation

Experiment 1

mix time	Pixel size		Pixel change	Cm change		Time change	rate
5	0,012069		54	0,651724138		7,5	86,89655
10	0,012727		52	0,661818182		7,8	84,84848
15	0,012844		54	0,693577982		9	77,06422
20	0,012727		53	0,674545455		8,4	80,30303
25	0,012281		53	0,650877193		11,4	57,09449
30	0,012444		54	0,672		13,8	48,69565
45	0,011966		54	0,646153846		8,7	74,27056
60	0,012069		54	0,651724138		10,8	60,34483
90	0,011715		53	0,620920502		8,1	76,65685

Experiment 2

5	0,012281		53	0,650877193		6,6	98,61776
10	0,012121		53	0,642424242		4,8	133,8384
15	0,012227		54	0,660262009		11,4	57,91772
20	0,012389		54	0,669026549		8,4	79,64602
25	0,012335		54	0,666079295		9,6	69,38326
30	0,012069		54	0,651724138		8,4	77,58621
45	0,0125		54	0,675		12	56,25
60	0,012121		53	0,642424242		13,5	47,58698
90	0,012389		54	0,669026549		12,9	51,86252

Experiment 3

90	0,011523		61	0,702880658		45	15,61957
60	0,01157		62	0,717355372		46	15,59468
45	0,012017		63	0,757081545		37	20,46166
30	0,011915		60	0,714893617		25	28,59574
25	0,011475		60	0,68852459		24	28,68852
20	0,011618		67	0,778423237		10	77,84232
15	0,01098		63	0,691764706		11	62,8877
10	0,01157		65	0,752066116		10	75,20661
5	0,011618		67	0,778423237		11	70,76575

Appendix B

Contact Angle

Aluminum sputtered 5 min

Al5	Degrees
1	72
2	71
3	68
4	73
5	68
6	74
7	76
8	63
9	66
10	68

Glass surface on the aluminum sample sputtered 5 min

Al5 Glass	Degrees
1	29
2	32
3	22
4	25
5	28
6	31
7	27
8	25
9	21
10	24

Aluminum sputtered 10 min

Al10	Degrees
1	58
2	60
3	61
4	61
5	74
6	70
7	72
8	69
9	68
10	62

Glass surface on alumium sample sputtered 10 min

Al10 Glass	Degrees
1	28
2	32
3	31
4	30
5	36
6	25
7	28
8	28
9	33
10	32

Aluminum sputtered 15 min

Al15	Degrees
1	69
2	65
3	58
4	61
5	60
6	62
7	60
8	55
9	55
10	61

Glass surface on the aluminum sample sputtered 15 min

Al15 Glass	Degrees
1	38
2	32
3	21
4	25
5	20
6	31
7	29
8	35
9	38
10	33

Aluminum sample sputtered 20 min

Al20	Degrees
1	60
2	59
3	60
4	60
5	53
6	60
7	59
8	56
9	62
10	59

Glass surface on aluminum sample sputtered 20 min

Al20 Glass	Degrees
1	25
2	30
3	29
4	24
5	30
6	29
7	25
8	23
9	33
10	26

Aluminum sputtered 30 min

Al30	Degrees
1	81
2	86
3	69
4	70
5	78
6	71
7	75
8	70
9	74
10	70

Glass surface on aluminum sample sputtered 30 min

Al30 Glass	Degrees
1	33
2	22
3	35
4	33
5	30
6	30
7	27
8	26
9	28
10	23

Aluminum sample sputtered 45 min

Al45	Degrees
1	88
2	87
3	91
4	86
5	76
6	80
7	84
8	70
9	85
10	82

Glass surface on aluminum sample sputtered 45 min

Al45 Glass	Degrees
1	32
2	30
3	32
4	29
5	29
6	31
7	25
8	27
9	26
10	26

ITO sample sputtered 10 min

ITO10	Degrees
1	71
2	69
3	85
4	80
5	85
6	85
7	88
8	78
9	84
10	82

Glass surface on ITO sample sputtered 10 min

ITO10 Glass	Degrees
1	27
2	29
3	30
4	29
5	31
6	30
7	32
8	32
9	31
10	32

ITO sample sputtered 20 min

ITO20	Degrees
1	41
2	48
3	44
4	43
5	49
6	42
7	38
8	42
9	35
10	38

Glass surface on ITO sample sputtered 20 min

ITO20 Glass	Degrees
1	31
2	31
3	30
4	29
5	31
6	30
7	30
8	31
9	30
10	31

ITO sample sputtered 30 min

ITO30	Degrees
1	95
2	93
3	102
4	101
5	85
6	85
7	92
8	85
9	86
10	90

Glass surface on ITO sample sputtered 30 min

ITO30 Glass	Degrees
1	29
2	32
3	33
4	30
5	32
6	32
7	29
8	32
9	28
10	26

Appendix C

Roughness

Root mean squared roughness

	5	10	15	20	30	45	60
AL	4,6258	4,6272	4,8525	7,1909	10,821	14,497	13,361
ITO		4,4471		4,1555	4,6153		
AL Glass	4,8603	5,5686	4,9664	5,102	4,6025	4,5043	5,7132
ITO Glass		5,3173		5,1556	4,3116		
Difference Al	-0,2345	-0,9414	-0,1139	2,0889	6,2185	9,9927	7,6478
Difference ITO		-0,8702		-1,0001	0,3037		

I-Gain

IG	SQ
0	0,111662
200	4,0881
500	4,1025
1000	4,7293
4000	4,8525
8000	5,1076
10000	5,1824
20000	5,6338